UNIVERSIDADE DE SÃO PAULO – USP
FACULDADE DE MEDICINA DE RIBEIRÃO PRETO
DEPARTAMENTO DE GENÉTICA

CARLOS HENRIQUE LOPES ROCHA

Atividade sinérgica do antidepressivo sertralina associada a caspofungina contra *Trichophyton rubrum* e avaliação dos mecanismos de resposta adaptativa

Ribeirão Preto – SP
2023

CARLOS HENRIQUE LOPES ROCHA

Atividade sinérgica do antidepressivo sertralina associada a caspofungina contra *Trichophyton rubrum* e avaliação dos mecanismos de resposta adaptativa

Versão corrigida

Tese apresentada ao programa de Pós-graduação em Genética da Faculdade de Medicina de Ribeirão Preto da Universidade de São Paulo, para obtenção do título de Doutor em Ciências Biológicas.

Área de Concentração: Genética

Orientadora: Profa. Dr[a]. Nilce Maria Martinez-Rossi
Coorientador: Prof. Dr. Antonio Rossi Filho

Ribeirão Preto – SP
2023

FICHA CATALOGRÁFICA

Rocha, Carlos Henrique Lopes
Atividade sinérgica do antidepressivo sertralina associada a caspofungina contra *Trichophyton rubrum* e avaliação dos mecanismos de resposta adaptativa. Ribeirão Preto, 2023.
134 p.: il.

Tese de doutorado, apresentada à Faculdade de Medicina de Ribeirão Preto/USP. Área de concentração: Ciências Biológicas (Genética).
Orientadora: Martinez-Rossi, Nilce Maria.
Coorientador: Rossi Filho, Antonio.

1. *Trichophyton rubrum*. 2. Dermatófito. 3. Sinergismo. 4. Resistência antifúngica. 5. Sertralina. 6. Caspofungina. 7. Biofilme.

Nome: Rocha, Carlos Henrique Lopes

Título: Atividade sinérgica do antidepressivo sertralina associada a caspofungina contra *Trichophyton rubrum* e avaliação dos mecanismos de resposta adaptativa

Tese apresentada ao programa de Pós-graduação em Genética da Faculdade de Medicina de Ribeirão Preto da Universidade de São Paulo, para obtenção do título de Doutor em Ciências Biológicas (Genética).

Aprovado em:

BANCA EXAMINADORA

Prof(a). Dr(a). _____
Instituição: _____Julgamento:_____

Prof(a). Dr(a). _____
Instituição: _____Julgamento:_____

Prof(a). Dr(a). _____
Instituição: _____Julgamento:_____

APOIO E SUPORTE FINANCEIRO

Este projeto foi realizado com o apoio financeiro das seguintes entidades e instituições:

Faculdade de Medicina de Ribeirão Preto – FMRP/USP.

Fundação de Amparo à Pesquisa do Estado de São Paulo – FAPESP.

Coordenação de Aperfeiçoamento de Pessoal de Nível Superior – Brasil (CAPES) - Código de financiamento 001.

Conselho Nacional de Desenvolvimento Científico e Tecnológico – Brasil – CNPq.

Fundação de Apoio ao Ensino, Pesquisa e Assistência – FAEPA (FMRP/USP).

Normalização Adotada

Este documento foi elaborado de acordo com:

As normas brasileiras em documentação do Comitê Brasileiro (ABNT/CB-014): NBR 6023, NBR 6024, NBR 6027 e NBR 6028.

Universidade de São Paulo. Sistema Integrado de Bibliotecas. Diretrizes para apresentação de dissertações e teses da USP: documento eletrônico e impresso Parte I (ABNT), São Paulo, 2020.

Dedico este trabalho em primeiro lugar, ao Senhor meu Deus, que nos criou e foi quem me deu toda sabedoria e criatividade para questionar a realidade e o mundo que me cerca. Dedico também e principalmente a minha família que sempre esteve ao meu lado.

AGRADECIMENTOS

Obrigado em primeiro lugar, ao meu Deus que diante de tantas dificuldades, foi aonde encontrei forças para continuar.

Obrigado aos meus pais, Maria José Lopes e Raimundo Rocha, por toda educação, conhecimento e experiência que colocaram na minha vida. Obrigado especialmente a meu pai, que dedicou toda a sua vida ao trabalho e a criação de seus filhos, por ser um homem íntegro e de garra. Obrigado aos dois por toda a força, honestidade, perseverança e sabedoria.

Agradeço a força que a mim foi fornecida, através dos meus irmãos, Iraneide dos Anjos Rocha, Cláudio Jorge Lopes Rocha e Virgínia Lucia Lopes Rocha. Obrigado pelo incentivo e cumplicidade.

Dedico esta tese especialmente a minha irmã Neíze Rocha por me mostrar o poder da superação. Também dedico especialmente ao meu sogro que partiu e como ele dizia, sem poder me chamar de doutor.

Aos meus queridos e amados sobrinhos e tios que trazem alegria a minha vida. Em resumo a toda a minha família que de alguma forma estão presentes nesta tese.

A professora Drª Nilce M. Martinez Rossi, que aceitou me orientar, compartilhar sua experiência e por ter me aceitado em seu laboratório. Agradeço também o meu coorientador professor Dr. Antonio Rossi Filho.

Um agradecimento especial a Flaviane Maria Galvão Rocha, que esteve ao meu lado, contribuindo com sua inteligência, carinho e dando força. Que Deus abençoe e fortaleça você e sua família. Obrigado Vi!

A todos os amigos e colegas do laboratório de Genética e Biologia Molecular de Fungos do Departamento de Genética da Faculdade de Medicina de Ribeirão Preto.

Obrigado a Drª Maíra P. Martins, Drª Tamires A. Bitencourt e Dr. Pablo R. Sanches por compartilhar suas experiências e contribuir diretamente com esta tese.

Agradeço especialmente a Vanderci Massaro de Oliveira (Cuca), ao Marcos Martins e Mendel Mazucato, por compartilhar suas experiências e pela “paciência”.

Meu muito obrigado ao Comitê de Ética do Hospital Universitário da Faculdade de Medicina de Ribeirão Preto, que aprovou este estudo.

Agradeço ao Departamento de Genética, a Faculdade de Medicina de Ribeirão Preto, a USP, FAPESP, CAPES, CNPQ e a FAEPA, pelo suporte estrutural e financeiro.

RESUMO

Rocha, C.H.L. **Atividade sinérgica do antidepressivo sertralina associada a caspofungina contra *Trichophyton rubrum* e avaliação dos mecanismos de resposta adaptativa.** 2023. Tese (Genética) – Faculdade de Medicina da USP de Ribeirão Preto, Universidade de São Paulo, Ribeirão Preto – SP.

As infecções fúngicas em humanos têm aumentado em incidência, principalmente em imunocomprometidos. *Trichophyton rubrum* é o fungo mais prevalente nas dermatofitoses. As condições climáticas, fatores culturais, padrões de migração populacional e até mesmo o nível socioeconômico da população são algumas características que determinam o desenvolvimento de infecções causadas por dermatófitos. Para tratamentos dessas infecções existem poucas opções terapêuticas que atuam em alvos celulares limitados. Além disso, os fungos desenvolvem mecanismos para resistir ao estresse causado pelos antifúngicos disponíveis. Dessa forma, novas estratégias destinadas a controlar esses patógenos estão sendo investigadas. Nesse contexto e assumindo que a sertralina (SRT) tem sido explorada por suas propriedades antifúngicas, objetivamos avaliar alterações na expressão de genes relacionados ao mecanismo de adaptação e resistência em *T. rubrum*. Para isso, realizamos um sequenciamento de alto rendimento do RNA de *T. rubrum* cultivado na presença de dose subletal de SRT. Também investigamos neste estudo a atividade antifúngica do antidepressivo SRT, isoladamente ou em combinação com a caspofungina (CASP). Calculamos as concentrações inibitórias mínimas de SRT e CASP contra *T. rubrum*. Além disso, as interações entre SRT e CASP foram avaliadas usando um método de microdiluição em "xadrez'. Usamos ensaios de MTT e cristal violeta para comparar o efeito de SRT e da combinação de SRT com CASP no biofilme de *T. rubrum*. Também realizamos um ensaio de infecção de unha humana. O RNA-seq revelou 541 genes modulados em 3 h e 1.569 genes modulados em 12 h de cultivo na presença de SRT. Identificamos alguns genes possivelmente relacionados ao efluxo da SRT e sugerimos alvos terapêuticos promissores em alguns componentes da parede celular. SRT sozinha, ou em combinação com CASP, exibiu atividade antifúngica contra *T. rubrum*. A combinação SRT/CASP reprime genes essenciais relacionados à virulência e resistência. A SRT tem como alvos prioritários genes envolvidos na biossíntese da parede celular e do ergosterol. Além disso, a atividade metabólica do biofilme de *T. rubrum* e sua biomassa foram afetadas pela SRT e pela combinação de SRT e CASP. SRT sozinha, ou em combinação, mostra potencial como uma abordagem para minimizar a resistência e reduzir a virulência fúngica.

Palavras-chave: *Trichophyton rubrum*; Dermatófito; Sinergismo; Resistência antifúngica; Sertralina; Caspofungina e Biofilme.

ABSTRACT

Rocha, C.H.L. **Synergistic activity of the antidepressant sertraline associated with caspofungin against *Trichophyton rubrum* and assessment of adaptive response mechanisms.** 2023. Tese (Genética) – Faculdade de Medicina da USP de Ribeirão Preto, Universidade de São Paulo, Ribeirão Preto – SP.

Fungal infections in humans have increased in incidence, especially in immunocompromised. *Trichophyton rubrum* is the most prevalent fungus in dermatophytosis. The climate conditions, cultural factors, population migration patterns, and even the population's socioeconomic level are some features that determine the development of infections caused by dermatophytes. Few therapeutic options exist for treatments of these infections that act in limited cellular targets. In addition, the fungi develop mechanisms to resist the stress caused by the available antifungals. Thus, novel strategies aimed at controlling this pathogen are being investigated. In this context, assuming that sertraline (SRT) has been explored for its antifungal properties, we aimed to evaluate alterations in the expression of genes related to the adaptation mechanism and resistance in *T. rubrum*. For this, we performed high-throughput sequencing of RNA after *T. rubrum* was cultivated in the presence of a sublethal dose of SRT. We also aimed to investigate the antifungal activity of the antidepressant sertraline (SRT), alone or in combination with caspofungin (CASP). We calculated the minimum inhibitory concentrations of SRT and CASP against *T. rubrum*. Furthermore, a broth microdilution chequerboard evaluated interactions between SRT and CASP. We used MTT and violet crystal assays to compare the effect of SRT alone and in combination with CASP on *T. rubrum* biofilms. We also performed a human nail infection trial. RNA-seq showed 541 genes modulated at 3 h and 1,569 genes modulated at 12 h. We identified some genes possibly related to the efflux of the SRT and suggested therapeutic targets promising in some wall cell components. SRT, alone or combined with CASP, exhibited antifungal activity against *T. rubrum*. The combination of SRT/CASP represses essential genes related to virulence and resistance. SRT targets genes involved in the biosynthesis of cell wall and ergosterol. Furthermore, the metabolic activity of the *T. rubrum* biofilm and its biomass were affected by SRT and the combination of SRT and CASP. SRT, alone or in combination, shows the potential to minimize resistance and reduce fungal virulence.

Keywords: *Trichophyton rubrum*; Dermatophyte; Synergism; Antifungal resistance; Sertraline; Caspofungin and Biofilm.

Índice de Figuras

Figura 1: Morfologia de *T. rubrum* 18
Figura 2: Colônias de *T. rubrum* cultivadas em meio sólido (Ágar extrato de malte)..... 19
Figura 3: Mecanismos de ação dos medicamentos azólicos e alilaminas na via da biossíntese do ergosterol 22
Figura 4: Estrutura molecular da caspofungina (CASP)..... 25
Figura 5: Esquematização da formação, maturação e proliferação de biofilmes de fungos filamentosos..... 27
Figura 6: Estrutura molecular da sertralina (SRT). 29
Figura 7: Esquema da representação da microdiluição em xadrez para a obtenção das CIMs combinadas e dos ICIFs. 41
Figura 8: Qualidade e integridade das réplicas biológicas (**rep**) das amostras de RNA extraído 50
Figura 9: Distribuição dependente do tempo de genes diferencialmente expressos em *T. rubrum* após exposição a SRT..... 51
Figura 10: Categorização funcional de genes diferencialmente expressos 53
Figura 11: Genes expressos diferencialmente em resposta a SRT, identificados usando análise RT-qPCR 54
Figura 12: Genes expressos diferencialmente em resposta a combinações de SRT com CASP, identificados usando análise RT-qPCR 55
Figura 13: Expressão dos genes após a exposição SRTcs 56
Figura 14: Genes diferencialmente expressos após exposição a CASPcs. 57
Figura 15: Metabolismo do biofilme de *T. rubrum*..... 58
Figura 16: Avaliação do efeito de SRT, CASP e da combinação sinérgica (SRT + CASP) na biomassa do biofilme de *T. rubrum* corado com cristal violeta. 59
Figura 17: Efeito de SRT, CASP e SRT + CASP na biomassa do biofilme de *T. rubrum*. 59
Figura 18: Microscopia eletrônica de varredura do biofilme de *T. rubrum* em uma unha humana. 61

Índice de Tabelas

Tabela 1: Composição do meio RPMI – 1640 37
Tabela 2: Conjuntos de primers usados para reação em cadeia da polimerase em tempo real (RT-qPCR). 44
Tabela 3: CIMs de sertralina (SRT) e caspofungina (CASP) contra formas planctônicas de *T. rubrum* 49
Tabela 4: Valores MICcb (MICs combinados) para análise de sinergismo entre sertralina (SRT) e caspofungina (CASP) em ensaios realizados em meio RPMI e meio Sabouraud (SB) 49

SUMÁRIO

1. Introdução 17
1.1 As dermatofitoses e *T. rubrum* 17
1.2 Relação patógeno-hospedeiro e *T. rubrum* 19
1.3 Tratamento das infecções fúngicas 21
1.4 Caspofungina 24
1.5 Biofilmes 26
1.6 SRT e combinações farmacológicas 28
2. Justificativa 33
3. Hipótese 33
4. Objetivos 35
5. Estratégias 35
6. Material e Métodos 37
6.1 Meios de cultivo: Extrato de malte (MEA), Sabouraud (SB) e RPMI-1640 37
6.2 Linhagem e condições de cultivo 38
6.3 Concentração Inibitória Mínima (CIM) 39
6.4 Interação entre SRT e CASP 40
6.5 Extração total de RNA 41
6.6 Qualidade e integridade do RNA 42
6.7 RNA-seq e análise de dados 42
6.8 Síntese de DNA complementar (cDNA) 43
6.9 Análise RT-qPCR 43
6.10 Formação de biofilme *in vitro* 45
6.11 Quantificação da atividade metabólica do biofilme por ensaio de MTT 45
6.12 Quantificação da biomassa do biofilme *in vitro* por cristal violeta 45
6.13 Avaliação de biofilmes em unhas humanas 46
6.14 Microscopia eletrônica de varredura 47
6.15 Análise Estatística 47
7. Resultados 49
7.1 Suscetibilidade antifúngica e interação entre SRT e CASP 49
7.2 Qualidade das amostras de RNA 49
7.3 Modulação da expressão gênica em resposta a SRT 50

7.4 RT-qPCR 54
7.5 Efeitos da SRT e sua combinação com CASP na atividade do biofilme de *T. rubrum* 57
8. Discussão 63
9. Conclusão 70
10. Referências Bibliográficas 72

Introdução

1. Introdução

1.1 As dermatofitoses e *T. rubrum*

As infecções fúngicas em humanos vem adquirindo crescente importância especialmente em pacientes imunodeprimidos (Korecka *et al.*, 2021; Seagle *et al.*, 2021; Spallone and Schwartz, 2021; Zeeshan *et al.*, 2023). Uma das infecções fúngicas mais prevalentes são as dermatofitoses, que acometem tanto indivíduos imunocompetentes quanto imunocomprometidos. Essas infecções são causadas por uma classe de patógenos denominados dermatófitos, que obtêm nutrientes de tecidos queratinizados, como cabelo, pele e unhas (Martinez-Rossi *et al.*, 2021). Os dermatófitos são fungos primários, ou seja, não oportunistas, que são divididos em espécies antropofílicas, zoofílicas e geofílicas. Os antropofílicos estão associados principalmente aos seres humanos e raramente infectam outros animais (Martinez-Rossi *et al.*, 2018; Moskaluk and Vandewoude, 2022).

Desde 2017 as relações taxonômicas desses dermatófitos veem sendo reagrupadas e atualmente as espécies estão organizadas em sete gêneros: *Trichophyton*, *Microsporum*, *Epidermophyton*, *Arthroderma*, *Lophophyton*, *Nannizzia* e *Paraphyton*. Estima-se que esses grupos de dermatófitos afetem aproximadamente 25% da população mundial, sendo que 30 a 70% dos adultos agem como portadores, mas não apresentam manifestações clínicas (De Hoog *et al.*, 2017). O clima úmido e as temperaturas elevadas das regiões tropicais e subtropicais, além do modo de vida como a falta de higiene adequada, a estrutura socioeconômica e o convívio com um grande número de pessoas, contribuem para o alto índice de dermatofitoses (Jain *et al.*, 2020; Martinez-Rossi *et al.*, 2021).

As lesões causadas pelos dermatófitos, podem não levar a condições graves em um primeiro momento, mas causam muito desconforto, podendo evoluir para feridas que geram constrangimento estético. São lesões circulares, eritematosas e pruriginosas. São classificadas de acordo com o sítio anatômico de infecção: tinea pedis (pé), tinea corporis (corpo) tinea carpitis (cabelo) e tinea unguium (unha), sendo que esta última também pode ser denominada onicomicose (Ran *et al.*, 2015; Velásquez *et al.*, 2019; Gupta and Venkataraman, 2022; Moseley *et al.*, 2023).

Apesar de fungos dermatófitos causarem principalmente infecções dérmicas cutâneas, em alguns casos, podem provocar infecções mais profundas, além da camada queratinizada da pele (Yun *et al.*, 2022). De forma invasiva, essas infecções provocam diferentes tipos de lesões subcutâneas e profundas, causando condições graves, disseminadas para órgãos internos, que podem levar a um problema de saúde pública (Hu *et al.*, 2023; Simonsen *et al.*, 2023).

Em sua imensa maioria, as dermatofitoses são predominantemente causadas por *Trichophyton rubrum* (Martinez-Rossi *et al.*, 2018; Petrucelli *et al.*, 2019; Martinez-Rossi *et al.*, 2021). É um dermatófito pertencente a um complexo clinicamente relevante, que apresenta uma variedade de fenótipos, mas mostra relativamente poucas diferenças genéticas, sendo cada vez mais prevalente na América do Norte, Europa, Austrália e Leste Asiático (Cornet *et al.*, 2021). É uma espécie frequentemente isolada de infecções em unhas, principalmente em hospedeiros humanos imunocomprometidos (Song *et al.*, 2022; Navarro-Pérez *et al.*, 2023).

T. rubrum é uma espécie que apresenta estruturas morfológicas bem características, com hifas multisseptadas e de crescimento lento (**Figura 1**). Quando é cultivado em meio sólido apresenta uma coloração branca, com aspecto cotonoso. O reverso de uma placa contendo colônias de *T. rubrum* apresenta uma pigmentação bem clássica, vermelho escura, em decorrência de pigmentos produzidos pelo fungo e que acabam se difundindo no meio de cultura (**Figura 2**) (Cornet *et al.*, 2021).

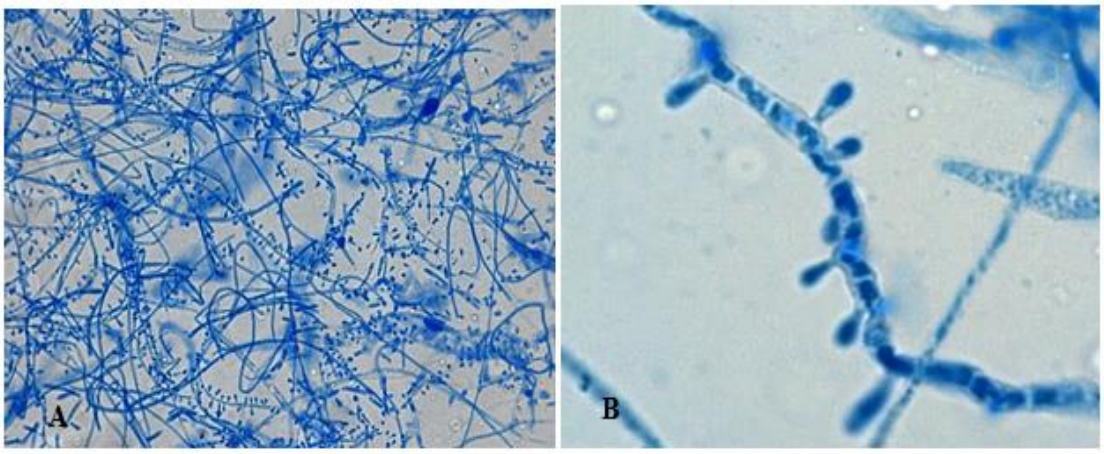

Figura 1: Morfologia de *T. rubrum*. **A**: Microscopia de luz de *T. rubrum* corado com azul de algodão destacando suas hifas septadas hialinas. **B**: Microconídios típicos. **Fonte:** Disponível em: http://thunderhouse4-yuri.blogspot.com/2012/02/trichophyton-rubrum.html.

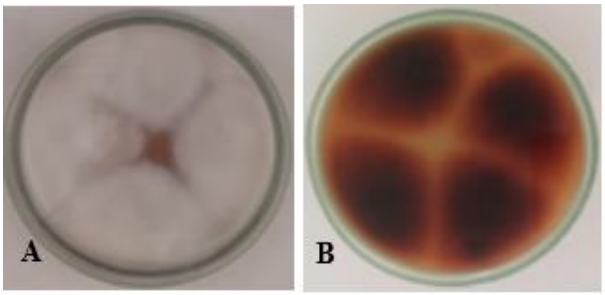

Figura 2: Colônias de *T. rubrum* cultivadas em meio sólido (Agar extrato de malte) com coloração branca, e com aspecto cotonoso (**A**) e o reverso da placa apresenta cor vermelho escuro (**B**). **Fonte**: Próprio autor 2023.

1.2 Relação patógeno-hospedeiro e *T. rubrum*

A patogênese das infecções por *T. rubrum* e pelos demais dermatófitos envolve alguns fatores que incluem a sua capacidade de adesão a um substrato, a supressão da resposta inflamatória, a produção de metabólitos com atividade imunomoduladora e a capacidade de sobreviver em diferentes condições ambientais. Esses mecanismos permitem que o fungo se estabeleça, se multiplique e cause infecções persistentes (Gupta *et al.*, 2021).

A adesão aos substratos específicos como pele e unha é a primeira etapa da infecção. *T. rubrum* possui uma variedade de receptores que iniciam a infecção; ele adere a célula do hospedeiro através de glicoproteínas, proteínas presentes na parede celular dos fungos que são cruciais para a fixação inicial, também denominadas adesinas (Kar *et al.*, 2019). Essas glicoproteínas se ligam aos resíduos de manose e galactose presentes na superfície da célula hospedeira, uma estratégia para não ser eliminado juntamente com a descamação do epitélio. Posteriormente ocorre a germinação dos artroconídios e as hifas entram rapidamente na estrutura hospedeira a ser infectada (Sardana *et al.*, 2021).

Durante a infecção, os principais mecanismos de defesa do hospedeiro incluem descamação da pele, diminuição da umidade, pH da pele, temperatura elevada e ácidos graxos (Martinez-Rossi *et al.*, 2017; Celestrino *et al.*, 2021). Em contraste, *T. rubrum* desenvolve respostas adaptativas para superar esses desafios (Mendes *et al.*, 2018). Ele modula a resposta imune do hospedeiro, causa lesões leves com inflamação mínima ou persistem por tempo suficiente para se tornarem crônicos. Além disso, esse patógeno tem a capacidade de reduzir a produção de citocinas pró inflamatórias (Celestrino *et al.*, 2021). *T. rubrum* pode causar infecções crônicas, através da liberação de glicopeptídeos que

possivelmente inibem a proliferação de linfócitos T, suprimindo assim a imunidade do hospedeiro (Sardana *et al.*, 2021). Além disto, o mutante *ap1* de *T. rubrum* cresce mais que a linhagem selvagem em fragmentos de unhas humanas ou em queratinócitos. Estes dados sugerem que o gene $ap1^{+}$ controla negativamente a virulência e contribui para a cronicidade de *T. rubrum*, principalmente nas onicomicoses (Peres *et al.*, 2022).

Assim que o fungo se instala no hospedeiro, busca nutrientes para o seu crescimento. Para isso, conta com auxílio das permeases, enzimas da parede celular e da secreção de uma variedade de enzimas hidrolíticas, como as nucleases, queratinases, lipases, fosfatases, fosfolipases (Nenoff *et al.*, 2014; Elavarashi *et al.*, 2017; Zhan *et al.*, 2018; Chen *et al.*, 2023). Essas enzimas são críticas no estabelecido da infecção por *T. rubrum*, pois auxiliam na invasão dos tecidos (Cruz *et al.*, 2022). No caso específico de *T. rubrum*, uma resposta ao pH ambiental acontece. A quebra da queratina e sua posterior utilização como fonte de carbono, resulta em metabólitos que modificam o pH do ambiente para alcalino. Neste ambiente, ocorre transcrição de genes que codificam proteases cuja atividade ótima é em pH alcalino (Martinez-Rossi *et al.*, 2017). Ademais, enzimas proteolíticas inespecíficas e queratinases são desreprimidas, fenômeno que também pode estar diretamente relacionado com a resposta ao pH, que na pele humana é ácido. Essa resposta transcricional ao pH é governada por uma via conservada de transdução de sinal, regida pelo fator de transcrição PacC/Rim101p, e também relacionada com outros eventos metabólicos (Silveira *et al.*, 2010).

Outra adaptação de *T. rubrum* ao invadir o tecido hospedeiro, é a superexpressão de várias proteínas de choque térmico (HSPs). Essas proteínas são responsivas ao calor e aos desafios ambientais, entre eles o tratamento com drogas antifúngicas e o estresse oxidativo (Sardana *et al.*, 2021). A presença dessas proteínas em fungos, geralmente estão associadas a patogenicidade, transição de fase em fungos dimórficos e resistência a drogas antifúngicas (Jacob *et al.*, 2015). Em *T. rubrum* quando cultivado em unhas humanas e *in vitro*, por exemplo, observa-se uma expressão aumentada dos genes *hsp60*, *hsp70* e *hsp78*, e quanto *T. rubrum* é cultivado na pele, a *hsp70, hsp90*, e alguns genes relacionados, *hsf1* e *hspSSc1* são superexpressos (Martinez-Rossi *et al.*, 2017).

1.3 Tratamento das infecções fúngicas

O tratamento das infecções por *T. rubrum* é desafiador, porque apenas algumas opções terapêuticas, como azóis e alilaminas que interferem na via de biossíntese do ergosterol, estão disponíveis (Li *et al.*, 2021). Além disso, o tratamento é longo e caro e vários casos de resistência antifúngica vem sendo relatados (Perlin *et al.*, 2017; Khan *et al.*, 2022; Mohammadifard *et al.*, 2022; Branco *et al.*, 2023; Martinez-Rossi *et al* 2021).

Apesar disto, os medicamentos azólicos, por exemplo, ainda têm sido bastante utilizados no tratamento de dermatofitoses (Khurana *et al.*, 2019). Esses compostos atuam na biossíntese do ergosterol, mais precisamente na enzima que converte lanosterol em ergosterol (**Figura 3**), no estágio de desmetilação, uma reação oxidativa que ocorre em três etapas catalisada pela enzima citocromo P450 – 14α-lanosterol, codificada por *ERG11* em leveduras como *Candida albicans* e *Cryptococcus neoformans* e por *cyp51A* e *cyp51B* em alguns fungos filamentosos como em *Aspergillus fumigatus* (Khurana *et al.*, 2019; Shafiei *et al.*, 2020).

O ergosterol é um componente fundamental da membrana e contribui com diversas funções celulares, principalmente para fluidez e a integridade, sendo importante para o crescimento e proliferação celular (Petrucelli *et al.*, 2019; Choy *et al.*, 2023). Esse mecanismo de ação dos azóis causam o acúmulo de esteróis intermediários, que podem ser desviados para uma via metabólica alternativa, prejudicando ainda mais a célula (Bhattacharya *et al.*, 2018).

Esse acúmulo de esteróis intermediários e tóxicos, que perturbam a estabilidade da membrana é um mecanismo que também está associado ao surgimento da resistência. Ele permite a sobrevivência de populações fúngicas, um efeito tipicamente fungistático e, juntamente com o uso extensivo de azóis, resulta em resistência generalizada (Robbins *et al.*, 2017; Ganesan *et al.*, 2022). Outro mecanismo bastante comum e que permite o surgimento de cepas resistentes, é consequência de mutações no gene que codifica o alvo do fármaco, reduzindo a ligação com esse alvo e, portanto, a eficácia do fármaco (Robbins *et al.*, 2017). Esse mecanismo é frequentemente observado na resistência aos azóis (Ahangarkani *et al.*, 2020; Li *et al.*, 2023).

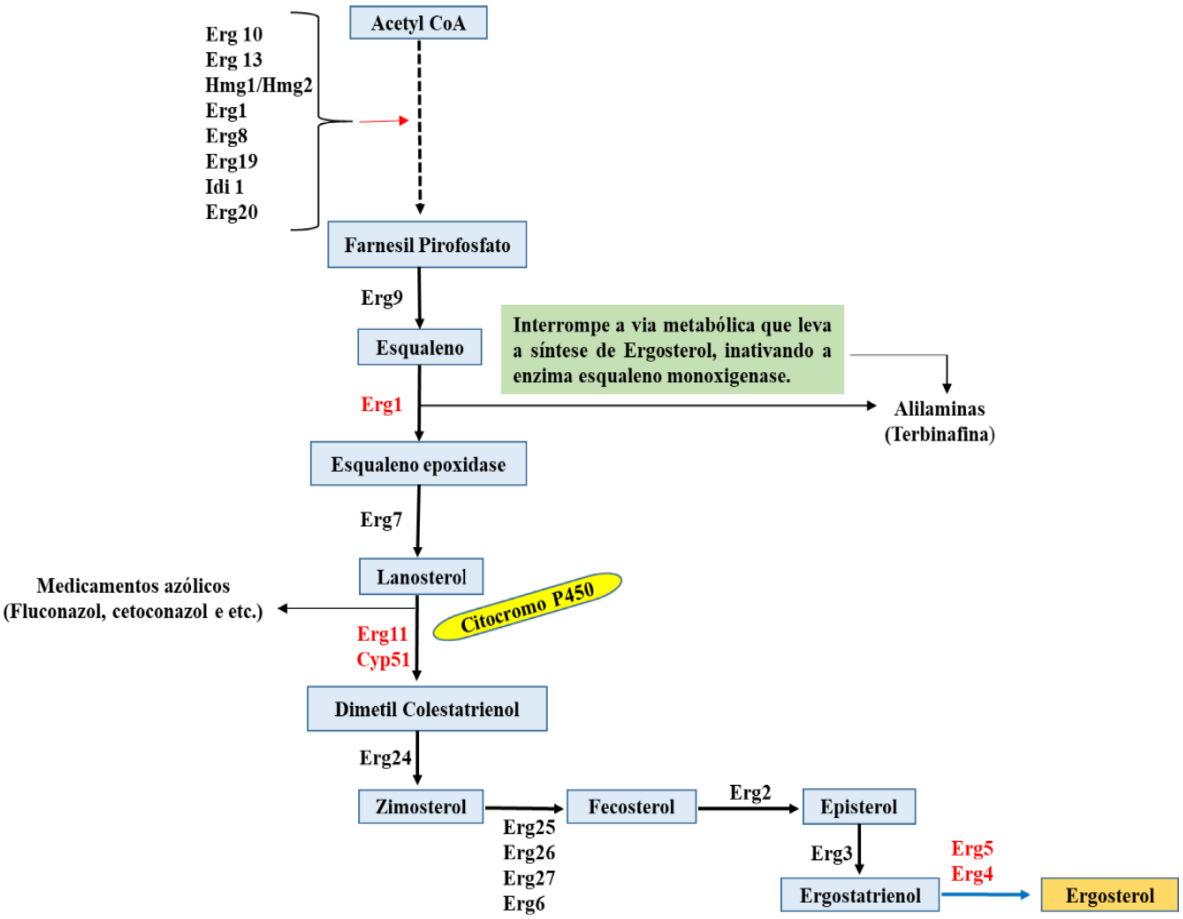

Figura 3: Mecanismos de ação dos medicamentos azólicos e alilaminas na via da biossíntese do ergosterol. Os azólicos atuam na enzima que converte lanosterol em ergosterol, que é codificada pelo gene *Erg11* ou *Cyp51*. Alilaminas atuam na enzima esqualeno epoxidase, que é codificada pelo gene *Erg1*. *Erg5* e *Erg4* são genes críticos na conversão de ergostrienol em ergosterol. **Fonte:** Próprio autor 2023.

Outra possibilidade, é através de uma chaperona molecular a Hsp90, que os fungos utilizam para regular a estabilidade e a ativação de diversas proteínas, possibilitando uma maior tolerância aos antifúngicos e como consequência gerando resistência, especialmente aos azóis (Fu *et al.*, 2022). A adaptação a diversas perturbações ambientais, também é uma aliada a resistência fúngica, em diversas espécies (Robbins *et al.*, 2017). Outro processo, é o aumento da expressão de um alvo de droga que também pode conferir resistência (Paul *et al.*, 2019).

A problemática da resistência fúngica é constante e extremamente urgente. É um fenômeno crítico e evolutivo observado em diversas espécies fúngicas, que proporciona aos

fungos a capacidade de tolerar e se adaptar aos fármacos destinados à sua inibição (Martins-Santana *et al.*, 2023). Especificamente em *T. rubrum*, essa adaptação é modulada e orquestrada por diversos fatores que sustentam também a virulência, como a expressão de genes envolvidos na interação patógeno-hospedeiro e a ativação de mecanismos compensatórios (Martins *et al.*, 2016; Martins *et al.*, 2020).

Recentemente um trabalho realizado no Japão demonstrou os primeiros isolados de *T. rubrum* resistentes a itraconazol, nesse país (Hiruma *et al.*, 2023). Outro trabalho mostrou que *T. rubrum* está presente em feridas crônicas de pacientes diabéticos, uma condição que favorece a resistência fúngica (Ge and Wang, 2022). Uma cepa multirresistente de *T. rubrum* foi isolada de um paciente com tinea corporis recorrente. Nesse trabalho, foi identificado um aumento na expressão de genes que codificam proteínas transportadoras, uma forte evidência da resistência intimamente associadas à azóis (Kano *et al.*, 2022).

Atualmente os relatos de resistência aos medicamentos azólicos só aumentam (Khurana *et al.*, 2019; Gupta *et al.*, 2021; Kano *et al.*, 2022; Yamada *et al.*, 2022). Um caso muito interessante foi descrito em um trabalho realizado com cepas do complexo interdigital de *Trichophyton mentagrophytes.* Nesse estudo, foi quantificado o conteúdo de ergosterol de duas cepas, uma resistente e uma outra cepa de referência, sem resistência. A cepa padrão de *T. mentagrophytes* tinha metade do conteúdo de ergosterol que a cepa resistente. Além disso, através de uma análise genômica, constatou-se mutações nos genes *SQLE*, *ERG4*, *ERG11*, *MDR1*, *MFS* e uma nova mutação no *ERG3* (Bhattacharyya *et al.*, 2023). Outros trabalhos realizados com outros patógenos, *Aspergillus* e *Candida*, já vem demonstrando casos de resistência aos antifúngicos mais recentes, como posaconazol e voriconazol. Além disso, esses fungos também desenvolveram resistência a azóis clássicos, como itraconazol e fluconazol (Gupta *et al.*, 2021).

O maior representante das alilaminas contra dermatófitos**,** é a terbinafina (TRB), um fármaco bastante utilizado contra a maioria das dermatofitoses, onicomicoses e até micoses sistêmicas (Lipner and Scher, 2019; Pinto *et al.*, 2021). Contra *T. rubrum* é bastante recomendada, além de ser usada para tratamento de outras doenças fúngicas, como pitiríase versiculor e candidíase cutânea (Dall'oglio *et al.*, 2022; Shen *et al.*, 2022). A TRB atua através da inibição da enzima esqualeno epoxidase (SQLE), bloqueando a síntese de 2,3

óxido esqualeno, o que consequentemente leva ao acúmulo de esqualeno e depleção de ergosterol (Lipner and Scher, 2019; Maxfield *et al.*, 2023).

A resistência a TRB pode acontecer devido a mutações no gene da esqualeno epoxidase, do aumento da expressão desse gene alvo da droga, resistência natural e, assim como a resistência aos azóis, também pode ocorrer devido a atuação das bombas de efluxo (Astvad *et al.*, 2022; Khurana *et al.*, 2022; Shen *et al.*, 2022). Recentemente um caso intrigante de multirresistência natural de *Trichophyton indotineae* à TRB foi detectado na China (Jia *et al.*, 2023). Ainda no contexto atual, outro trabalho identificou a ocorrência de dermatofitoma causado por *T. rubrum* resistente à TRB em um paciente com diabete tipo 2 (Noguchi *et al.*, 2022).

Com os trabalhos publicados atualmente, fica bastante claro que a principal causa de resistência dos dermatófitos, incluindo *T. rubrum* à TRB são as mutações no gene que codifica a esqualeno epoxidase (Hsieh *et al.*, 2019; Ebert *et al.*, 2020; Kong *et al.*, 2021; Burmester *et al.*, 2022). Um trabalho realizado recentemente na Dinamarca, mostrou uma grande preocupação com o número crescente de isolados de *Trichophyton* resistentes à TRB, devido principalmente a mutações no gene da SQLE. Os autores concluíram nesse estudo, que a maioria dos isolados de *T. rubrum* e *T. mentagrophytes/interdigitale* possuíam mutações nesse gene que consequentemente refletia na resistência desses isolados (Astvad *et al.*, 2022).

Um trabalho pioneiro demonstrou um novo mecanismo de resistência a TRB em fungos dermatófitos. Nesse trabalho, foi construída uma cepa de *T. rubrum* com múltiplas cópias do gene que codifica a salicilato 1-monooxigenase (*sal*A). Essa cepa apresentou aumentada expressão de *salA* e resistência a TRB, demonstrando a importância deste gene na resistência de *T. rubrum* a esse fármaco (Santos *et al.*, 2018). Apesar de ser um mecanismo que até então não havia sido descrito, a resistência a TRB mediada por *Sal*A já tinha sido sugerida pela primeira vez em *Aspergillus nidulans* (Graminha *et al.*, 2004).

1.4 Caspofungina

Outro medicamento bastante utilizado contra infecções fúngicas, principalmente contra o gênero *Candida* é a CASP, pertencente a classe das equinocandinas (**Figura 4**) (Itoh

et al., 2022; Badiee *et al.*, 2023; Thompson *et al.*, 2023). CASP é um dos mais recentes antifúngicos desenvolvidos para a terapia clínica (Sucher *et al.*, 2009). Seu espectro de atuação tem sido bastante estudado, mas apenas alguns trabalhos relatam sua eficiência contra fungos filamentosos, incluindo os dermatófitos (Colabardini *et al.*, 2022; Szymański *et al.*, 2022; Zhao *et al.*, 2022; Fortes *et al.*, 2023).

Recentemente um trabalho demonstrou que CASP apresentou excelentes resultados contra diversos dermatófitos, especialmente do gênero *Trichophyton*: *T. mentagrophytes, T. rubrum, Trichophyton tonsurans, Trichophyton violaceum, e Trichophyton benhamiae* (Badiee *et al.*, 2023). Contra o gênero *Microsporum* CASP também demonstrou resultados promissores, necessitando baixas concentrações para inibir algumas espécies desse gênero (Katiraee *et al.*, 2021). A atividade de CASP também foi demonstrada contra isolados clínicos de dermatófitos. Nesse estudo realizado com 100 pacientes com tinea capitis, CASP apresentou uma atividade considerável contra *Microsporum canis*, *Microsporum gypseum* e *Microsporum audouinii*, apesar de ter sido menos eficiente que outros antifúngicos (Doss *et al.*, 2018).

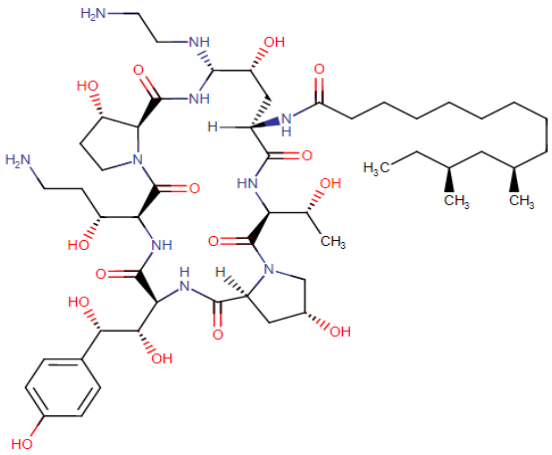

Figura 4: Estrutura molecular da caspofungina (CASP). **Fonte:** Disponível em https://go.drugbank.com/structures/DB00520/image.svg.

O mecanismo de ação da CASP, assim como as demais equinocandinas, é através da inibição da enzima beta-(1,3)-D-glucana sintase, que é um componente essencial na formação da parede celular fúngica (Szymański *et al.*, 2022). CASP não é substrato para transportadores multidrogas em algumas espécies. Dessa forma, um dos principais

mecanismos de resistência está relacionado com a aquisição de mutações no gene FKS (Accoceberry *et al.*, 2019; Hirayama *et al.*, 2023; Memon *et al.*, 2023). Esse fenômeno ocorre devido as substituições de aminoácidos em regiões pontuais na subunidade catalítica de 1,3-β-D-glucana sintase, um produto do gene FKS (Fayed *et al.*, 2021). Em um trabalho publicado em 2021 os autores sugeriram que uma ATPase do tipo P e a biossíntese de ubiquinona metiltransferase podem estar envolvidas na resistência de *Aspergillus flavus* a CASP (Yassin *et al.*, 2021). Em *A. fumigatus*, ocorre o chamado efeito paradoxal da CASP, um fenômeno existente quando o fungo é exposto a altas concentrações de CASP, também associado com a evolução da resistência as drogas (Valero *et al.*, 2020).

Assim, apesar de CASP ser um fármaco relativamente novo no mercado, comparada a outros antifúngicos, os casos de resistência já estão sendo descritos (Papon and Goldman, 2021; Moreira-Walsh *et al.*, 2022; Perrine-Walker, 2022; Wang *et al.*, 2023). Recentemente foi demonstrado a ocorrência de *splicing* alternativo em *T. rubrum* em resposta a CASP, uma resposta pós-transcricional altamente relacionada ao estresse causado por drogas antifúngicas (Lopes *et al.*, 2022).

O combate as infecções fúngicas torna-se a cada dia um verdadeiro desafio. Aliado a toda essa problemática da resistência fúngica, poucas opções terapêuticas e alvos limitados, ainda existem os biofilmes. Estes são complexos de população celulares geralmente fixados a uma superfície, que contribuem para a resistência as drogas, principalmente por dificultarem a sua penetração. Essas estruturas complexas se manifestam na forma de uma matriz extracelular, caracterizada por heterogeneidade metabólica e genes relacionados à bomba de efluxo superexpressos (Pereira, 2021; Kaur and Nobile, 2023; Ramage *et al.*, 2023).

1.5 Biofilmes

Praticamente qualquer microrganismo é capaz de formar um biofilme (**Figura 5**). Essas estruturas podem ser caracterizadas como sendo uma coleção de organismos, como bactérias, fungos, vírus, protozoários e outros microrganismos (Mishra *et al.*, 2023). Biofilmes são tridimensionais e complexos, podem ser formados por uma comunidade de uma única espécie ou de várias espécies aderidas a superfícies abióticas ou tecidos vivos,

envolvidas em uma substância polissacarídica extracelular, a matriz extracelular, que fornece proteção (Pereira, 2021). Os biofilmes promovem a tolerância a altas concentrações de antifúngicos (Kaur and Nobile, 2023). Assim, para inibir biofilmes fúngicos são necessárias concentrações de antifúngicos muito maiores do que as concentrações inibitórias mínimas (CIMs) que normalmente inibem células planctônicas (Liu *et al.*, 2022).

Os biofilmes têm sido bem caracterizados em bactérias e leveduras como *Candida* ssp, no entanto, alguns trabalhos já vêm caracterizando biofilmes em fungos filamentosos (Diban *et al.*, 2023; Khari *et al.*, 2023; Markantonatou *et al.*, 2023). Biofilme de dermatófitos foi demonstrado pela primeira vez em cepas referência de *T. rubrum* e *T. mentagrophytes* (Costa-Orlandi *et al*., 2014).

Figura 5: Esquematização da formação, maturação e proliferação de biofilmes de fungos filamentosos. **Fonte:** Próprio autor 2023.

A formação de biofilme também já foi investigada em fragmentos de unha infectados por vários isolados dermatófitos: *T. rubrum*, *T. tonsurans*, *T. mentagrophytes*, *M. canis e M. gypseum* (Brilhante *et al*., 2017).

Para iniciar a formação de um biofilme o processo de adesão é primordial, por isso a células fúngicas acabam superexpressando proteínas essenciais como as adesinas, que aderem a um determinado substrato. Em um segundo momento, ocorre a proliferação dessas células, o aparecimento das hifas e por fim a formação da matriz extracelular (Pereira *et al.*, 2021; Markantonatou *et al.*, 2023).

Os biofilmes dificultam a penetração de antifúngicos, pois estruturalmente, constitui uma densa rede de mistura de formas morfológicas, células de levedura, hifas, pseudo-hifas e hifas vegetativas multinucleadas ramificadas interconectadas e possuem uma matriz extracelular bastante heterogênea, com um metabolismo extremamente dinâmico (Lohse *et al.*, 2018; Morelli *et al.*, 2021; Nett and Pohl, 2021).

A matriz de *A. fumigatus*, por exemplo, contém α-glucanas abundantes, que também estão entre os principais polissacarídeos da parede celular. Essa matriz também é composta principalmente por estruturas que medeiam o processo de resistência, como as proteínas de adesão, DNA extracelular, polióis, lipídios e exopolissacarídeos, incluindo galactomanana e galactosaminogalactana (Reichhardt *et al.*, 2019; Kowalski *et al.*, 2020).

Diante de todas essas estratégias que os fungos desenvolvem para resistir ao tratamento, como a degradação de drogas, superexpressão de genes, mutações em genes alvo, transportadores de múltiplas drogas e entre outros, a resistência torna-se uma problemática emergente para todas as infecções geradas por fungos, em especial pelos dermatófitos (Martinez-Rossi *et al.*, 2021). Dessa forma, o rastreamento e a identificação de compostos com atividade antifúngica são urgentemente necessários (Wang *et al.*, 2023).

1.6 SRT e combinações farmacológicas

SRT (**Figura 6**) é um antidepressivo muito usado contra vários transtornos psiquiátricos, sendo considerado um fármaco de primeira linha para o tratamento dessas alterações em todo o mundo (Szuhany and Simon, 2022). Em mamíferos esse antidepressivo inibe seletivamente a receptação da serotonina, bloqueando o transportador 5-hidroxitriptamina (5-HT) (Lochmann and Richardson, 2019). Além de seu uso como antidepressivo, o reposicionamento da SRT também tem sido bastante explorado em

promissoras terapias (Baú-Carneiro *et al.*, 2022; Kutkat *et al.*, 2022; Tseng *et al.*, 2022; Wang *et al.*, 2023).

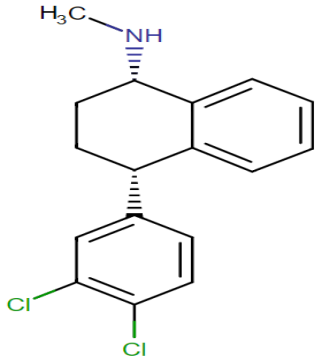

Figura 6: Estrutura molecular da sertralina (SRT). **Fonte:** Disponível em: https://go.drugbank.com/drugs/DB01104.

O reposicionamento de fármacos é uma alternativa bastante válida, principalmente para os tratamentos das infecções fúngicas (Martinez-Rossi *et al.*, 2018). A possibilidade de usar um medicamento existente no mercado contra uma outra enfermidade tem várias vantagens, como por exemplo, a toxicidade e a farmacocinética, já foram estabelecidas. Reposicionar um fármaco é ganhar tempo e diminuir os custos necessários para o desenvolvimento de uma nova formulação (Rossi *et al.*, 2021). E no contexto da resistência fúngica, é importante redirecionar drogas já existentes, não antifúngicas, mas com um potencial antifúngico, possibilitando descobertas importantes que gerem alternativas para o tratamento das infecções (Zhang *et al.*, 2021).

SRT tem sido explorada por suas propriedades antifúngicas (Katende *et al.*, 2019; Villanueva-Lozano *et al.*, 2019; Villanueva-Lozano *et al.*, 2020). O primeiro uso de SRT demonstrando sua capacidade de inibir fungos patogênicos foi em 2001, quando três pacientes com transtorno disfórico pré-menstrual e candidíase vulvovaginal recorrente (CVV) foram tratadas com SRT. Os sintomas clínicos de CVV desapareceram durante a terapia com SRT, e esse antidepressivo atuou como fungicida para todos os fungos testados: isolados de *C. albicans, Candida glabrata* e *Candida tropicalis* (Lass-Flörl *et al*., 2001).

Recentemente um trabalho relatou que a SRT induz a formação de gotículas lipídicas superdimensionadas em *C. neoformans*, *C. albicans*, *Saccharomyces cerevisiae* e *A.*

fumigatus (Breuer *et al*., 2022). SRT exibe atividade antifúngica contra a maioria dos isolados clínicos de *Cryptococcus in vitro* (Treviño-Rangel *et al.*, 2016; Boulware *et al.*, 2020). Além disso, contra essa levedura SRT apresenta uma peculiaridade, que auxilia na sua eficácia contra o fungo, ela penetra efetivamente na barreira hematoencefálica e se acumula em altas concentrações no sistema nervoso central, extremamente afetado em casos graves de criptococose (Nedahl *et al.*, 2018).

Contra as espécies do gênero *Candida*, vários trabalhos relatam a atividade de SRT contra biofilmes (Rodrigues *et al.*, 2023). SRT reduz o metabolismo do biofilme em *Candida krusei* e *Candida parapsilosis* e a biomassa do biofilme em *C. glabrata* (Oliveira *et al*., 2018). Contra *Candida auris*, um patógeno emergente nos últimos anos, a SRT demonstrou-se muito promissora, inibindo a conversão da levedura em hifas, a formação de biofilme, reduzindo a porcentagem de ergosterol e atuando diretamente na esterol 14 alfa demetilase, enzima envolvida na biossíntese do ergosterol (Gowri *et al.*, 2020).

De forma pioneira um estudo avaliou a atividade antifúngica da SRT contra *A. fumigatus* em um modelo alternativo usando *Galleria mellonella* e em um modelo murino de aspergilose pulmonar invasiva. Os resultados em conjunto, também indicaram a possível opção promissora de SRT para o tratamento adjuvante da aspergilose pulmonar (Treviño-Rangel *et al.*, 2019). Um trabalho do nosso grupo, também demonstrou o efeito da SRT em em *T. rubrum*. Nesse fungo, SRT afetou a sinalização celular e o metabolismo. Além disso, identificamos que SRT pode alterar a expressão de genes envolvidos na manutenção da parede celular fúngica e estabilidade da membrana plasmática (Galvão-Rocha *et al.*, 2023).

SRT então, representa uma alternativa no tratamento das infecções fúngicas. Ademais, para melhorar sua atividade, vários trabalhos sugerem a possibilidades de combinações da SRT com antifúngicos comerciais, o que representaria uma abordagem terapêutica promissora que aumentaria a eficácia terapêutica (Katende *et al.*, 2019). Essa abordagem vem sendo bastante utilizada, porque possibilita superar a resistência antifúngica, diminuir os efeitos tóxicos dos antifúngicos utilizados e aumentar a eficiência dos compostos testados, especialmente se os mecanismos de ação forem diferentes (Jafri and Ahmad, 2020; Jiang *et al.*, 2022; Rossato *et al.*, 2022).

Desde a descoberta do potencial antifúngico de SRT até o cenário atual, alguns trabalhos foram realizados para mostrar interações sinérgicas entre SRT e outros compostos.

Interações sinérgicas entre SRT e micafungina ou voriconazol foram obtidas contra isolados clínicos de *C. auris* (Alanís-Ríos *et al*., 2022). Ensaios com *C. neoformans* evidenciaram a atividade antifúngica da SRT, seja em monoterapia ou em combinação sinérgica com fluconazol (Breuer *et al.*, 2022). Além disso, SRT exibiu efeitos sinérgicos com CASP contra células planctônicas de *Trichosporon asahii* (Cong *et al.*, 2016).

A combinação de SRT e anfotericina B apresentou sinergismo contra a neurocriptococose (Rossato *et al.*, 2016). Combinações de fluconazol com SRT mostraram efeito sinérgico promissor contra cepas resistentes de *C. glabrata* (Alkhalifa *et al.*, 2022). SRT e paroxetina também foram sinérgicos contra seis isolados de *Candia ssp* (Tekintaş *et al*., 2020). Assim, SRT sozinha, ou em combinação com alguns antifúngicos, apresenta-se como uma abordagem promissora para minimizar a resistência e reduzir a virulência.

Justificativa e Hipótese

2. Justificativa

T. rubrum é o dermatófito predominante nos casos de dermatofitoses em todo mundo, inclusive no Brasil (Martinez-Rossi *et al.*, 2021; Mularoni *et al.*, 2022; Yun *et al.*, 2022). A grande problemática no tratamento das infecções causadas por este dermatófito é a resistência e a cronicidade (Branco *et al.*, 2023). Neste fungo, responder adequadamente às mudanças ambientais é necessário para sobreviver ao estresse celular, como aqueles causados pela exposição a fármacos e neste sentido ele desenvolve diversos mecanismos de adaptação com circuitos complexos incluindo a interação entre moléculas de sinalização (Monod *et al.*, 2019; Martinez-Rossi *et al.*, 2021).

Em *T. rubrum*, os mecanismos moleculares relacionados com a resposta ao estresse, a tolerância ou resistência, são pouco conhecidos (Martinez-Rossi *et al.*, 2018). Traçar o perfil de expressão de genes, fornece conhecimento para o desenvolvimento de novos fármacos e auxilia na compreensão dos processos envolvidos na resposta a um medicamento (Galvão-Rocha *et al.*, 2023). Encontrar novos compostos com atividade antifúngica e novos alvos moleculares torna-se necessário e, neste sentido o reposicionamento de fármacos e combinações sinérgicas com antifúngicos clássicos revela-se como uma estratégia promissora (An *et al.*, 2023; Andriani *et al.*, 2023).

Nessa perspectiva, investigar uma interação sinérgica entre SRT e CASP em um dermatófito é uma abordagem bastante válida. Um trabalho pioneiro demonstrou o efeito de SRT associada a CASP contra uma levedura, o patógeno *Trichosporon asahi* (Cong *et al.*, 2016). Recentemente, outros trabalhos identificaram que CASP tem sua atividade antifúngica potencializada quando associada a fluconazol, posiconazol, anfotericina B, terbinafina e nicomicina Z, contra espécies do gênero *Candida* (Caballero *et al.*, 2021; Su *et al.*, 2022). Entretanto, a atividade de SRT e CASP contra dermatófitos ainda não estão bem definidas.

3. Hipótese

A combinação sinérgica de SRT com outros antifúngicos tradicionais constitui uma estratégia terapêutica contra *T. rubrum* e pode minimizar a ocorrência de mecanismos associados a resistência e adaptação.

Objetivos e Estratégias

4. Objetivos

O objetivo deste estudo foi avaliar a atividade antifúngica do antidepressivo sertralina (SRT), isoladamente ou em combinação com a caspofungina (CASP) contra *T. rubrum*.

5. Estratégias

✓ Determinar as concentrações inibitórias mínimas (CIM) de CASP e SRT, contra *T. rubrum* CBS 118892.

✓ Analisar a ocorrência de sinergismo entre SRT e CASP contra *T. rubrum*.

✓ A partir de um RNA-seq validado, identificar genes envolvidos na resistência e adaptação de *T. rubrum* a SRT.

✓ Quantificar a expressão gênica por RT-qPCR de genes relacionados aos mecanismos de resistência e de adaptação de *T. rubrum*, após o tratamento com a SRT, CASP e combinação de SRT com CASP.

✓ Verificar a formação do biofilme de *T. rubrum in vitro* e em fragmentos de unha.

✓ Quantificar a atividade metabólica e a biomassa do biofilme de *T. rubrum*, após o tratamento com SRT, CASP ou combinação de SRT e CASP.

Material e Métodos

6. Material e Métodos

6.1 Meios de cultivo: Extrato de malte (MEA), Sabouraud (SB) e RPMI-1640

O MEA foi preparado utilizando 20 g de extrato de malte (Becton Dickinson, Franklin Lakes, NJ, EUA), 20 g de glicose (Becton Dickinson) e 1 g de peptona (Becton Dickinson) dissolvidos em 900 mL de água destilada (qsp). Após esse procedimento, o pH do meio foi ajustado para 5,7 e o volume final para 1000 mL. Após isso, acrecentou-se 20 g de ágar na solução, que então foi autoclavada a 1 atm de pressão a 120 ºC. Para preparar o meio SB, foi utilizado 20 g de glicose (Becton Dickinson) e 10 g de peptona (Becton Dickinson). Esses componentes foram então adicionados em 900 mL de água destilada (qsp) e o pH ajustado para 5,7. O volume final da solução foi ajustada para 1000 mL. Em seguida, o SB foi autoclavado a 1 atm de pressão a 120 ºC. O meio RPMI foi preparado dissolvendo 10,4 g do meio RPMI-1640 (Sigma-Aldrich, St Louis, MO, EUA) em 900 mL de água destilada. Após isso, o meio foi tamponado com ácido morfolinopropanossulfônico (MOPS) 0,165 M (Sigma-Aldrich), o pH ajustado para 7,0 e adicionado água destilada (qsp) para completar um volume final de 1000 mL. O meio foi então esterilizado utilizando um sistema de filtração com membrana de náilon de 22 µm (Sigma-Aldrich) e estocado a 4 °C. Para o ajuste do pH no preparo dos meios, foi utilizado hidróxido de sódio 1 M. A composição do meio RPMI é mostrada na tabela 1.

Tabela 1: Composição do meio RPMI – 1640.

Componentes	Concentração (mg/L)	Componentes	Concentração (mg/L)
L-Ácido aspártico	20	Ácido para-aminobenzóico	1
L-Ácido glutâmico	20	Biótina	0,2
L-Arginina	200	Cloreto de colina	3
L-Asparagina	50	i-Inositol	35
L-Cisteína 2 HCL	65	Niacinamida	1

L-Fenilamina	15	D-Pantotenato de cálcio	0,25
Glicina	10	Piridoxina HCL	1
L-Glutamina	300	Riboflavina	0,2
L-Hidroxiprolina	20	Tiamina HCL	1
L-Histidina	15	Vitamina B12	0,005
L-Isoleucina	50	Nitrato de cálcio	100
L-Leucina	50	Sulfato de magnésio	48,84
L-Lisina HCL	40	Cloreto de potássio	400
L-Metionina	15	Cloreto de sódio	6000
L-Prolina	20	Fosfato de sódio dibásico	800
L-Serina	30	D-Glicose (Dextrose)	2000
L-Treonina	20	Glutationa	1
L-Triptofano	5	Vermelho de fenol	5
L-Tirosina 2Na	29		
L-Valina	20		
Ácido Fólico	1		

6.2 Linhagem e condições de cultivo

A cepa de *T. rubrum*, CBS118892 (Westerdijk Fungal Biodiversity Institute, Utrecht, Holanda), obtida de um paciente com onicomicose, foi cultivada em ágar extrato de malte por 35 dias a 28 °C, conforme descrito anteriormente (Peres *et al.*, 2016), para extração de RNA total. A suspensão fúngica foi preparada em NaCl 0,9% e a concentração de conídios foi estimada usando uma câmara de Newbauer. Aproximadamente 1×10^6 conídios foram adicionados a 100 mL de Sabouraud líquido (SB) seguido de incubação a 28 °C por 96 h sob agitação contínua. Os micélios resultantes foram então transferidos para 100 mL de SB na

presença de uma dose subletal (70 mg/L) de SRT (Cayman Chemical, Ann Arbor, MI, EUA) para os experimentos de RNAseq. Para avaliar o efeito da combinação de SRT + CASP na expressão gênica, *T. rubrum* também foi cultivado na presença de uma combinação subletal de 0,273 mg/L SRT + 10,93 mg/L CASP (Merck Sharp & Dohme, São Paulo, SP, Brasil) e na presença desses valores de combinação separados, 0,273 mg/L SRT (SRTcs) e 10,93 mg/L CASP (CASPcs). O controle para todos os experimentos foi usado o fungo cultivado na ausência de drogas. Os cultivos foram incubados a 28 °C com agitação continua a 120 rpm por 3 h e 12 h.

6.3 Concentração Inibitória Mínima (CIM)

As CIMs foram obtidas de acordo com o método de referência M38-A recomendado pelo Clinical and Laboratory Standards Institute (CLSI), com as seguintes modificações: 100 μL da suspensão de conídios, totalizando 6×10^4 conídios/mL, estimado usando uma câmara de Newbauer, foram adicionados a cada poço na placa de microtitulação de 96 poços. A concentração final de conídios foi ajustada para aproximadamente 3×10^4 conídios por poço em meio RPMI 1640 ou meio SB. SRT e CASP foram preparadas como soluções estoque em dimetilsulfóxido (DMSO, Sigma-Aldrich): SRT (50.000 mg/L) e CASP (10.000 mg/L). Após isso, foi preparada uma diluição de SRT a 5.000 mg/L e CASP a 1000 mg/L afim de reduzir a concentração final do DMSO, previnindo sua possível interferência nos experimentos.

Diluições seriadas de SRT e CASP foram realizadas em meio RPMI, tamponado com ácido morfolinapropanossulfônico (MOPS) 0,165 M ou meio SB. As concentrações finais de SRT variaram entre 0,78–200 mg/L, enquanto as de CASP variaram entre 0,98–250 mg/L. As placas de ensaios que foram usadas para determinar as CIMs foram incubadas a 28 °C por sete dias. Os controles de crescimento foram realizados em poços contendo apenas a suspensão fúngica. Outro controle foi realizado em poços contendo apenas a suspensão fúngica e DMSO na concentração de 4%. As CIMs foram definidas por comparação com controles de crescimento realizados em poços contendo apenas suspensão fúngica e meio, com inibição completa do crescimento. Todos os experimentos foram realizados em triplicata biológicas e técnicas.

6.4 Interação entre SRT e CASP

As interações entre SRT e CASP foram avaliadas usando o método *chequerboard* de microdiluição em caldo (CLSI). Esse método fornece uma matriz em "xadrez" que permite uma interação de todas as concentrações testadas de SRT e CASP, possibilitanto analisar diversas combinações, para classificá-las como sinérgicas ou não (**Figura 7**). Algumas modificações foram realizadas. A partir das soluções de 5.000 mg/L de SRT e 1000 mg/L de CASP foram realizadas diluições seriadas em meio RPMI, tamponado com ácido morfolinapropanossulfônico (MOPS) 0,165 M ou meio SB. As concentrações finais de SRT variaram entre 0,78–200 mg/L, enquanto as de CASP variaram entre 0,98–250 mg/L. As interações entre SRT e CASP foram quantificadas usando o índice de concentração inibitória fracionada (ICIF), obtido a partir da fórmula: ICIF = (*Sc* / *S*) + (*Cc* / *C*), onde *Sc* é a CIM de SRT combinada, *S* é a CIM da SRT obtida individualmente, *Cc* é a CIM da CASP combinada e *C* é a CIM da CASP obtida individualmente. As interações com ICIF $\leq$ 0,5, foram categorizadas como sinérgicas, com ICIF > 0,5 a $\leq$ 4,0 como indiferentes e ICIF > 4,0 foram categorizadas como antagônicas (Gómez-López *et al.*, 2003).

Os ICIFs foram calculados para todas as combinações possíveis de diferentes concentrações. Os resultados foram expressos como média de ICIFs. As placas de ensaios que foram usadas para determinar os ICIFs foram incubadas a 28 °C por sete dias. Conforme descrito para o cálculo dos CIMs, os controles de crescimento foram realizados em poços contendo apenas a suspensão fúngica e o meio e em poços contendo a suspensão fúngica e DMSO na concentração de 4%. As CIMs combinadas foram definidas por comparação com controles de crescimento realizados em poços contendo apenas suspensão fúngica e meio, com inibição completa do crescimento. Todos os experimentos foram realizados em triplicatas biológicas e técnicas.

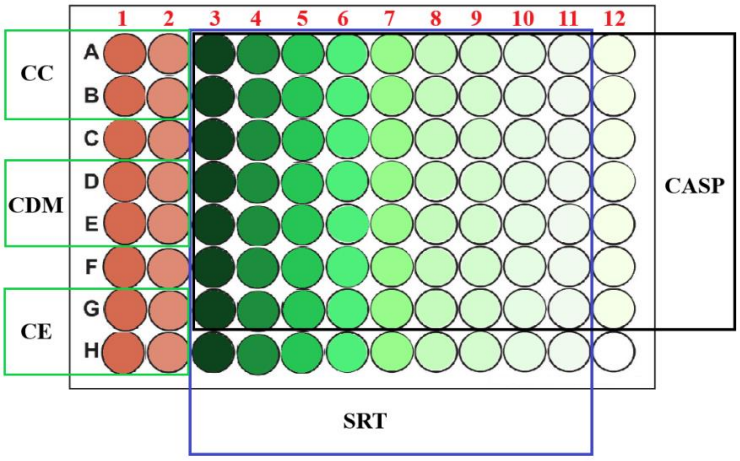

Figura 7: Esquema da representação da microdiluição em xadrez para a obtenção das CIMs combinadas e dos ICIFs. As concentrações testadas para SRT foram colocadas nas colunas de 3 a 11 e as concentrações testadas para CASP foram colocadas nas linhas de A a G. A coluna 12 e a linha H foram usadas para obtenção da CIM de CASP e SRT, respectivamente. As concentrações foram dispostas em ordem decrescente. CC é controle de crescimento, CDM é controle do DMSO e CE controle de esterilidade. Os poços da linha C, das colunas 1 e 2 e da linha F, das colunas 1 e 2, não foram utilizados no experimento. **Fonte:** Próprio autor 2023.

6.5 Extração total de RNA

O RNA total foi extraído de *T. rubrum*, cultivado na presença de SRT sozinha, CASP sozinha e SRT combinada com CASP, usando um kit de mini-isolamento Illustra RNAspin (GE Healthcare, Chicago, IL, EUA), com algumas adaptações. Os micélios foram macerados por meio de pulverização mecânica usando um almofariz e pilão em nitrogênio líquido até obter uma massa de micélio de aproximadamente 30 mg. O RNA foi extraido da massa resultante acrescentando 350 µL de solução de lise. Acrescentou-se então 3,5 µL de β-mercaptoetanol (Sigma-Aldrich) em cada amostra, levou-se ao vórtex por 10 s. O conteúdo foi transferido cuidadosamente para o sistema de filtração do kit (coluna roxa) e centrifugou-se as amostras a 11.000 × g por 1 minutos a 4 ºC. Em seguida adicionou-se 350 µL de etanol (70%) gelado e o conteúdo foi levado ao vórtex novamente por duas vezes durante 5 s. Posteriormente o sobrenadante foi transferido para outro sistema de filtração do kit (coluna azul) e centrifugado a 8.000 × g por 30 s. O tubo coletor foi trocado e a coluna transferida para outro tubo. Acrescentou-se 350 µL de tampão dessalinizador (*Desalting buffer*) e centrifugou-se a 11.000 × g por 1 minuto. Descartou-se o sobrenadante e acrescentou-se 95

µL de DNase I livre de RNase (Sigma-Aldrich) previamente preparada com tampão do kit (10 µL + 90 µL de DNase *Reaction Buffer*), no centro da coluna de filtração.

O conteúdo foi deixado por 15 minutos em temperatura ambiente. Após isso, foi realizada uma lavagem com um tampão do kit (*Wash Buffer I*) e uma centrifugação a 11.000 × g por 1 minuto. Novamente uma lavagem foi realizada com outro tampão do kit (*Wash Buffer II*) e em seguida centrifugou-se a 11.000 × g por 2 miuntos. Descartou-se o eluído e manteve-se a coluna. A coluna de centrifugação foi transferida para um tubo do kit e adicionado 40 µL de água deionizada livre de RNase. O conteúdo foi centrifugado a 11.000 × g por 1 minuto. Descartou-se a coluna e o tubo com RNA foi utilizado na etapa seguinte. As amostra foram estocadas a -80 ºC para sua utilização posteriormente.

6.6 Qualidade e integridade do RNA

Após a extração, a concentração de RNA foi determinada por um NanoDrop. Com o intuito de verificar se o RNA extraído se encontrava livre de DNA contaminante, foi realizada uma reação de PCR seguida por eletroforese em gel de agarose 1,5 % (m/v), utilizando oligonucleotídeos que flanqueiam o gene que codifica a β-tubulina. O DNA genômico de *T. rubrum* foi utilizado como um controle de amplificação. Para certificação da qualidade e integridade das amostras, também foi realizada uma eletroforese microfluída e o resultado analizado em um bionalizador. Nesse equipamento, o resultado da quantificação da fluorescência é determinada por um índice denominado RIN (Integridade do RNA). O RIN é classificado em uma escala de 1 a 10 e quanto maior o valor maior a qualidade e integridade do RNA. As amostras que apresentaram RIN superiores a 7.0, foram classificadas como ideais para o uso.

6.7 RNA-seq e análise de dados

Uma alíquota de RNA de três réplicas biológicas independentes em cada ponto de tempo (3 e 12 h) de *T. rubrum* cultivado em 70% da CIM de SRT foi usada para realizar o sequenciamento em um sequenciador HiSeq 2000 (Illumina, San Diego, CA, EUA). Após obtenção dos dados brutos as sequências de baixa qualidade foram retiradas utilizando a

ferramenta *FastQC*. O Trimmomatic foi aplicado para remover adaptadores e outras sequências específicas do Illumina (Bolger *et al.*, 2014). Em seguida, leituras de extremidades pareadas e trimadas foram alinhadas ao genoma de referência de *T. rubrum* (ftp://ftp.broadinstitute.org/pub/annotation/fungi) usando o alinhador STAR (Dobin *et al.*, 2013) e inspecionado com o software Visualizador de Genômica Integrativa (IGV) (Thorvaldsdóttir *et al.*, 2013). A análise de expressão diferencial foi realizada utilizando o pacote DESeq do Bioconductor e manipulado no ambiente estatístico R (Love *et al.*, 2014). O valor P ajustado de Benjamin-Hochberg foi definido como 0,05 (Benjamini and Hochberg, 1995), e um corte de ± 1,5 log2 foi definido para revelar diferenças de expressão estatisticamente significativas. A categorização funcional foi realizada usando os termos do Gene Ontology (GO) atribuídos pelo algaritmo Blast2GO. As categorias altamente representadas foram determinadas pela análise de enriquecimento usando o algoritmo BayGO (Vêncio *et al.*, 2006).

6.8 Síntese de DNA complementar (cDNA)

Após a verificação de ausência de contaminação, as amostras de RNA foram submetidas à síntese de DNA complementar (cDNA). O cDNA foi sintetizado a partir de cada condição usando 1 µL de RNA total a 1000 ng em um volume de reação de 20 mL, com um kit de síntese de cDNA de alta capacidade (Applied Biosystems, Waltham, MA, EUA) de acordo com o protocolo estabelecido pelo fabricante. Após a conversão as amostras de cDNA foram confirmadas por gel de agarose 1,5 % (m/v). As amostras foram estocadas a -80 ºC. Quantidades iguais de RNA de três réplicas biológicas independentes foram usadas para sintetizar o cDNA.

6.9 Análise RT-qPCR

A expressão gênica foi quantificada via qPCR usando um sistema StepOnePlus Real-Time PCR (Applied Biosystems). Um grupo de genes foi selecionado para estender a análise da expressão gênica ao crescimento de *T. rubrum* na presença de combinações de SRT com CASP. Para essa análise e para efeito de comparação, o nível de expressão também foi

quantificado na presença de SRT sozinha. As reações de PCR foram realizadas com pares de primers específicos projetados usando o software Prime3Plus (https://www.bioinformatics.nl/cgi-bin/primer3plus/primer3plus.cgi (acessado em 4 de julho de 2022)) e especificidade (**Tabela 2**). Para exclusão de produtos inespecíficos da reação uma curva de dissociação foi realizada com diferentes concentrações de cDNA (600 ng, 300 ng, 150 ng, 75 ng e 37,5 ng). Também foram estabelecidas as concentrações para cada *primer*. Para isso, fixou-se a concentração de cDNA em 70 ng e variou-se as concentrações dos primers em 600 nM, 400 nM, 300 nM, 200 nM e 100 nM. Em seguida foi realizada a qPCR, usando um volume final de 12,5 µL: 0,125, 0,25 ou 0,375 µL de primers (dependendo da concentração do primer), 6,25 µL SYBR Green PCR Master Mix (Applied Biosystem, Waltham, MA, EUA) 1 µL de cDNA a 70 ng e o volume final ajustado com água ultrapura (qsp). As condições do termociclador para RT-qPCR foram as seguintes: 95 °C por 10 minutos, seguido de 40 ciclos de 95°C por 15 segundos e 60°C por 1 minuto. Selecionamos genes que codificam as enzimas gliceraldeído 3 fosfato desidrogenase (*gapdh*) e RNA polimerase II dependente de DNA (*rpb2*) como controles endógenos. Os dados foram derivados de três réplicas independentes, e o método $2^{-\Delta\Delta ct}$ foi usado para avaliar a quantificação relativa de genes responsivos (Livak and Schmittgen, 2001).

Tabela 2: Conjuntos de primers usados para reação em cadeia da polimerase em tempo real (RT-qPCR).

Proteína/gene	ID	Sequência dos Primers (5´- 3´)	Eficiência (%)	Concentração (nM)
C-8 Esterol isomerase	TERG_06755	Fwd: GGTGGGCTTTAGAGTTAG Rev: GCAGTCAAGTAGCAAGTC	110	200
Hidrofobina	TERG_04234	Fwd: GGCATACATCTTGGTGGTTTC Rev: CAGACAGTGGAGGTGGATGTT	103	300
MFS transportador multidroga	TERG_00162	Fwd: CTCCTTTGGACCTTTGATCG Rev: TGACGAAGAGAACGTTGCAG	102	100
Quitina sintase2	TERG_12319	Fwd: AGCCAACTGCCTTGTACCAT Rev: GTAATCCGACCCATCCCTTT	103.5	200
rpb II	TERG_05742	Fwd: TGCAGGAGCTGGTGGAAGA Rev: GCTGGGAGGTACTGTTTGATCAA	94.99	300
gapdh	TERG_04402	Fwd: GCGTGACCCAGCCAACA Rev: CGGTGGACTCGACGATGTAGT	99.90	200

6.10 Formação de biofilme *in vitro*

Os biofilmes de *T. rubrum* foram formados de acordo com método previamente descrito (Costa-Orlandi *et al.*, 2014), com algumas modificações. *T. rubrum* CBS118892 foi cultivado em ágar de extrato de malte por 15 dias a 28 °C. A suspensão fúngica foi preparada em NaCl 0,9% e a concentração de conídios foi ajustada para aproximadamente 1×10^6 conídios/mL. As placas foram inicialmente incubadas a 37 °C por 4 h sem agitação para pré-adesão.

6.11 Quantificação da atividade metabólica do biofilme por ensaio de MTT

O ensaio de MTT (Sigma-Aldrich) é baseado na capacidade de conversão do composto MTT (brometo de 3-(4,5-dimetiltiazol-2-il)-2,5-difeniltetrazólio) solúvel em água em um produto insolúvel (cristal de formazan). Para tanto, o MTT foi preparado na ausência de luz, em uma solução estoque de 50.000 mg/mL e em seguida foi diluido em solução salina esterilizada NaCl 0,9% para a concentração de uso. Tanto a solução estoque quanto a solução de uso foram mantidas a 4 ºC. Após a pré-adesão, os tratamentos consistindo em 200 µL cada de SRT (12,5 mg/L e 3,12 mg/L), CASP (15,62 mg/L e 1,95 mg/L) e SRT + CASP (3,12 mg/L + 1,95 mg/L respectivamente) preparados em meio RPMI 1640, suplementado com 2% de glicose, foram adicionados aos poços contendo os conídios aderidos. Os biofilmes foram preparados em diferentes tempos (0, 24, 48, 72 e 96 h). Após cada incubação, 2 µL de menadiona (Sigma-Aldrich) e 20 µL de MTT (Sigma-Aldrich) a 5.000 mg/L foram adicionados a cada poço. As placas foram incubadas a 37 °C por 4 horas. As alterações colorimétricas foram medidas usando um leitor de ELISA (Thermo Fisher Scientific, Waltham, MA, EUA) a 550 nm. Um controle foi preparado adicionando 200 µL de suspensão de conídios não tratados em cada poço. Todos os experimentos foram realizados em triplicatas biológicas e técnicas.

6.12 Quantificação da biomassa do biofilme *in vitro* por cristal violeta

Após a pré-adesão, o sobrenadante foi removido dos poços e lavado três vezes com solução salina esterilizada 0,9% e em seguida 200 µL de meio RPMI 1640 suplementado com 2% de glicose foram adicionados a cada poço. Três réplicas biológicas independentes, cada uma com 3 repetições, foram incubadas a 37 °C por 72 h para a maturação do biofilme. Após a formação do biofilme, o meio de cultura foi removido e os poços foram lavados novamente por três vezes com solução salina esterilizada 0,9%. Os tratamentos compreendendo 200 µL cada um de SRT 25 mg/L, SRT 6,25 mg/L, CASP 62,50 mg/L, CASP 1,95 mg/L e SRT 6,25 mg/L + CASP 1,95 mg/ L foram adicionados aos poços. Os tratamentos foram preparados em meio RPMI 1640 suplementado com 2% de glicose.

As réplicas foram incubadas a 37 °C por 3 e 7 dias. Em seguida, as drogas foram removidas e cada poço foi lavado três vezes com PBS 0,01 M (pH 7,2), em seguida 100 µL de solução de cristal violeta (0,5 %) foi adicionada a cada poço para quantificar a biomassa. Então, cada poço foi lavado duas vezes com água esterilizada, tratado com 100 µL de etanol 95% e cuidadosamente homogeneizado. A solução resultante foi transferida para uma nova placa de 96 poços e o valor da absorbância foi obtido usando um leitor de ELISA em um comprimento de onda de 550 nm. Poços contendo 200 µL de suspensão de conídios não tratados foram utilizados como controle.

6.13 Avaliação de biofilmes em unhas humanas

O ensaio de infecção em unha humana foi realizado conforme descrito anteriormente (Costa-Orlandi *et al.*, 2014; Ferreira-Nozawa *et al* 2006), com algumas modificações. As unhas humanas, obtidas de doadores saudáveis foram inicialmente cortados em fragmentos de 1 mm^2 e esterilizados em autoclave a 1 atm de pressão a 120 ºC. Esses fragmentos foram transferidos para placas de 24 poços contendo ágar-água (20 g de ágar em 1000 mL de água). Os fragmentos foram infectados com 2 mL de um suspensão fúngica de *T. rubrum* preparada em solução salina esterilizada 0,9% (NaCl), a uma concentração de conídios ajustada para aproximadamente 3×10^4 conídios por poço. Essa fase inicial foi caracterizada como o estágio de pré-adesão dos conídios aos fragmentos de unhas. Após 4 h de pré-adesão a 37 °C, a suspensão foi removida cuidadosamente e cada poço foi lavado três vezes com solução salina esterilizada 0,9%. Em seguida, 2 mL de solução salina esterilizada 0,9% foram

adicionados a cada poço. Após isso, as placas foram incubadas por 20 dias a 28 °C. Depois desse tempo, 2 mL de tratamentos com SRT 50 mg/L, SRT 12,5 mg/L, CASP 62,50 mg/L, CASP 3,90 mg/L e SRT 12,5 mg/L + CASP 3,90 mg/L preparados em solução salina esterilizada a 0,9% foram adicionados em cada poço diariamente, durante sete dias. Após sete dias, os fragmentos de unha foram retirados dos poços cuidadosamente e devidamente tratados para os biofilmes serem analisados por microscopia eletrônica de varredura. O ensaio foi conduzido de acordo com o Comitê de Ética da Faculdade de Medicina e aprovado pelo protocolo número 4.304.317/2020.

6.14 Microscopia eletrônica de varredura

As amostras foram inicialmente fixadas com glutaraldeído 3% em tampão fosfato 0,1% (v/ v) (pH 7,2) a 4 °C por 24 h e lavadas com tampão fosfato 0,1% (pH 7,2). O tetróxido de ósmio (1%) foi utilizado na etapa de pós-fixação. Posteriormente, as amostras foram desidratadas em gradiente crescente de etanol envolvendo banhos sucessivos de concentrações crescentes de etanol. As amostras foram então revestidas com spray de ouro para visualizar os biofilmes formados nas unhas humanas. Um microscópio eletrônico de varredura JEOL JSM-6610 LV a uma voltagem de aceleração de 25 kV foi usado para visualização.

6.15 Análise Estatística

A expressão gênica foi calculada usando o método comparativo $2^{-\Delta\Delta CT}$. O *teste t* de Student pareado foi usado para comparar a expressão gênica entre as condições de tratamento e controle em cada tempo. Os resultados foram relatados como a média ± desvio padrão de três réplicas biológicas independentes. Para comparação da atividade metabólica do biofilme e quantificação da biomassa, foi utilizada a ANOVA one-way, seguida do teste *post hoc* de Tukey. Para todos os testes, a significância estatística foi adotada em $p < 0,05$. Prism v. 5.1 (GraphPad Software, San Diego, CA, EUA) foi usado para gerar os gráficos e as análises estatísticas.

Resultados

7. Resultados

7.1 Suscetibilidade antifúngica e interação entre SRT e CASP

SRT sozinha ou em combinação com CASP exibiu atividade antifúngica contra células planctônicas de *T. rubrum*. A CIM da SRT necessária para inibir *T. rubrum* em meio RPMI foi de 25 mg/L, enquanto a da CASP foi de 31,25 mg/L. As CIMs de SRT e CASP aumentaram consideravelmente quando o ensaio foi realizado no meio SB. Nesse meio, a SRT apresentou CIM de 100 mg/L, enquanto a CASP apresentou CIM de 62,50 mg/L. As interações entre SRT/CASP em ambos os meios de cultura (RPMI ou SB) podem ser consideradas sinérgicas (ICIF ≤ 0,5). Os ensaios realizados em ambos os meios indicaram que os ICIFs correspondentes à combinação SRT/CASP variaram entre 0,1–0,5. Os ICIFs médios no meio RPMI e SB foram 0,28 e 0,25, respectivamente (**Tabela 3**). Os valores das CIMs combinadas que resultaram em uma interação sinérgica entre SRT e CASP são exibidos (**Tabela 4**).

Tabela 3: CIMs de sertralina (SRT) e caspofungina (CASP) contra formas planctônicas de *T. rubrum*. ICIF e a média do ICIF das interações entre SRT e CASP.

Meio	CIM_{100} - mg/L		Variação do ICIF	ICIF (média)
	SRT	CASP	SRT/CASP	SRT/CASP
SB	100	62.50	0.1 - 0.50	0.25
RPMI	25	31.25	0.1 - 0.50	0.28

ICIF ≤ 0,5, ICIF > 0,5 a ≤4,0 e ICIF > 4,0 foram categorizados como sinergismo, indiferença e antagonismo, respectivamente.

Tabela 4: Valores MICcb (MICs combinados) para análise de sinergismo entre sertralina (SRT) e caspofungina (CASP) em ensaios realizados em meio RPMI e meio Sabouraud (SB).

Meio	Antifúngico	Concentrações de SRT (mg/L)								
		200	100	50	25	12.5	6.25	3.12	1.56	0.78
SB	CASP (mg/L)	0	0	1.95	1.95	1.95	1.95	7.81	15.62	15.62
RPMI		0	0	0	0	0.98	0.98	1.95	1.95	3,90

7.2 Qualidade das amostras de RNA

As amostras obtidas nas nossas extrações foram consideradas de excelente qualidade. As amostras apresentaram um RIN variando entre 8,3 e 10, sendo que apenas uma amostra apresentou RIN menor que 8 (**Figura 8**). Essa amostra apresentou um RIN igual a 7,90. Ainda assim foi utilizada, porque apresentava uma qualidade próxima de excelente. Além disso, essas amostras estavam puras sem presença de DNA contaminante.

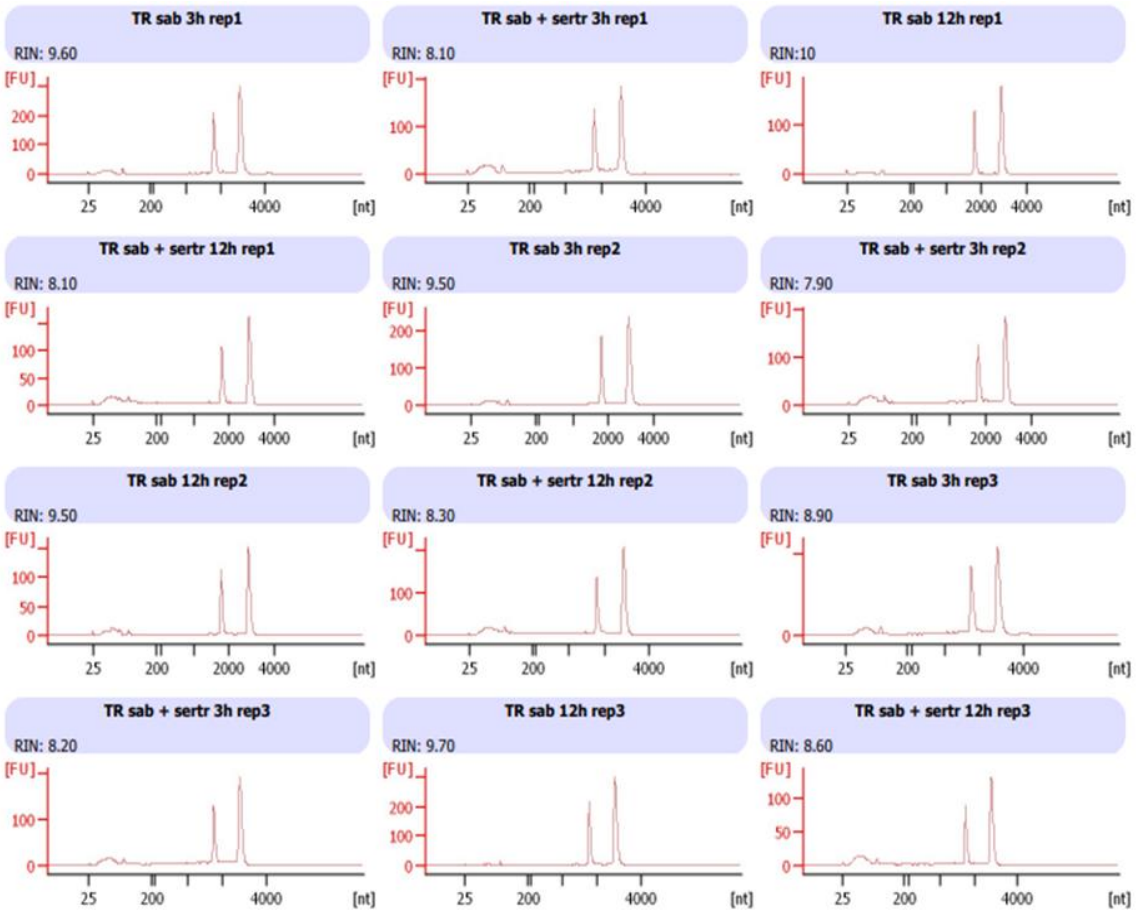

Figura 8: Qualidade e integridade das réplicas biológicas (**rep**) das amostras de RNA extraído. Amostras de *T. rubrum* (**TR**) em 3 h e 12 h, cultivadas na presença (**TR sab + sertr**) ou ausência de SRT (**TR sab**). No eixo "y" é representada a intensidade de fluorescência e no eixo "x" o número de nucleotídeos.

7.3 Modulação da expressão gênica em resposta a SRT

O RNA-seq de *T. rubrum* após o tratamento com uma dose subinibitória de SRT foi considerado de alto rendimento, produzindo mais de 500 milhões de sequências *paired-end*

de leituras de alta qualidade, correspondendo a seis bibliotecas. A comparação com os genes anotados no genoma de *T. rubrum*, disponível no Broad Institute, revelou leituras alinhadas de cerca de 99,54% para bibliotecas de 3 h e 99,57% para bibliotecas de 12 h. Além disso, dos 8.616 genes anotados no genoma de *T. rubrum*, 8.585 genes apresentaram pelo menos 1 read mapeado ao longo de sua sequência (99,64%).

Para quantificar os níveis de expressão de genes, diferentes pontos de tempo foram comparados aos pares na razão log2 da contagem de leitura em cada ponto de tempo versus o valor mediano normalizado da contagem de leitura para cada gene. Um limite de corte de -1,5 e 1,5 log2-expressão relativa, que corresponde a pelo menos 2,8 vezes de expressão relativa, foi usado para minimizar a ocorrência de falsos positivos devido a genes com baixa expressão. Além disso, um limite de significância estatística de $P < 0,05$ foi usado para definir transcritos regulados positiva ou negativamente. No total, 541 genes foram modulados em resposta a SRT em 3 h vs SB (controle) e 1.569 genes foram modulados em resposta a SRT em 12 h vs. SB (controle). Em resposta a SRT 3 h vs. SB (controle), 452 genes foram regulados positivamente e 89 genes foram regulados negativamente. Além disso, 768 genes foram regulados positivamente em resposta a SRT em 12 h vs. SB (controle) e 801 genes foram regulados negativamente em resposta a SRT em 12 h vs. SB (controle). Independentemente do tempo, 372 genes foram modulados em resposta a SRT (interseção), e todos os genes modulados estão representados (**Figura 9**).

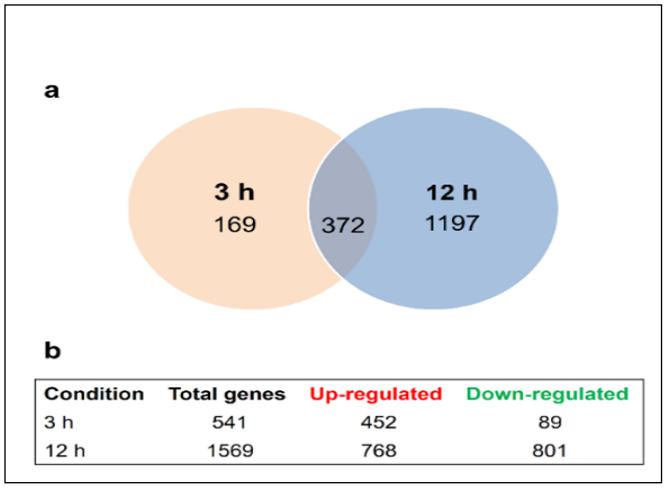

Condition	Total genes	Up-regulated	Down-regulated
3 h	541	452	89
12 h	1569	768	801

Figura 9: Distribuição dependente do tempo de genes diferencialmente expressos em *T. rubrum* após exposição a SRT. (**A**) Diagrama de Venn mostrando expressão diferencial entre SRT e controle (ausência de droga). (**B**) Genes regulados negativamente (*down-regulated*) e genes regulados positivamente (*up-regulated*) em 3 h e 12 h.

Esse transcriptoma de *T. rubrum* revelou vários genes associados à resistência a drogas e mecanismos adaptativos. Mais de 40 genes que codificam transportadores da superfamília facilitadora principal (MFS) foram modulados em resposta à exposição a SRT em 3 horas e 12 horas. Apenas 4 genes dessa família foram regulados positivamente em 3 h (TERG_07040, TERG_04764, TERG_08336 e TERG_04765). A maioria dos transportadores contendo o domínio MFS foram regulados negativamente em 12 h, como os transportadores TERG_12504, TERG_11600 e TERG_05342. Neste mesmo tempo, vários transportadores foram regulados positivamente, como os transportadores TERG_05429, TERG_02265, TERG_05575 e TERG_00776. A SRT também reprimiu dois genes que codificam o transportador de membrana do tipo superfamília e de ligação com ATP (ABC) (TERG_08130 e TERG_12194). Em contraste, induziu os genes transportadores do tipo (ABC) TERG_08613, TERG_05126, TERG_00286, TERG_08751, TERG_00402 e TERG_04224. Entre as proteínas multirresistentes moduladas no transcriptoma de *T. rubrum*, três foram reguladas negativamente (TERG_07539, TERG_12373 e TERG_12372) e uma foi regulada positivamente (TERG_04952). Um gene importante que codifica um β-1,6-glucano que atua como o núcleo central da rede proteína-carboidrato na parede celular (TERG_12043) foi reprimido em resposta a SRT.

Três genes que codificam quitinases moduladas no transcriptoma foram regulados negativamente em 12 h (TERG_05626, TERG_05625 e TERG_06638) e uma única em 3 h (TERG_06638). Genes que codificam duas quitinas sintase foram reprimidas em 12 h (TERG_12318 e TERG_12319), e uma hidrofobina (TERG_04234) foi regulada negativamente.

Alguns genes que codificam hidrolases associadas à morfogênese da parede celular foram induzidos, como o da glucanase da parede celular (TERG_04268). Também foram induzidos genes das acetiltransferases da família GNAT (Gcn5-related N-acetiltransferase) (TERG_07408, TERG_02517, TERG_08151, TERG_00563 e TERG_04021). Uma proteína contendo o domínio LysM TERG_05627, que mascara os componentes da parede celular do patógeno, foi reprimida em 12 h e uma catalase foi regulada negativamente em ambos os tempos (TERG_01252). Três Hsps foram moduladas no transcriptoma, uma reprimida em 3 h e 12 h, a Hsp75 (TERG_01883), e duas reprimidas em 12 h, a Hsp70 (TERG_05615) e a Hsp30 (TERG_01659).

O software Blast2GO foi usado para categorizar as distribuições funcionais de genes que foram diferencialmente expressos em resposta a SRT vs. SB (controle) nos pontos de tempo 3 h e 12 h. Os genes modulados em resposta a SRT estão envolvidos em diversos processos biológicos, componentes celulares e funções moleculares.

No geral, a maioria dos genes categorizados foram superexpressos após 3 h na presença de SRT. Esses genes participam principalmente de processos de oxidação-redução, transporte transmembrana, proteólise e atividades de transferase, catalítica e hidrolase. Após 12 h na presença da droga, vários genes pertencentes a essas mesmas categorias mostraram-se regulados negativamente, sugerindo uma resposta adaptativa ao estresse da droga. Além disso, em 12 h, a SRT reprimiu mais de 50 genes envolvidos na tradução. No entanto, os genes envolvidos nas atividades da membrana são os mais representados entre os componentes celulares e permanecem superexpressos independentemente de quanto tempo a SRT desafiou o fungo (**Figura 10**).

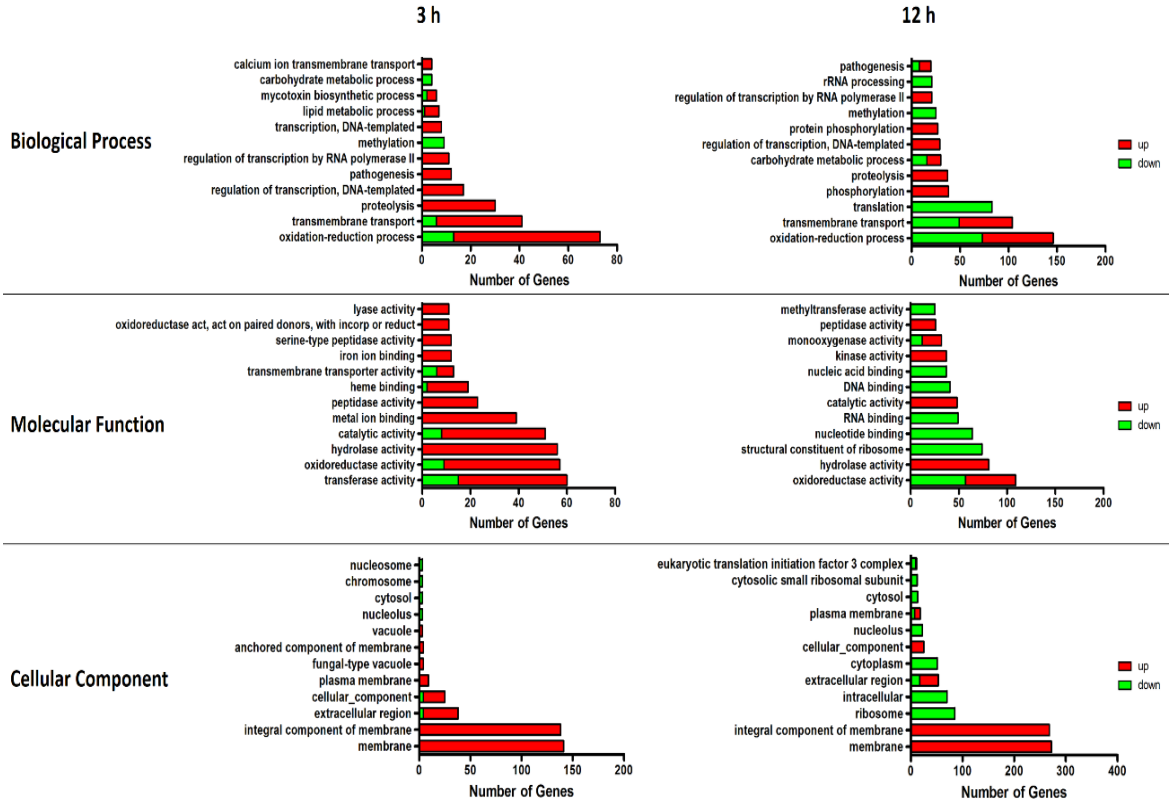

Figura 10: Categorização funcional de genes diferencialmente expressos. As barras vermelhas indicam o número de genes regulados positivamente, e as barras verdes indicam o número de genes regulados negativamente.

7.4 RT-qPCR

Inicialmente a eletroforese em gel de agarose mostrou que amostras foram convertidas adequadamente em cDNA. Então, foi realizada análise por RT-qPCR.

A análise da expressão gênica baseada em RT-qPCR revelou que 70% da CIM de SRT induziu um gene que codifica um transportador (TERG_00162) pertencente à superfamília de facilitadores principais (MFS) em 3 e 12 h. Em contraste, a exposição a SRT por 3 e 12 h regulou negativamente a TERG_12319, um gene crítico associado à quitina sintase ligado à virulência fúngica e remodelamento da parede celular. Além disso, a TERG_04234, que codifica um hidrofobina, uma proteína essencial para a patogênese fúngica, e a TERG_06755, que codifica a proteína c-8 esterol isomerase, necessária para a via do ergosterol, foram regulados negativamente em 3 e 12 h, respectivamente (**Figura 11**).

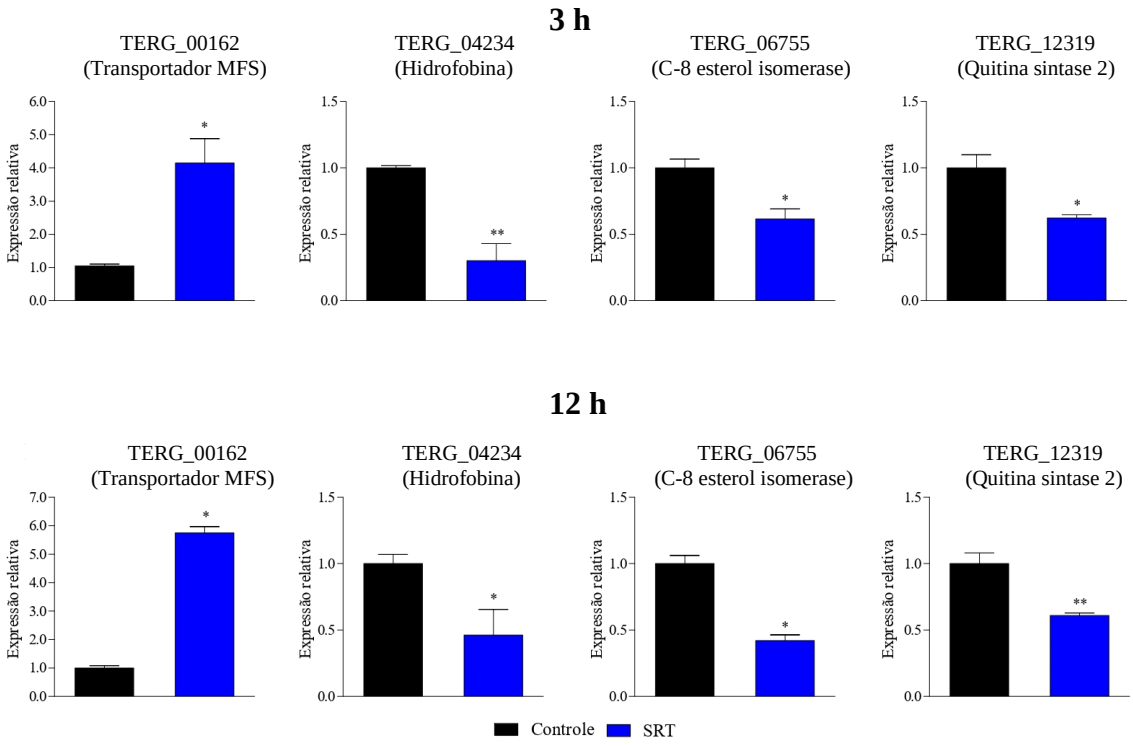

Figura 11: Genes expressos diferencialmente em resposta a SRT, identificados usando análise RT-qPCR. Os asteriscos indicam a significância estatística do *teste t* em comparação com o controle (ausência da droga SB). * $p < 0,05$; e ** $p < 0,01$.

Para avaliar a influência de SRT + CASP em genes relacionados a resistência e virulência em *T. rubrum*, foi realizada uma análise de expressão gênica usando RT-qPCR

estendida à combinação de SRT + o antifúngico CASP. Essas situações foram examinadas comparando os tratamentos com um controle na ausência de qualquer medicamento. A exposição a SRT + CASP diminuiu a transcrição do gene que codifica o transportador pertencente a superfamilia de transportadores multidrogas (MFS), TERG_00162 nos dois tempos analisados, 3 e 12 h. Em oposição a isso, a indução desse gene, foi observada quando SRT foi utilizada sozinha. Em contraste, SRT + CASP regulou negativamente os genes TERG_04234 e TERG_06755, bem como o gene que codifica uma enzima essencial na estrutura da parede celular de *T. rubrum* a quitina sintase, TERG_12319, o que foi semelhante ao observado em condições envolvendo o uso da SRT sozinha (**Figura 12**).

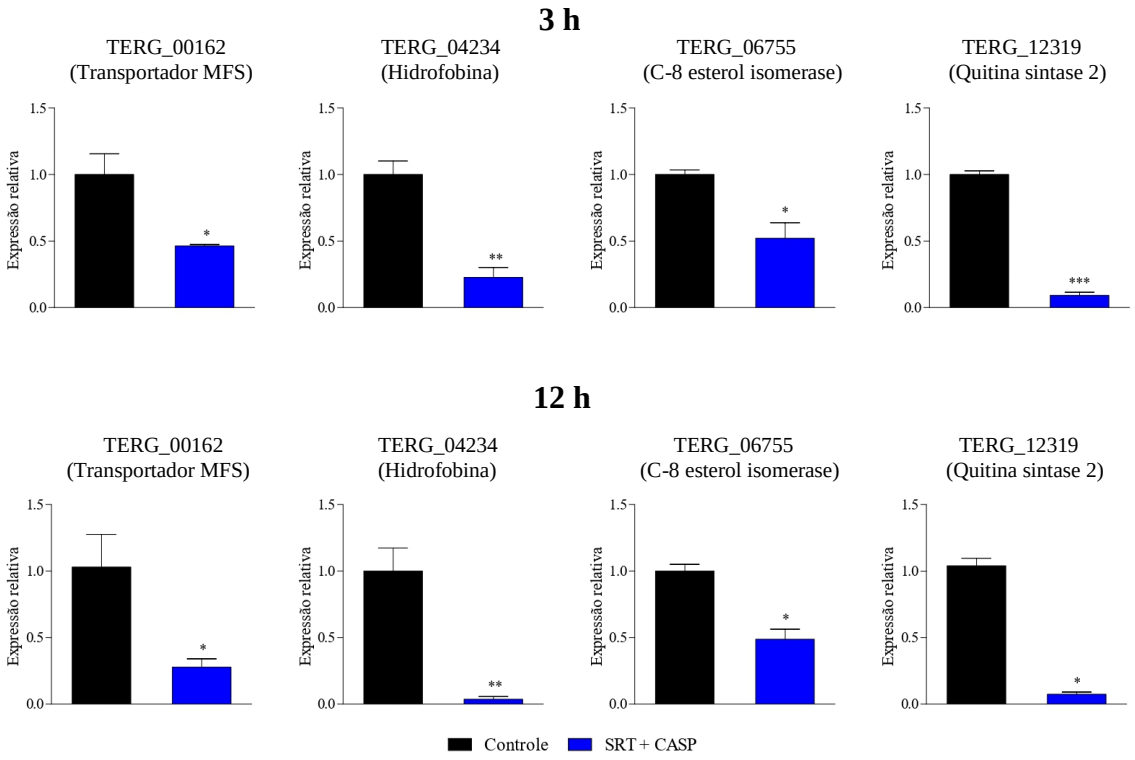

Figura 12: Genes expressos diferencialmente em resposta a combinações de SRT com CASP, identificados usando análise RT-qPCR. Os asteriscos indicam a significância estatística determinada pelo *teste t* em comparação com o controle (ausência de droga, SB) em 3 h e 12 h; * p <0,05; ** p < 0,01; *** p < 0,001.

Foram analisados os efeitos de baixas concentrações de CASP e SRT nos níveis de expressão desses genes em *T. rubrum* cultivado na presença de CASPcs ou SRTcs nas concentrações que foram sinérgicas, só que agora usadas individualmente. Os resultados mostraram que a SRTcs manteve o nível de expressão do gene TERG_00162, que codifica

um transportador multidroga, em nível semelhante ao observado no controle em 3 h. Em contraste, a expressão do gene TERG_00162 aumentou em 12 h. Além disso, existe uma diferença significativa entre os níveis de expressão mostrados nessas condições comparado ao controle ($p < 0,05$). A expressão do gene TERG_06755 foi regulada negativamente em 3 h, mas sua expressão em 12 h foi semelhante ao do controle. Os genes TERG_04234 e TERG_12319 mantiveram sua expressão em ambas as condições (controle e SRTcs) em 3 h e 12 h (**Figura 13**).

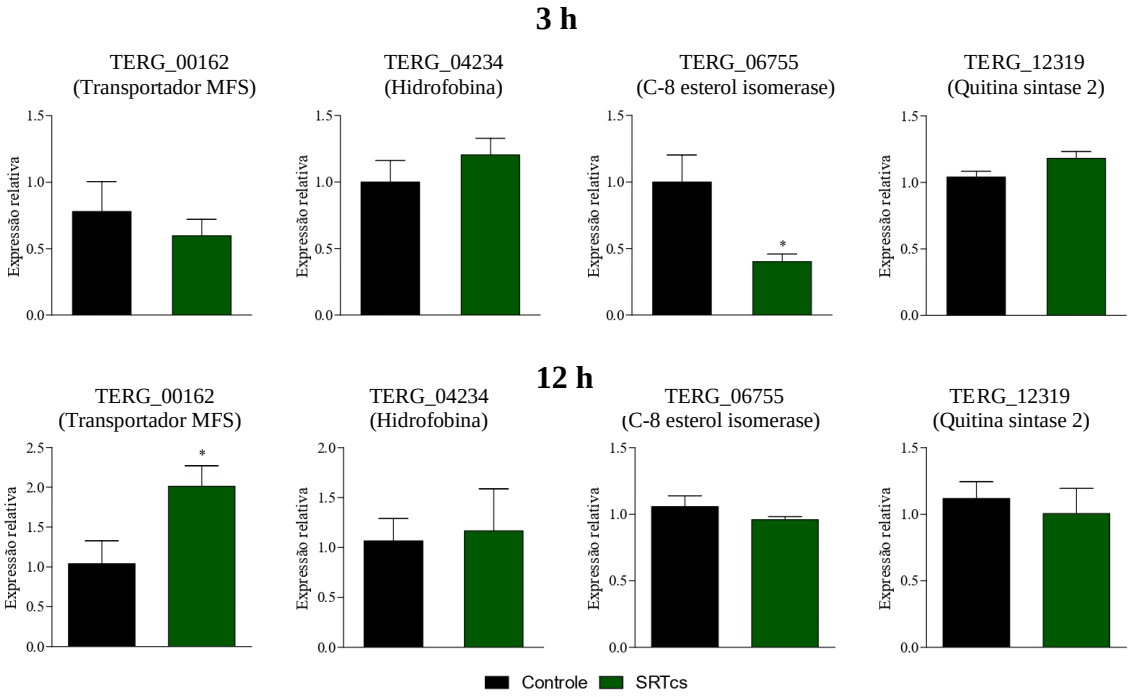

Figura 13: Expressão dos genes após a exposição SRTcs. Os asteriscos indicam significância estatística determinada pelo *teste t*, em comparação com o controle (ausência de droga) em 3 h e 12 h; *P < 0,05.

Para verificar se os efeitos nos genes de *T. rubrum* era consequência da interação entre CASP e SRT ou se era simplesmente resultado das drogas utilizadas individualmente nas concentrações que foram combinadas, os níveis de expressão também foram quantificados após a exposição a CASPcs. A exposição de *T. rubrum* a CASPcs mostrou que a expressão dos genes que codificam o transportador multidrogas (TERG_00162), a hidrofobina (TERG_04234), a C-8 esterol isomerase (TERG_06755) e a quitina síntase 2 (TERG_12319) eram semelhantes ao controle não tratado, em 3 h ou em 12 h. Portanto, não

existem diferenças estatisticamente significativas entre essas condições de tratamento (**Figura 14**).

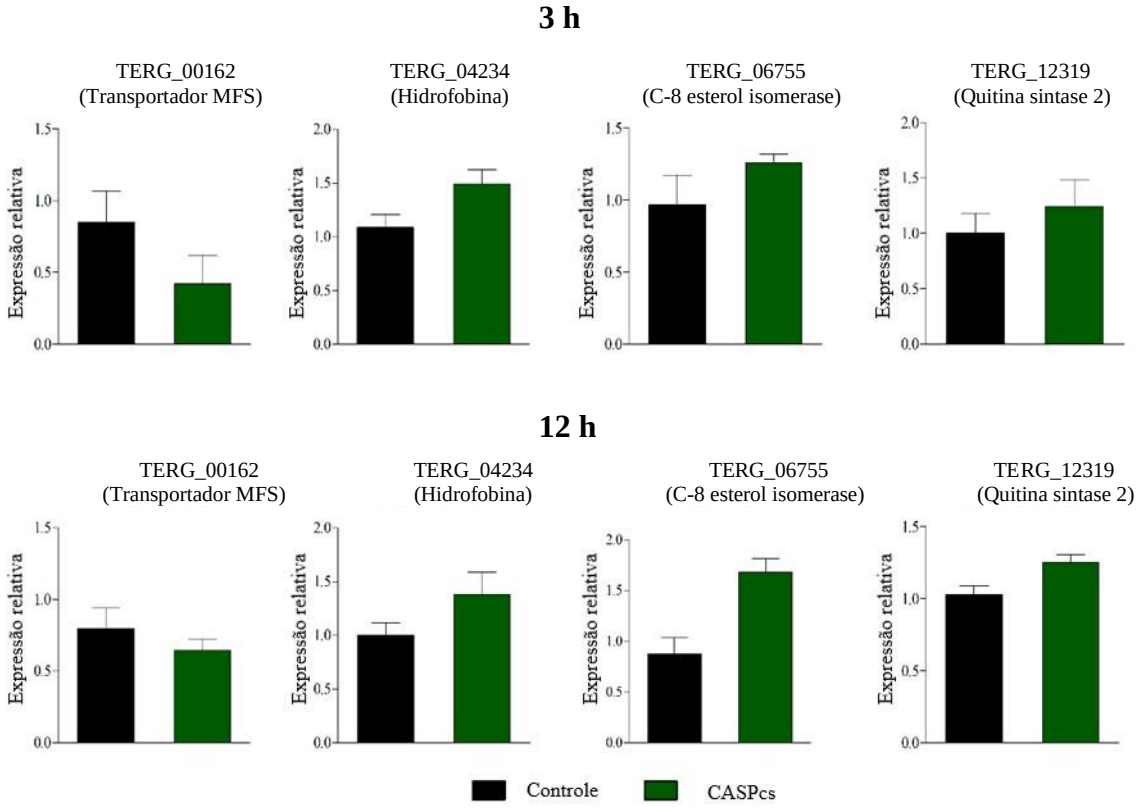

Figura 14: Genes diferencialmente expressos após exposição a CASPcs em comparação com o controle (ausência de drogas SB) em 3 h e 12 h.

7.5 Efeitos da SRT e sua combinação com CASP na atividade do biofilme de *T. rubrum*

Durante o ensaio com MTT, as células fúngicas viáveis com metabolismo ativo convertem esta substância em formazan. De forma aposta, células fúngicas mortas perdem essa capacidade. Assim, a formação de cor característica desse composto, após a reação catalizada pela desidrogenase mitocondrial, serve como um marcador útil e conveniente apenas das células viáveis. A absorbância medida em densidade óptica (DO) 550 nm é proporcional ao número de células viáveis.

Assim, a atividade metabólica no biofilme foi medida a cada 24 horas. Um aumento significativo nessa atividade foi observado até 72 h, após isso a atividade se estabilizou. Apesar de uma pequena elevação na atividade metabólica em 96 h, não houve alterações

significativas se comparada com 72 h. Portanto, 72 h foi considerado o tempo ideal para formação de biofilme de *T. rubrum in vitro*. Os resultados do ensaio com MTT indicaram que SRT sozinha na concentração de 12,5 mg/L, CASP sozinha na concentração de 15,62 mg/L, bem como as baixas concentrações obtidas da combinação de SRT + CASP (3,12 mg/L SRT+ 1,95 mg/L CASP), reduziram significativamente a atividades metabólicas do biofilme. O tratamento com SRTcs ou CASPcs não reduziu a atividade metabólica dos biofilmes de *T. rubrum* comparada ao controle. Um resultado indicativo da ineficiência dessas concentrações quando usadas individualmente (**Figura 15**).

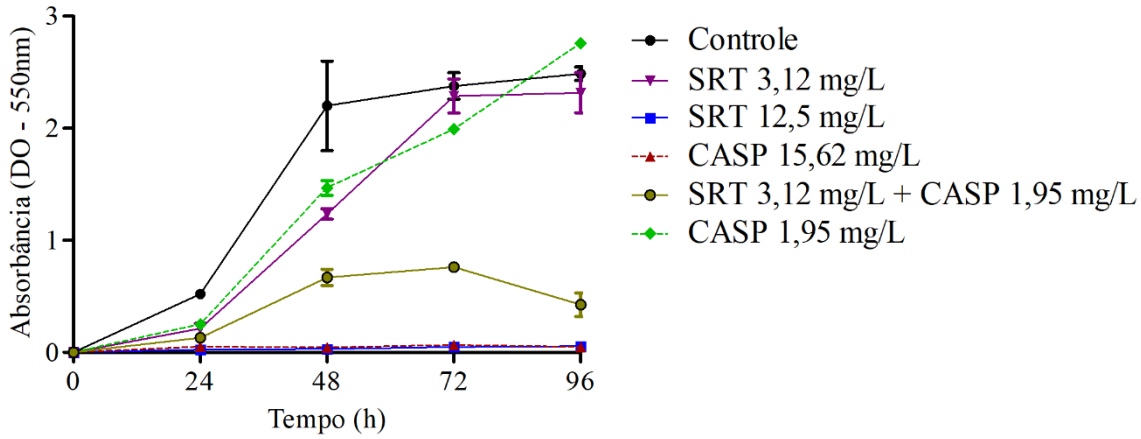

Figura 15: Metabolismo do biofilme de *T. rubrum*. Efeitos da sertralina (SRT), caspofungina (CASP) e SRT + CASP na atividade metabólica do biofilme de *T. rubrum.*

Diferente do MTT, o cristal violeta não é um composto indicativo da viabilidade celular. Na realidade, ele se adere a parede celular fúngica, permitindo avaliar a quantidade de biofilme formado, ou seja, o quanto de biomassa foi produzida pelo fungo durante a maturação. Nesse sentido, constatamos que a biomassa do biofilme também foi afetada pelos tratamentos com SRT, CASP e SRT + CASP. Três dias após o biofilme ter sido tratado com 62,50 mg/L CASP, uma redução significativa foi observada na biomassa em comparação com o controle ($p < 0,01$). O tratamento com 25 mg/L SRT, bem como 6,25 mg/L SRT + 1,95 mg/L CASP reduziu significativamente a biomassa. Por outro lado, 6,25 mg/L SRT ou 1,95 mg/L CASP não reduziram a biomassa. Na realidade, mantiveram a produção de biomassa de modo semelhante a do controle, sem diferença estatística significativa (**Figura 16**).

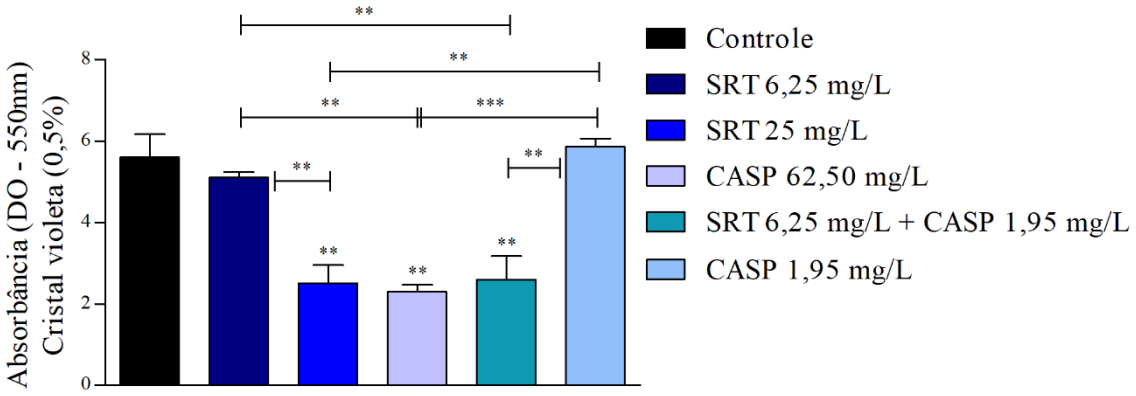

Figura 16: Avaliação do efeito de SRT, CASP e da combinação sinérgica (SRT + CASP) na biomassa do biofilme de *T. rubrum* corado com cristal violeta. Os tratamentos foram realizados 3 dias após a maturação do biofilme. As análises estatísticas mostrando diferenças significativas ($p < 0,05$) entre os compostos testados e o controle de crescimento foram estimadas usando ANOVA e teste *post hoc* de Tukey; ** $p < 0,01$ e *** $p < 0,001$.

Após o biofilme amadurecer e os tratamentos serem realizados por sete dias, os tratamentos com 25 mg/L SRT, 62,50 mg/L CASP ou 6,25 mg/L SRT + 1,95 mg/L CASP reduziram significativamente a biomassa quando comparados com o controle ($p < 0,001$). No entanto, o tratamento com 6,25 mg/L SRT ou 1,95 mg/L CASP não reduziu a biomassa do biofilme, assim como observado após os tratamentos por três dias. A biomassa produzida por esses tratamentos foi semelhante à observada na ausência de drogas (**Figura 17**).

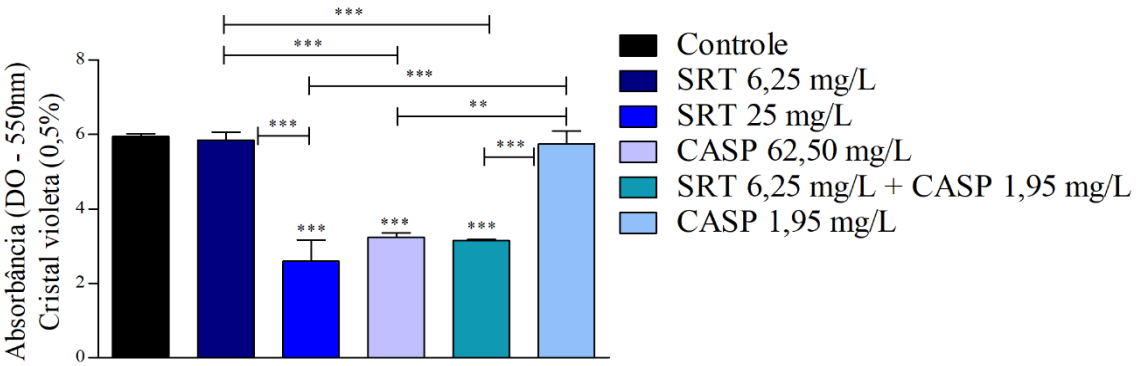

Figura 17: Efeito de SRT, CASP e SRT + CASP na biomassa do biofilme de *T. rubrum*. Os tratamentos foram realizados 7 dias após o biofilme maturado e corado com cristal violeta. Diferenças significativas entre compostos testados e controle de crescimento foram obtidas usando ANOVA e teste *post hoc* de Tukey. Os asteriscos indicam significância estatística: ** $p < 0,01$ e *** $p < 0,001$.

Os resultados do ensaio de infecção em unha humana corroboraram com a redução da biomassa e da atividade metabólica do biofilme, observadas pelos ensaios de MTT e cristal violeta. A microscopia eletrônica de varredura revelou que *T. rubrum* forma biofilmes maduros em fragmentos de unhas humanas após 20 dias. Seu crescimento no substrato foi caracterizado por filamentos infinitos, densos, interligados e espalhados em todas as direções para formar uma verdadeira rede de hifas conectadas. A alta tolerância antifúngica em *T. rubrum* pode ser atribuída a esta rede de hifas conectadas. Assim, a maturação do biofilme em fragmentos de unhas humanas foi consideravelmente afetada pela SRT.

A densidade do filamento foi significativamente reduzida pelos tratamentos em comparação com o controle não tratado. Observou-se redução significativa na espessura dos filamentos que formavam a rede hifálica. Além disso, a maioria das hifas não conseguiu completar seu desenvolvimento a um nível que lhes permitisse criar um biofilme mais uniforme. Nesse contexto, a maior atividade foi observada após *T. rubrum* ser tratado com SRT e CASP em concentrações correspondentes a 2 × CIMs, que totalizaram 50 mg/L e 62,50 mg/L, respectivamente. Destaca-se a excelente redução do biofilme decorrente do tratamento com 12,5 mg/L SRT + 3,90 mg/L CASP. No entanto, não verificamos a redução da densidade do filamento e as alterações mencionadas anteriormente em condições isoladas e não combinadas (**Figura 18**).

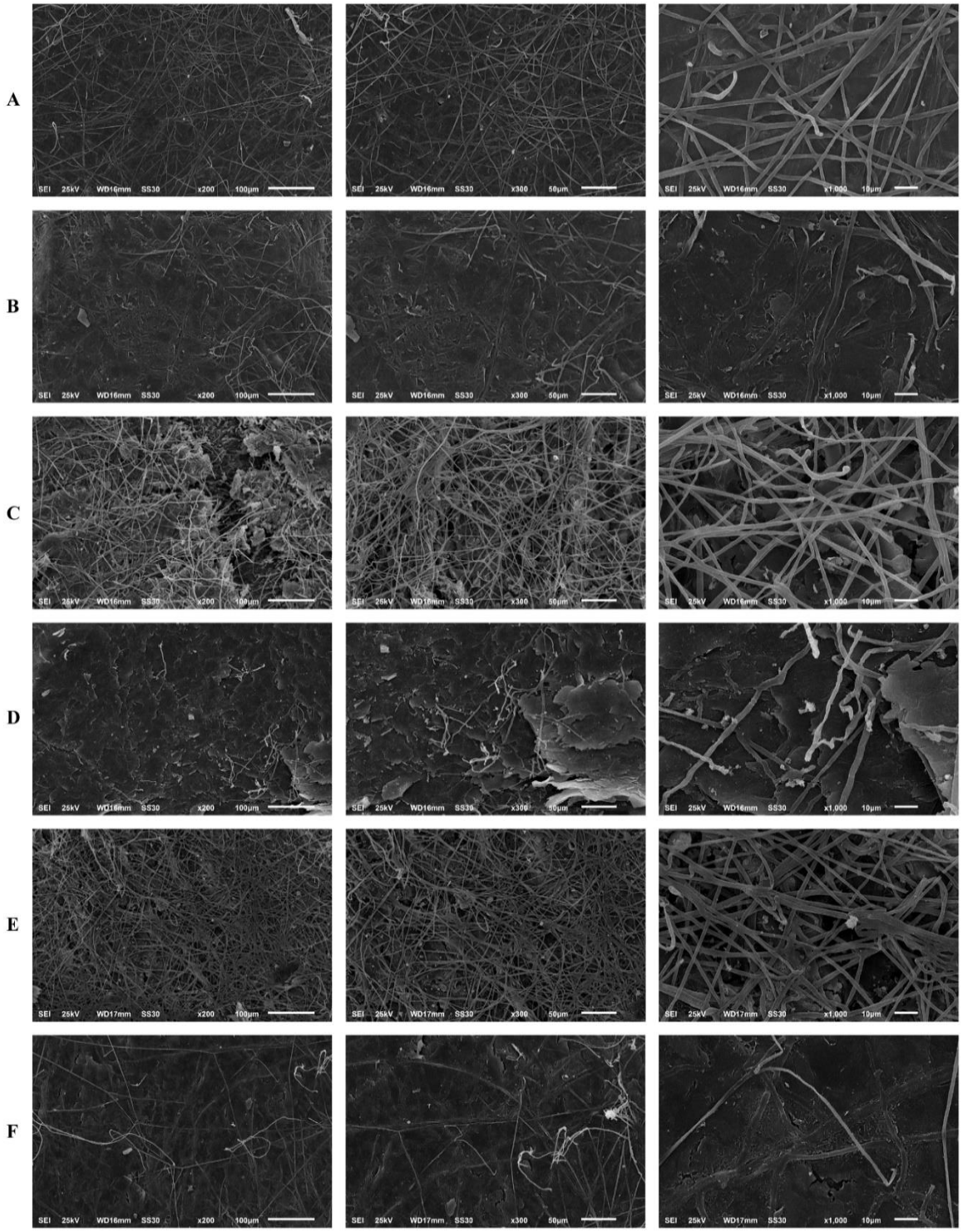

Figura 18: Microscopia eletrônica de varredura do biofilme de *T. rubrum* em uma unha humana. Crescimento da cepa de *T. rubrum* em fragmentos de unha na ausência de drogas (**A**) Tratamento com SRT 50 mg/L (**B**), SRT 12,5 mg/L (**C**), CASP 62,50 mg/L (**D**), CASP 3,90 mg/L (**E**) e SRT 12,5 mg/L + CASP 3,90 mg/L (**F**), 20 dias após a maturação do biofilme. As 3 colunas representam aumentos de 200, 300 e 1000 vezes, respectivamente.

Discussão

8. Discussão

O antidepressivo humano, SRT, exibiu atividade antifúngica contra formas planctônicas de *T. rubrum* (100 mg/L SB e 25 mg/L RPMI). Quando combinado com CASP, SRT mostrou excelentes efeitos sinérgicos inibindo *T. rubrum in vitro*. Os resultados da interação mostraram que à combinação de SRT e CASP diminuiu a concentração de antifúngicos necessários para inibir o fungo em até 30 vezes em comparação com os antifúngicos usados individualmente.

Esses resultados sugerem que reposicionar a SRT e combiná-la com a CASP constitui uma terapia promissora contra o *T. rubrum*. Vários relatos descrevem a atividade de SRT contra fungos patogênicos *in vitro* e *in vivo*, com referência particular a *Cryptococcus*, *Candida* e *Aspergillus* (Gowri *et al.,* 2020; Villanueva-Lozano *et al.,* 2020; Fortes *et al.,* 2023). Até onde sabemos, somos os primeiros a demonstrar seu efeito sozinha e em combinação com CASP contra o dermatófito *T. rubrum*, embora um estudo anterior tenha discutido as vantagens de usar uma combinação de SRT e CASP contra a levedura *T. asahii* (Cong *et al.,* 2016). Além disso, a concentração de SRT na pele é muito maior do que no sangue; assim, a utilidade da SRT como tratamento contra dermatofitose parece ser promissora (Tremaine *et al.*, 1989).

O sequenciamento de RNA (RNA-seq) de *T. rubrum* cultivado na presença de 70% da CIM da SRT revelou novos *insights* sobre os mecanismos usados pelo dermatófito para superar a exposição a SRT. A categorização funcional mostrou um número significativo de genes *upregulated* relacionados ao processo de oxidação e componentes da membrana. Esses dados demonstram uma tentativa de *T. rubrum* de manter a integridade da membrana e degradar a droga. A SRT afetou diversos processos biológicos relacionados ao transporte transmembrana e interferiu nas estruturas citoplasmáticas. Além disso, o processo de tradução de proteínas foi bastante afetado pela exposição a SRT. Este efeito já havia sido sugerido em *Cryptococcus* (Zhai *et al.*, 2012).

Identificamos a repressão dos únicos genes que codificam *hsp*s modulados no transcriptoma, um fenômeno diferente da indução que normalmente é observada em resposta à drogas. As HSPs em fungos desempenham um papel crítico na sobrevivência e na adaptação a diferentes condições ambientais desfavoráveis, como o estresse oxidativo e a

presença de fármacos (Martinez-Rossi *et al.*, 2016). É provável que SRT possa ter modulado vias de sinalização específícas envolvidas na regulação da expressão dessas HSPs, inibindo um fator de transcrição que normalmente induz a expressão das HSPs. Recentemente foi demonstrado que SRT atua em diferentes vias de sinalização, inclusive inibindo alguns fatores de transcrição (Galvão-Rocha *et al.*, 2023).

Quando analisamos um grupo de genes por RT-qPCR, observamos que uma concentração sub inibitória de SRT induziu um gene que codifica um transportador transmembrana (TERG_00162) pertencente à superfamília de facilitadores principais (MFS). Esses transportadores medeiam o aumento do efluxo de drogas, um dos principais mecanismos de resistência em dermatófitos (Yamada *et al.*, 2022). A combinação de SRT e CASP reduziu os níveis de transcrição do gene TERG_00162. Além disso, a exposição de *T. rubrum* a SRTcs ou CASPcs (0,273 mg/L SRT ou 10,93 mg/L CASP) mostrou que o nível de expressão do gene TERG_00162 estava associado à quantidade de SRT na célula e à atividade da combinação. Os transportadores da superfamília facilitadora principal (MFS) possibilitam o transporte de diversas compostos pela célula, contra ou a favor de um gradiente de concentração (Drew *et al.*, 2021).

Encontrar alvos moleculares associados a esses transportadores é uma estratégia bastante significativa, na busca de tratamentos, principalmente no contexto do surgimento de cepas resistentes. Nos diversos patógenos fúngicos, como *Aspergillus*, *Cryptococcus* e *Candida*, vários trabalhos tem destacado esses transportadores como alvos moleculares promissores (Cavalheiro *et al.*, 2018; Pérez-Cantero *et al.*, 2020; Qadri *et al.*, 2022). Em *T. rubrum* e nos demais dermatófitos, a expressão dos genes que codicam esses transportadores pode está relacionada com a resistência (Petrucelli *et al.*, 2019; Yamada *et al.*, 2022).

A exposição de *T. rubrum* a SRT 70% da CIM, induziu diversos genes que codificam transportadores do tipo ABC e reprimiu apenas dois. Esses transportadores são codificados por genes críticos, os genes de resistências a múltiplas drogas (MDRs), que estão relacionados diretamente com a necessidade do trasporte de drogas nas células fúngicas. Esses transportadores são ATPases, proteínas altamente conservados e bastante especificas, que fazem parte de um mecanismo complexo e eficiente, necessário para a extrusão de antifúngicos do interior celular para o ambiente externo, denominado bomba de efluxo (Martins *et al.*, 2016; Monod *et al.*, 2019).

Os fungos podem desenvolver vários mecanismos de adaptação em resposta a mudanças ambientais. A parede celular fúngica, que permite que os fungos interajam dinamicamente com o ambiente, também constitui um alvo antifúngico promissor. Além disso, sua integridade estrutural, que é ativamente modulada em resposta a condições de estresse, desempenha um papel na adesão, sinalização e colonização, tornando-a essencial para a sobrevivência do patógeno (Chevalier *et al.*, 2023; Gow and Lenardon, 2023).

Nós revelamos outros alvos antifúngicos promissores após SRT reprimir genes importantes que codificam quitinases (TERG_05626, TERG_05625 e TERG_06638), e quitinas sintases (TERG_12318 e TERG_01231). Ademais SRT + CASP, reprimiram genes críticos que codificam a quitina sintase (TERG_12319) e a hidrofobina (TERG_04234). No entanto, a expressão desses genes não mudou quando *T. rubrum* foi cultivado com SRTcs ou CASPcs em comparação com o controle. Isso sugeriu que a eficácia da atividade contra TERG_04234 e TERG_12319 se deve exclusivamente à combinação de drogas e não a cada droga usada isoladamente. A quitina, é uma proteína linear que fornece força e proteção a muitos eucariotos e é vital para a morfogênese da parede celular (Breuer *et al.*, 2022). A quitina está ausente em células de mamíferos; assim, seu metabolismo é um alvo atraente para agentes antifúngicos altamente específicos (Martins *et al.*, 2019). As quitinases clivam as quitinas durante a remodelação da parede celular. A repressão de genes que codificam quitinases representa uma interrupção desse processo e afeta a virulência e a sobrevivência dos fungos (Rush *et al.*, 2010).

Normalmente, a regulação positiva de genes relacionados à síntese de quitina é a resposta primária ao estresse da parede celular (Ries *et al.*, 2017; Li, J. *et al.*, 2023). A quitina sintase é essencial para a síntese de quitina nos septos primários de fungos (Silverman *et al.*, 1988). Por muitos anos a síntese de quitina foi de interesse científico como possível alvo para terapias antifúngicas (Chaudhary *et al.*, 2013; Ji *et al.*, 2016). E, assim como nosso trabalho, atualmente outras pesquisas tem explorado a biossíntese de quitina e consequentemente a quitina sintase (Ibe and Munro, 2021; Ji *et al.*, 2021; Xu *et al.*, 2022).

O gene TERG_12043 também se mostrou um excelente alvo antifúngico. Ele codifica um componente essencial e específico do fungo, o β-1,6-glucano, que liga outros componentes da parede e associa as manoproteínas ao β-1,3-glucano e à quitina (Horváthová

and Farkaš, 2022). A repressão de β-1,6-glucana leva a uma restrição na formação da parede celular.

Como mencionamos anteriormente, uma hidrofina também foi alvo da SRT. As hidrofobinas, são proteínas ricas em cisteína, elas reduzem a tensão superficial da água e auxiliam na adesão do fungo (Tanaka *et al.*, 2022). As hidrofobinas são secretadas apenas por fungos filamentosos, além de ser bastante conservadas nesses organismos (Stanzione *et al.*, 2022; Tanaka *et al.*, 2022).

A identificação de medicamentos que regulam negativamente os genes que codificam a hidrofobina pode ajudar a desenvolver novas estratégias para tratar infecções causadas por *T. rubrum*. Esta proteína regula o fluxo de água através da parede celular fúngica e medeia a fixação de estruturas infecciosas associadas à patogênese fúngica. Essas proteínas formam uma camada hidrofóbica, que se acumulam nas faces da parede celular tornando-a impermeável, mas com uma pecularidade, permitindo as trocas gasosas (Gow and Lenardon, 2023). Assim, como observado em nossos resultados e descrito na literatura, sua regulação negativa está associada à diminuição da virulência fúngica (Martins *et al.*, 2019; Lang *et al.*, 2020).

Também identificamos os efeitos da SRT e SRT + CASP na via do ergosterol. SRT na concentração de 70% de sua CIM e baixas concentrações de SRT + CASP regulou negativamente o gene TERG_06755, que codifica uma C-8 esterol isomerase. Essa enzima está envolvida na cascata da biossíntese do ergosterol (Petrucelli *et al.*, 2019). A relevância de fármacos que têm como alvo genes ou proteínas envolvidas na biossíntese do ergosterol tem sido relatada (Sun and Liao, 2020; Behbehani *et al.*, 2023; Galvão-Rocha *et al.*, 2023). Apesar da via do ergosterol ser descrita muitas vezes como um alvo favorito de muitos antifúngicos, a interferência da SRT e da sua combinação com CASP, ocorreu em um alvo não usual, uma enzima necessária no processo de isomerização na cadeia da biossíntese do ergosterol.

Outra proteína, contendo o domínio LysM (TERG_05627), foi reprimida por SRT. Foi relatado previamente que o gene que codifica esta proteina é induzido quando o fungo é cultivado presença dessas proteínas contendo LysM secretadas por fungos pode diminuir o reconhecimento da quitina fúngica livre pelo sistema imunológico do hospedeiro. Assim, essas proteínas funcionam como um forte fator de virulência. Elas protegem a quitina da

parede da célula hospedeira do sistema imunológico humano. Essas proteínas que contém o domínio LysM, contêm o domínio catalítico quitinase II, importante para a virulência fúngica (Lopes *et al.*, 2020). Além dessas funções, as proteínas que contenham o domínio LysM contribuem para a adesão do patógeno à pele humana (Kar *et al.*, 2019).

Diante do estresse causado pela SRT, observamos *T. rubrum* tentando manter sua virulência e seu desenvolvimento por meio da indução de genes que codificam proteínas associadas à morfogênese da parede celular e responsivas ao estresse (família GNAT acetiltransferase). Os membros da família GNAT estão envolvidos na modificação pós-traducional; eles transferem grupos acetil do acetil-CoA para seus substratos cognatos e regulam as respostas ao estresse oxidativo, bem como a baixa disponibilidade de nutrientes (Favrot *et al.*, 2016).

Nossos ensaios demonstraram o impacto da SRT e sua combinação sinérgica no metabolismo e biomassa de biofilmes de *T. rubrum*. Demonstramos que mesmo em baixas concentrações de SRT, quando combinadas com CASP, são eficazes contra biofilmes de *T. rubrum*; os resultados da microscopia eletrônica de varredura comprovaram esse efeito inibitório.

Esses nossos achados complementam a ideia de que SRT, sua combinação com CASP e até mesmo a CASP, representam possibilidades no tratamento das infecções fungicas, especialmente contra *T. rubrum*. Atuar de forma eficiente contra essas comunidades de infecção, indica o potencial alternativo do fármaco. Isso porque, os biofilmes fornecem proteção aos patógenos, tanto da ação de drogas quanto do sistema imunológico. Assim, esses organimos conseguem sobreviver em ambientes os mais inadequados possíveis, ambientes hostis, com baixo oxigênio, escacez de nutrientes e resposta do hospedeiro ativa. Nesse conjunto, muitas populações insistem em se manterem vivas, se "unindo" e produzindo um verdadeiro arsenal contra essa guerra, provocando uma heterogeinidade metabólica e provocando recidivas das infecções, consequentemente resultando na resistência (Armbruster *et al.*, 2023).

Assim, nossos resultados indicam que a atividade da SRT em altas concentrações, bem como em combinação com a CASP, regula negativamente genes essenciais relacionados à formação e constituição da parede celular e um gene associado à via do ergosterol.

Apesar dos mecanismos que fundamentam os efeitos da CASP na parede celular de leveduras serem conhecidos (Odds *et al.*, 2003), excluímos a possibilidade de que alterações nos níveis de expressão de genes possam ser causadas por essa droga em baixas concentrações. Nossos estudos indicaram que CASP isoladamente (CASPcs) não alterou a expressão de genes envolvidos na constituição da parede celular. Também não afetou significativamente os biofilmes de *T. rubrum* em nenhum dos aspectos estudados.

Em resumo, o fungo desenvolve vários mecanismos de adaptação em resposta às mudanças ambientais. Demonstramos o impacto da SRT e suas combinações sinérgicas no metabolismo e na biomassa do biofilme de *T. rubrum*. Um exemplo é a produção de vários componentes da parede celular que suportam o crescimento e desenvolvimento do fungo, proporcionando adaptação a condições ambientais hostis e neutralizando os efeitos do estresse induzido por drogas. Nosso estudo contribui significativamente para o enriquecimento da literatura e promove uma perspectiva promissora no desenvolvimento de antifúngicos alternativos contra as complexas comunidades de biofilmes.

Conclusão

9. Conclusão

- SRT foi capaz de inibir consideravelmente o crescimento de *T. rubrum in vitro* e em *ex vivo*.
- CASP também foi atuante contra *T. rubrum,* apesar das estatísticas mostrarem que sua atividade não foi tão eficiente quanto a da SRT.
- SRT e CASP representam também uma estratégia contra as comunidades práticas de infecção, os biofilmes.
- SRT e CASP são sinérgicas contra *T. rubrum*.
- SRT sozinha ou em combinação com CASP promoveu efeitos significativos em importantes genes relacionados com as estruturas da parede celular, adesão e genes diretamente relacionados com resistência e adaptação.
- SRT sozinha ou em combinação com CASP revelou um novo alvo, não usual, necessário na biossíntese do ergosterol.

Referências Bibliográficas

10. Referências Bibliográficas

ACCOCEBERRY, I. et al. Challenging SNP impact on caspofungin resistance by full-length FKS1 allele replacement in *Candida* lusitaniae. **Journal of Antimicrobial Chemotherapy,** v. 74, n. 3, p. 618-624, Mar. 2019. ISSN 0305-7453.

AHANGARKANI, F. et al. First azole-resistant *Aspergillus fumigatus* isolates with the environmental TR(46) /Y121F/T289A mutation in Iran. **Mycoses,** v. 63, n. 5, p. 430-436, May. 2020. ISSN 0933-7407.

ALANÍS-RÍOS, S. A. et al. Evaluation of the synergistic antifungal activity of micafungin and voriconazole plus sertraline against *Candida auris*. **Brazilian Journal of Microbiology,** v. 53, n. 4, p. 2003-2008, Dec. 2022. ISSN 1517-8382.

ALKHALIFA, B. A. et al. Serotonin reuptake inhibitors effect on fluconazole activity against resistant *Candida glabrata* strains. **Journal of Global Antimicrobial Resistance,** v. 29, p. 49-54, Jun. 2022. ISSN 2213-7165.

AN, J. X. et al. Drug repurposing strategy II: from approved drugs to agri-fungicide leads. **Journal of Antibiotics (Tokyo),** v. 76, n. 3, p. 131-182, Mar. 2023. ISSN 0021-8820.

ANDRIANI, G. M. et al. Synergistic antifungal interaction of N-(butylcarbamothioyl) benzamide and amphotericin B against *Cryptococcus neoformans*. **Frontiers in Microbiology,** v. 14, p. 1040671, Mar. 2023. ISSN 1664-302X.

ARMBRUSTER, C. E. et al. Editorial: Rising stars in biofilms 2022. **Frontiers in Cellular and Infection Microbiology,** v. 13, p. 1169998, Mar. 2023. ISSN 2235-2988.

ASTVAD, K. M. T. et al. Increasing Terbinafine Resistance in Danish *Trichophyton* Isolates 2019-2020. **Journal of Fungi (Basel),** v. 8, p. 801, n. 2, Jan. 2022. ISSN 2309-608x.

BADIEE, P. et al. Comparison of *in vitro* activities of newer triazoles and classic antifungal agents against dermatophyte species isolated from Iranian University Hospitals: a multi-central study. **Annals of Clinical Microbiology Antimicrobials,** v. 22, n. 1, p. 15, Feb. 2023. ISSN 1476-0711.

BAGHI, N. et al. *In vitro* activity of new azoles luliconazole and lanoconazole compared with ten other antifungal drugs against clinical dermatophyte isolates. **Medical Mycology,** v. 54, n. 7, p. 757-63, Oct. 2016. ISSN 1369-3786.

BAÚ-CARNEIRO, J. L. et al. Sertraline repositioning: an overview of its potential use as a chemotherapeutic agent after four decades of tumor reversal studies. **Translational Oncology,** v. 16, p. 101303, Dec. 2022. ISSN 1936-5233.

BEHBEHANI, J. M. et al. Anticandidal Activity of Capsaicin and Its Effect on Ergosterol Biosynthesis and Membrane Integrity of *Candida albicans*. **International Journal of Molecular Sciences,** v. 24, n. 2, Jan. 2023. ISSN 1422-0067.

BENJAMINI, Y.; HOCHBERG, Y. Controlling the False Discovery Rate: A Practical and Powerful Approach to Multiple Testing. **Journal of the Royal Statistical Society: Series B (Methodological),** v. 57, n. 1, p. 289-300, Jan. 1995. ISSN 0035-9246.

BHATTACHARYA, S.; ESQUIVEL, B. D.; WHITE, T. C. Overexpression or Deletion of Ergosterol Biosynthesis Genes Alters Doubling Time, Response to Stress Agents, and Drug Susceptibility in *Saccharomyces cerevisiae*. **mBio,** v. 9, n. 4, Jul. 2018.

BHATTACHARYYA, A. et al. Treatment of recalcitrant cases of tinea corporis/cruris caused by *T. mentagrophytes* - interdigitale complex with mutations in *ERG11*, *ERG* 3, *ERG4*, *MDR1*, *MFS* genes & *SQLE* and their potential implications. **International Journal of Dermatology**, v. 62, n. 5, p. 637-648, Mar. 2023. ISSN 0011-9059.

BOLGER, A. M.; LOHSE, M.; USADEL, B. Trimmomatic: a flexible trimmer for Illumina sequence data. **Bioinformatics,** v. 30, n. 15, p. 2114-2120, Aug. 2014. ISSN 1460-2059.

BOULWARE, D. R. et al. Adjunctive sertraline for asymptomatic cryptococcal antigenemia: A randomized clinical trial. **Medical Mycology,** v. 58, n. 8, p. 1037-1043, Nov. 2020. ISSN 1369-3786.

BRANCO, J.; MIRANDA, I. M.; RODRIGUES, A. G. *Candida parapsilosis* Virulence and Antifungal Resistance Mechanisms: A Comprehensive Review of Key Determinants. **Journal of Fungi (Basel),** v. 9, n. 1, Jan. 2023. ISSN 2309-608x.

BREUER, M. R. et al. The Antidepressant Sertraline Induces the Formation of Supersized Lipid Droplets in the Human Pathogen *Cryptococcus neoformans*. **Journal of Fungi (Basel),** v. 8, n. 6, Jun. 2022. ISSN 2309-608x.

BRILHANTE, R. S. N. et al. Quantitative and structural analyses of the *in vitro* and *ex vivo* biofilm-forming ability of dermatophytes. **Journal of Medical Microbiology,** v. 66, n. 7, p. 1045-1052, Jul. 2017. ISSN 0022-2615.

BURMESTER, A. et al. Point mutations in the squalene epoxidase *erg1* and sterol 14-α demethylase *erg11* gene of *T indotineae* isolates indicate that the resistant mutant strains evolved independently. **Mycoses,** v. 65, n. 1, p. 97-102, Jan. 2022. ISSN 0933-7407.

CABALLERO, U. et al. *In Vitro* Interaction and Killing-Kinetics of Amphotericin B Combined with Anidulafungin or Caspofungin against *Candida auris*. **Pharmaceutics,** v. 13, n. 9, Aug. 2021. ISSN 1999-4923.

CAVALHEIRO, M. et al. Host-Pathogen Interactions Mediated by MDR Transporters in Fungi: As Pleiotropic as it Gets! **Genes (Basel),** v. 9, n. 7, Jul. 2018. ISSN 2073-4425.

CELESTRINO, G. A. et al. Host immune responses in dermatophytes infection. **Mycoses,** v. 64, n. 5, p. 477-483, May. 2021. ISSN 0933-7407.

CHAUDHARY, P. M.; TUPE, S. G.; DESHPANDE, M. V. Chitin synthase inhibitors as antifungal agents. **Mini-Reviews in Medical Chemistry,** v. 13, n. 2, p. 222-36, Feb. 2013. ISSN 1389-5575.

CHEN, J. et al. Differential deuterolysin expression with a peak at low pH in human pathogenic fungi *Trichophyton rubrum* and *T. mentagrophytes*. **Medical Mycology,** v. 61, n. 4, Apr. 2023. ISSN 1369-3786.

CHEVALIER, L. et al. Cell wall dynamics stabilize tip growth in a filamentous fungus. **PLoS Biology,** v. 21, n. 1, Jan. 2023. ISSN 1544-9173.

CHOY, H. L.; GAYLORD, E. A.; DOERING, T. L. Ergosterol distribution controls surface structure formation and fungal pathogenicity. **mBio**, v. 14, n. 4, Feb. 2023.

COLABARDINI, A. C. et al. Heterogeneity in the transcriptional response of the human pathogen *Aspergillus fumigatus* to the antifungal agent caspofungin. **Genetics,** v. 220, n. 1, Jan. 2022. ISSN 0016-6731.

CONG, L. et al. *In vitro* antifungal activity of sertraline and synergistic effects in combination with antifungal drugs against planktonic forms and biofilms of clinical *Trichosporon asahii* isolates. **PloS one,** v. 11, n. 12, Dec. 2016. ISSN 1932-6203.

CORNET, L. et al. The taxonomy of the *Trichophyton rubrum* complex: a phylogenomic approach. **Microbial Genomics,** v. 7, n. 11, Nov. 2021. ISSN 2057-5858.

COSTA-ORLANDI, C. B. et al. *In vitro* characterization of *Trichophyton rubrum* and *T. mentagrophytes* biofilms. **Biofouling,** v. 30, n. 6, p. 719-27, Apr. 2014. ISSN 0892-7014.

CRUZ, A. H. S. et al. Relevance of Nutrient-Sensing in the Pathogenesis of *Trichophyton rubrum* and *Trichophyton interdigitale*. **Frontiers in Fungal Biology,** v. 3, Mar. 2022. ISSN 2673-6128.

DALL'OGLIO, F. et al. An Overview of the Diagnosis and Management of Seborrheic Dermatitis. **Clinical, Cosmetic and Investigational Dermatology,** v. 6, n. 15, p. 1537-1548, Aug. 2022. ISSN 1178-7015.

DE HOOG, S. et al. Skin Fungi from Colonization to Infection. **Microbiology Spectrum,** v. 5, n. 4, Jul. 2017. ISSN 2165-0497.

DIBAN, F. et al. Biofilms in Chronic Wound Infections: Innovative Antimicrobial Approaches Using the In Vitro Lubbock Chronic Wound Biofilm Model. **International Journal of Molecular Sciences,** v. 24, n. 2, Jan. 2023. ISSN 1422-0067.

DOBIN, A. et al. STAR: ultrafast universal RNA-seq aligner. **Bioinformatics,** v. 29, n. 1, p. 15-21, Jan. 2013. ISSN 1367-4803.

DOSS, R. W. et al. Antimicrobial Susceptibility of Tinea Capitis in Children from Egypt. **Indian Journal of Dermatology,** v. 63, n. 2, p. 155-159, Mar-Apr. 2018. ISSN 0019-5154.

DREW, D. et al. Structures and General Transport Mechanisms by the Major Facilitator Superfamily (MFS). **Chemical Reviews,** v. 121, n. 9, p. 5289-5335, May. 2021. ISSN 0009-2665.

EBERT, A. et al. Alarming India-wide phenomenon of antifungal resistance in dermatophytes: A multicentre study. **Mycoses,** v. 63, n. 7, p. 717-728, Jul. 2020. ISSN 0933-7407.

ELAVARASHI, E.; KINDO, A. J.; RANGARAJAN, S. Enzymatic and Non-Enzymatic Virulence Activities of Dermatophytes on Solid Media. **Journal of Clinical & Diagnostic Research,** v. 11, n. 2, p. 23-25, Feb. 2017. ISSN 2249-782X.

FAVROT, L.; BLANCHARD, J. S.; VERGNOLLE, O. Bacterial GCN5-Related N-Acetyltransferases: From Resistance to Regulation. **Biochemistry,** v. 55, n. 7, p. 989-1002, Feb. 2016. ISSN 0006-2960.

FAYED, B.; JAYAKUMAR, M. N.; SOLIMAN, S. S. M. Caspofungin-resistance in *Candida auris* is cell wall-dependent phenotype and potential prevention by zinc oxide nanoparticles. **Medical Mycology,** v. 59, n. 12, p. 1243-1256, Dec. 2021. ISSN 1369-3786.

FERREIRA-NOZAWA, S. M. et al. The pH signaling transcription factor PacC mediates the growth of *Trichophyton rubrum* on human nail *in vitro*. **Medical Mycology**, v. 44, n. 7, p. 41-645, Nov. 2006. ISSN 1460-2709.

FORTES, B. N. et al. Caspofungin alone or combined with polymyxin B are effective against mixed biofilm of *Aspergillus fumigatus* and carbapenem-resistant *Pseudomonas aeruginosa*. **Research in Microbiology,** v. 174, n. 1-2, p. 103993, Jan-Feb. 2023. ISSN 0923-2508.

FU, C. et al. Genetic analysis of Hsp90 function in *Cryptococcus neoformans* highlights key roles in stress tolerance and virulence. **Genetics,** v. 220, n. 1, Jan. 2022. ISSN 0016-6731.

GALVÃO-ROCHA, F. M. et al. The Antidepressant Sertraline Affects Cell Signaling and Metabolism in *Trichophyton rubrum*. **Journal of Fungi (Basel),** v. 9, n. 2, Feb. 2023. ISSN 2309-608x.

GANESAN, P. et al. Molecular Mechanisms of Antifungal Resistance in Mucormycosis. **Biomed Research International,** v. 2022, p. 6722245, Oct. 2022. ISSN 2314-6133.

GE, Y.; WANG, Q. Current research on fungi in chronic wounds. **Front Mol Biosci,** v. 9, p. 1057766, Oct. 2022. ISSN 2296-889X.

GOW, N. A. R.; LENARDON, M. D. Architecture of the dynamic fungal cell wall. **Nature Reviews Microbiology,** v. 21, n. 4, p. 248-259, Apr. 2023. ISSN 1740-1526.

GOWRI, M. et al. Sertraline as a promising antifungal agent: inhibition of growth and biofilm of *Candida auris* with special focus on the mechanism of action *in vitro*. **Journal of Applied Microbiology,** v. 128, n. 2, p. 426-437, Feb. 2020. ISSN 1364-5072.

GRAMINHA, M. A. et al. Terbinafine resistance mediated by salicylate 1-monooxygenase in *Aspergillus nidulans*. **Antimicrobial Agents and Chemotherapy,** v. 48, n. 9, p. 3530-5, Sep. 2004. ISSN 0066-4804.

GUPTA, A. K. et al. The Growing Problem of Antifungal Resistance in Onychomycosis and Other Superficial Mycoses. **American Journal Clinical Dermatology,** v. 22, n. 2, p. 149-157, Mar. 2021. ISSN 1175-0561.

GUPTA, A. K.; VENKATARAMAN, M. Antifungal resistance in superficial mycoses. **Journal of Dermatological Treatment,** v. 33, n. 4, p. 1888-1895, Jun. 2022. ISSN 0954-6634.

GÓMEZ-LÓPEZ, A. et al. *In vitro* evaluation of combination of terbinafine with itraconazole or amphotericin B against Zygomycota. **Diagnostic Microbiology and Infectious Disease,** v. 45, n. 3, p. 199-202, Mar. 2003. ISSN 0732-8893.

HIRAYAMA, T. et al. Echinocandin Resistance in *Candida auris* Occurs in the Murine Gastrointestinal Tract Due to FKS1 Mutations. **Antimicrobial Agents and Chemotherapy**, Mar. 2023. ISSN 0066-4804.

HIRUMA, J. et al. Epidemiological study of antifungal-resistant dermatophytes isolated from Japanese patients. **The Journal of Dermatology**, v. 50, n. 8, p. 1068-1071, Mar. 2023. ISSN 0385-2407.

HORVÁTHOVÁ, Á.; FARKAŠ, V. Effect of N-acetyl chito-oligosaccharides on the biosynthesis and properties of chitin in *Saccharomyces cerevisiae*. **Folia Microbiologica (Praha),** v. 67, n. 2, p. 285-289, Apr. 2022. ISSN 0015-5632.

HSIEH, A. et al. A new mutation in the SQLE gene of *Trichophyton mentagrophytes* associated to terbinafine resistance in a couple with disseminated tinea corporis. **Journal of Mycologie Medicale,** v. 29, n. 4, p. 352-355, Dec. 2019. ISSN 1156-5233.

HU, W. et al. A Typical but Rare Case of Solitary Tinea Auricularis. In: (Ed.). **Infection and Drug Resistance**. New Zealand: © 2023 Hu et al., v.16, 2023. p.239-241. ISBN 1178-6973.

IBE, C.; MUNRO, C. A. Fungal cell wall: An underexploited target for antifungal therapies. **PLoS Pathogens,** v. 17, n. 4, Apr. 2021. ISSN 1553-7366.

ITOH, K.; TSUTANI, H.; IWASAKI, H. Multifaceted efficacy of caspofungin against fungal infections in COVID-19 patients. **Medical Hypotheses,** v. 164, p. 110876, Jul. 2022. ISSN 0306-9877.

JACOB, T. R. et al. Heat shock protein 90 (Hsp90) as a molecular target for the development of novel drugs against the dermatophyte *Trichophyton rubrum*. **Frontiers in microbiology,** v. 6, p. 1241, Nov. 2015. ISSN 1664-302X.

JAFRI, H.; AHMAD, I. Thymus vulgaris essential oil and thymol inhibit biofilms and interact synergistically with antifungal drugs against drug resistant strains of *Candida albicans* and *Candida tropicalis*. **Journal of Mycologie Medicale,** v. 30, n. 1, p. 100911, Apr. 2020. ISSN 1156-5233.

JAIN, S.; KABI, S.; SWAIN, B. Current Trends of Dermatophytosis in Eastern Odisha. **Journal of Laboratory Physicians,** v. 12, n. 1, p. 10-14, Mar. 2020. ISSN 0974-2727.

JI, Q. et al. Synthesis and biological evaluation of novel phosphoramidate derivatives of coumarin as chitin synthase inhibitors and antifungal agents. **European Journal of Medical Chemistry,** v. 108, p. 166-176, Jan. 2016. ISSN 0223-5234.

JI, Q. et al. Design, synthesis and biological evaluation of novel diazaspirodecanone derivatives containing piperidine-4-carboxamide as chitin synthase inhibitors and antifungal agents. **Bioorganic Chemistry,** v. 114, p. 105108, Sep. 2021. ISSN 0045-2068.

JIA, S. et al. The epidemic of the multiresistant dermatophyte *Trichophyton indotineae* has reached China. **Frontiers in Immunology,** v. 13, p. 1113065, Feb. 2023. ISSN 1664-3224.

JIANG, H. et al. *In Vitro* Interactions of Antifungal Agents and Everolimus Against *Aspergillus* Species. **Frontiers in Cellular and Infection Microbiology,** v. 12, p. 936814, Jul. 2022. ISSN 2235-2988.

KANO, R. et al. Clinical Isolate of a Multi-Antifungal-Resistant *Trichophyton rubrum*. **Antimicrobial Agents and Chemother,** v. 66, n. 4, Apr. 19 2022. ISSN 0066-4804.

KAR, B.; PATEL, P.; FREE, S. J. *Trichophyton rubrum* LysM proteins bind to fungal cell wall chitin and to the N-linked oligosaccharides present on human skin glycoproteins. **PLoS One,** v. 14, n. 4, Apr. 2019. ISSN 1932-6203.

KATENDE, A. et al. Short-course amphotericin B in addition to sertraline and fluconazole for treatment of HIV-associated cryptococcal meningitis in rural Tanzania. **Mycoses,** v. 62, n. 12, p. 1127-1132, Dec. 2019. ISSN 0933-7407.

KATIRAEE, F. et al. Molecular Identification and Antifungal Susceptibility Patterns of Dermatophytes Isolated from Companion Animals with Clinical Symptoms of Dermatophytosis. **Journal of Veterinary Research,** v. 65, n. 2, p. 175-182, Jun. 2021. ISSN 2450-7393.

KAUR, J.; NOBILE, C. J. Antifungal drug-resistance mechanisms in *Candida* biofilms. **Current Opinion in Microbiology,** v. 71, p. 102237, Feb. 2023. ISSN 1369-5274.

KHAN, S. S.; HAY, R. J.; SAUNTE, D. M. L. A Review of Antifungal Susceptibility Testing for Dermatophyte Fungi and It's Correlation with Previous Exposure and Clinical Responses. **Jornal of Fungi (Basel),** v. 8, n. 12, Dec. 2022. ISSN 2309-608x.

KHARI, A. et al. *Candida auris* biofilm: a review on model to mechanism conservation. **Expert Review of Anti-Infective Therapy,** v. 21, n. 3, p. 295-308, Mar. 2023. ISSN 1478-7210.

KHURANA, A. et al. Multidrug resistant tinea corporis/cruris: Response to voriconazole. **Journal of Medical Mycology,** v. 32, n. 4, p. 101306, Nov. 2022. ISSN 1156-5233.

KHURANA, A.; SARDANA, K.; CHOWDHARY, A. Antifungal resistance in dermatophytes: Recent trends and therapeutic implications. **Fungal and Genetics and Biology,** v. 132, p. 103255, Nov. 2019. ISSN 1087-1845.

KONG, X. et al. Antifungal Susceptibility and Mutations in the Squalene Epoxidase Gene in Dermatophytes of the *Trichophyton mentagrophytes* Species Complex. **Antimicrobial Agents and Chemotherapy,** v. 65, n. 8, Jul. 2021. ISSN 0066-4804.

KORECKA, K. et al. Fungal infections of the feet in patients with erysipelas of the lower limb: is it a significant clinical problem? **Infection,** v. 49, n. 4, p. 671-676, Aug. 2021. ISSN 0300-8126.

KOWALSKI, C. H. et al. Fungal biofilm architecture produces hypoxic microenvironments that drive antifungal resistance. **Proceedings of the National Academy of Sciences of the United States of America,** v. 117, n. 36, p. 22473-22483, Sep. 2020. ISSN 0027-8424.

KUTKAT, O. et al. Robust antiviral activity of commonly prescribed antidepressants against emerging coronaviruses: *in vitro* and *in silico* drug repurposing studies. **Scientific Reports,** v. 12, n. 1, p. 12920, Jul. 2022. ISSN 2045-2322.

LANG, E. A. S. et al. The stuA gene controls development, adaptation, stress tolerance, and virulence of the dermatophyte *Trichophyton rubrum*. **Microbiological Research,** v. 241, p. 126592, Dec. 2020. ISSN 0944-5013.

LASS-FLÖRL, C. et al. Antifungal activity against *Candida* species of the selective serotonin-reuptake inhibitor, sertraline. **Clinical Infection Disease,** v. 33, n. 12, p. E135-6, Dec. 15 2001. ISSN 1058-4838.

LI, F. et al. The Effect of Cyclosporin A on *Aspergillus niger* and the Possible Mechanisms Involved. **Foods,** v. 12, n. 3, Jan. 2023. ISSN 2304-8158.

LI, J. et al. Novel *ERG11* and TAC1b mutations associated with azole resistance in *Candida auris*. **Antimicrobial Agents and Chemotherapy,** v. 65, n. 5, May. 2023. ISSN 0066-4804.

LI, T. et al. Activity and Mechanism of Action of Antifungal Peptides from Microorganisms: A Review. **Molecules,** v. 26, n. 11, Jun. 2021. ISSN 1420-3049.

LIPNER, S. R.; SCHER, R. K. Onychomycosis: Treatment and prevention of recurrence. **Journal of the American Academy of Dermatology,** v. 80, n. 4, p. 853-867, Apr. 2019. ISSN 0190-9622.

LIU, S. et al. Filamentous fungal biofilms: Conserved and unique aspects of extracellular matrix composition, mechanisms of drug resistance and regulatory networks in *Aspergillus fumigatus*. **NPJ Biofilms Microbiomes,** v. 8, n. 1, p. 83, Oct. 2022. ISSN 2055-5008.

LIVAK, K. J.; SCHMITTGEN, T. D. Analysis of relative gene expression data using real-time quantitative PCR and the $2^{-\Delta\Delta CT}$ method. **Methods,** v. 25, n. 4, p. 402-408, Dec. 2001. ISSN 1046-2023.

LOCHMANN, D.; RICHARDSON, T. Selective Serotonin Reuptake Inhibitors. **Handbook of Experimental Pharmacology,** v. 250, p. 135-144, Mar. 2019. ISSN 0171-2004.

LOHSE, M. B. et al. Development and regulation of single- and multi-species *Candida albicans* biofilms. **Nature Reviews Microbiology,** v. 16, n. 1, p. 19-31, Jan. 2018. ISSN 1740-1526.

LOPES, L. et al. Genes coding for LysM domains in the dermatophyte *Trichophyton rubrum*: A transcription analysis. **Medical Mycology,** v. 58, n. 3, p. 372-379, Apr. 2020. ISSN 1369-3786.

LOPES, M. E. R. et al. Alternative Splicing in *Trichophyton rubrum* Occurs in Efflux Pump Transcripts in Response to Antifungal Drugs. **Journal of Fungi (Basel),** v. 8, n. 8, Aug. 2022. ISSN 2309-608x.

LOVE, M. I.; HUBER, W.; ANDERS, S. Moderated estimation of fold change and dispersion for RNA-seq data with DESeq2. **Genome Biology,** v. 15, n. 12, p. 550, Dec. 2014. ISSN 1465-6906.

MARTINEZ-ROSSI, N. M. et al. Heat shock proteins in dermatophytes: current advances and perspectives. **Current genomics,** v. 17, n. 2, p. 99-111, Apr. 2016. ISSN 1389-2029.

MARKANTONATOU, A. M.; SAMARAS, K.; VYZANTIADIS, T. A. Dermatophytic Biofilms: Characteristics, Significance and Treatment Approaches. **Journal of Fungi (Basel),** v. 9, n. 2, Feb. 2023. ISSN 2309-608x.

MARTINEZ-ROSSI, N. M. et al. Dermatophyte Resistance to Antifungal Drugs: Mechanisms and Prospectus. **Frontiers in Microbiology,** v. 9, p. 1108, May. 2018. ISSN 1664-302X.

MARTINEZ-ROSSI, N. M.; PERES, N. T.; ROSSI, A. Pathogenesis of Dermatophytosis: Sensing the Host Tissue. **Mycopathologia,** v. 182, n. 1-2, p. 215-227, Feb. 2017. ISSN 0301-486x.

MARTINEZ-ROSSI, N. M. et al. State-of-the-Art Dermatophyte Infections: Epidemiology Aspects, Pathophysiology, and Resistance Mechanisms. **Journal of Fungi (Basel),** v. 7, n. 8, Aug. 2021. ISSN 2309-608x.

MARTINS, M. P. et al. Compensatory expression of multidrug-resistance genes encoding ABC transporters in dermatophytes. **Journal of Medical Microbiology,** v. 65, n. 7, p. 605-610, Jul. 2016. ISSN 0022-2615.

MARTINS, M. P. et al. Comprehensive analysis of the dermatophyte *Trichophyton rubrum* transcriptional profile reveals dynamic metabolic modulation. **Biochemical Journal,** v. 477, n. 5, p. 873-885, Mar. 2020. ISSN 0264-6021.

MARTINS, M. P. et al. Global Analysis of Cell Wall Genes Revealed Putative Virulence Factors in the Dermatophyte *Trichophyton rubrum*. **Frontiers in Microbiology,** v. 10, Sep. 2019. ISSN 1664-302X.

MARTINS-SANTANA, L. et al. Addressing Microbial Resistance Worldwide: Challenges over Controlling Life-Threatening Fungal Infections. **Pathogens,** v. 12, n. 2, Feb. 2023. ISSN 2076-0817.

MAXFIELD, L.; PREUSS, C. V.; BERMUDEZ, R. Terbinafine. In: (Ed.). **StatPearls**. Treasure Island (FL): StatPearls Publishing Copyright © 2023, StatPearls Publishing LLC., 2023.

MEMON, S. et al. Analysis of *fks1* and *fks2* gene mutations in invasive *Candida glabrata* strains from Pakistan. **Mycoses,** v. 66, n. 1, p. 52-58, Jan. 2023. ISSN 0933-7407.

MENDES, N. S. et al. Transcriptome-wide survey of gene expression changes and alternative splicing in *Trichophyton rubrum* in response to undecanoic acid. **Scientific Reports,** v. 8, n. 1, p. 2520, Feb. 2018. ISSN 2045-2322.

MISHRA, S. et al. Therapeutic Strategies against Biofilm Infections. **Life (Basel),** v. 13, n. 1, Jan. 2023. ISSN 2075-1729.

MOHAMMADIFARD, H. et al. Molecular study and antifungal susceptibility profile of *Trichophyton rubrum* and *Trichophyton mentagrophytes* strains isolated from lesions of humans and cattle. **Iranian Journal of Microbiology,** v. 14, n. 4, p. 587-597, Aug. 2022. ISSN 2008-3289.

MONOD, M. et al. *Trichophyton rubrum* Azole Resistance Mediated by a New ABC Transporter, TruMDR3. **Antimicrobial Agents and Chemother,** v. 63, n. 11, Nov. 2019. ISSN 0066-4804.

MOREIRA-WALSH, B. et al. Membrane Integrity Contributes to Resistance of *Cryptococcus neoformans* to the Cell Wall Inhibitor Caspofungin. **mSphere,** v. 7, n. 4, Aug. 2022. ISSN 2379-5042.

MORELLI, K. A.; KERKAERT, J. D.; CRAMER, R. A. *Aspergillus fumigatus* biofilms: Toward understanding how growth as a multicellular network increases antifungal resistance and disease progression. **PLoS Pathogens,** v. 17, n. 8, Aug. 2021. ISSN 1553-7366.

MOSELEY, I. et al. Onychomycosis in underrepresented groups: an all of us database analysis. **Archives of Dermatological Research,** v. 315, n. 3, p. 647-651, Apr. 2023. ISSN 0340-3696.

MOSKALUK, A. E.; VANDEWOUDE, S. Current Topics in Dermatophyte Classification and Clinical Diagnosis. **Pathogens,** v. 11, n. 9, Aug. 2022. ISSN 2076-0817.

MULARONI, A.; GRAZIANO, E.; TODARO, F. Invasive *Trichophyton* infection in a liver transplant recipient. **Transplant Infectious Disease,** v. 24, n. 2, Apr. 2022. ISSN 1398-2273.

NAVARRO-PÉREZ, D. et al. Onychomycosis associated with diabetic foot syndrome: A systematic review. **Mycoses,** v. 66, n. 6, p. 459-466, Jun. 2023. ISSN 0933-7407.

NEDAHL, M.; JOHANSEN, S. S.; LINNET, K. Reference Brain/Blood Concentrations of Citalopram, Duloxetine, Mirtazapine and Sertraline. **Journal of Analytical Toxicology,** v. 42, n. 3, p. 149-156, Apr. 2018. ISSN 0146-4760.

NENOFF, P. et al. Mycology - an update. Part 1: Dermatomycoses: causative agents, epidemiology and pathogenesis. **Journal Dtsch Dermatology Gesellschaft,** v. 12, n. 3, p. 188-209, Mar. 2014. ISSN 1610-0379.

NETT, J. E.; POHL, C. H. Editorial: Fungal Biofilms in Infection and Disease. **Frontiers Cellular in Infection Microbiology,** v. 11, p. 753650, Aug. 2021. ISSN 2235-2988.

NOGUCHI, H. et al. Dermatophytoma caused by terbinafine-resistant *Trichophyton rubrum* treated with fosravuconazole. **The Journal of Dermatology,** v. 49, n. 11, p. 407-408, Nov. 2022. ISSN 0385-2407.

ODDS, F. C.; BROWN, A. J.; GOW, N. A. Antifungal agents: mechanisms of action. **Trends in Microbiology,** v. 11, n. 6, p. 272-9, Jun. 2003. ISSN 0966-842X.

OLIVEIRA, A. S. et al. Anti-Candida activity of antidepressants sertraline and fluoxetine: effect upon pre-formed biofilms. **Medical Microbiology and Immunology,** v. 207, n. 3-4, p. 195-200, Aug. 2018. ISSN 0300-8584.

PAPON, N.; GOLDMAN, G. H. Unraveling Caspofungin Resistance in *Cryptococcus neoformans*. **mBio,** v. 12, n. 2, Mar. 2021.

PAUL, S. et al. AtrR Is an Essential Determinant of Azole Resistance in *Aspergillus fumigatus*. **mBio,** v. 10, n. 2, Mar. 2019.

PEREIRA, F. O. A review of recent research on antifungal agents against dermatophyte biofilms. **Medical Mycology,** v. 59, n. 4, p. 313-326, Apr. 2021. ISSN 1369-3786.

PEREIRA, R. et al. Biofilm of *Candida albicans*: formation, regulation and resistance. **Journal Applied Microbiology,** v. 131, n. 1, p. 11-22, Jul. 2021. ISSN 1364-5072.

PERES, N. T. A. et al. The bZIP Ap1 transcription factor is a negative regulator of virulence attributes of the anthropophilic dermatophyte *Trichophyton rubrum*. **Current Research in Microbial Sciences,** v. 3, p. 100132, Apr. 2022. ISSN 2666-5174.

PERES, N. T. D. A. et al. *In vitro* and *ex vivo* infection models help assess the molecular aspects of the interaction of *Trichophyton rubrum* with the host milieu. **Sabouraudia,** v. 54, n. 4, p. 420-427, May. 2016. ISSN 0036-2174.

PERLIN, D. S.; RAUTEMAA-RICHARDSON, R.; ALASTRUEY-IZQUIERDO, A. The global problem of antifungal resistance: prevalence, mechanisms, and management. **The Lancet Infectious Diseases,** v. 17, n. 12, p. 383-392, Dec. 2017. ISSN 1473-3099.

PERRINE-WALKER, F. Caspofungin resistance in *Candida albicans*: genetic factors and synergistic compounds for combination therapies. **Brazilian Journal of Microbiology,** v. 53, n. 3, p. 1101-1113, Sep. 2022. ISSN 1517-8382.

PETRUCELLI, M. F. et al. The transcriptional profile of *Trichophyton rubrum* co-cultured with human keratinocytes shows new insights about gene modulation by terbinafine. **Pathogens,** v. 8, n. 4, p. 274, Nov. 2019.

PINTO Â, V. et al. Potentiation of antifungal activity of terbinafine by dihydrojasmone and terpinolene against dermatophytes. **Letters in Applied Microbiology,** v. 72, n. 3, p. 292-298, Mar. 2021. ISSN 0266-8254.

PÉREZ-CANTERO, A. et al. Azole resistance mechanisms in *Aspergillus*: update and recent advances. **International Journal of Antimicrobial Agents,** v. 55, n. 1, p. 105807, Jan. 2020. ISSN 0924-8579.

QADRI, H. et al. Quinidine drug resistance transporter knockout *Candida* cells modulate glucose transporter expression and accumulate metabolites leading to enhanced azole drug resistance. **Fungal Genetics and Biology,** v. 161, p. 103713, Jul. 2022. ISSN 1087-1845.

RAMAGE, G. et al. Our current clinical understanding of *Candida biofilms*: where are we two decades on? **Journal of Pathology**, **Microbiology and Immunology**. v. 131, n. 11, p. 636-653, Mar. 2023. ISSN 0903-4641.

RAN, X.; ZHUANG, K.; RAN, Y. Tinea corporis on the stump leg with *Trichophyton rubrum* infection. **Medical Mycology Case Reports,** v. 9, p. 31-3, Sep. 2015. ISSN 2211-7539.

REICHHARDT, C. et al. Integration of electron microscopy and solid-state NMR analysis for new views and compositional parameters of *Aspergillus fumigatus* biofilms. **Medical Mycology,** v. 57, n. Supplement_2, p. S239-s244, Apr. 2019. ISSN 1369-3786.

RIES, L. N. A. et al. The *Aspergillus fumigatus* CrzA Transcription Factor Activates Chitin Synthase Gene Expression during the Caspofungin Paradoxical Effect. **mBio,** v. 8, n. 3, Jun. 2017.

ROBBINS, N.; CAPLAN, T.; COWEN, L. E. Molecular Evolution of Antifungal Drug Resistance. **Annual Review of Microbiology,** v. 71, p. 753-775, Sep. 2017. ISSN 0066-4227.

RODRIGUES, D. S. et al. Sertraline has *in vitro* activity against both mature and forming biofilms of different *Candida* species. **Journal of Medical Microbiology,** v. 72, n. 2, Feb. 2023. ISSN 0022-2615.

ROSSATO, L. et al. *In vitro* synergistic effects of chlorpromazine and sertraline in combination with amphotericin B against *Cryptococcus neoformans var. grubii*. **Folia Microbiology (Praha),** v. 61, n. 5, p. 399-403, Sep. 2016. ISSN 0015-5632.

ROSSATO, L. et al. *In vitro* activity of immunosuppressive agents against *Cryptococcus neoformans*. **Enfermedades Infecciosas y Microbiologia Clinica (Engl Ed),** v. 40, n. 2, p. 86-88, Feb. 2022. ISSN 2529-993x.

ROSSI, A. et al. Reassessing the Use of Undecanoic Acid as a Therapeutic Strategy for Treating Fungal Infections. **Mycopathologia,** v. 186, n. 3, p. 327-340, Jun. 2021. ISSN 0301-486x.

RUSH, C. L. et al. Natural product-guided discovery of a fungal chitinase inhibitor. **Chemistry & Biology,** v. 17, n. 12, p. 1275-81, Dec. 2010. ISSN 1074-5521.

SANTOS, H. L. et al. Terbinafine resistance conferred by multiple copies of the salicylate 1-monooxygenase gene in *Trichophyton rubrum*. **Medical Mycology,** v. 56, n. 3, p. 378-381, Apr. 2018. ISSN 1369-3786.

SARDANA, K.; GUPTA, A.; MATHACHAN, S. R. Immunopathogenesis of Dermatophytoses and Factors Leading to Recalcitrant Infections. **Indian Dermatology Online Journal,** v. 12, n. 3, p. 389-399, May-Jun. 2021. ISSN 2229-5178.

SEAGLE, E. E.; WILLIAMS, S. L.; CHILLER, T. M. Recent Trends in the Epidemiology of Fungal Infections. **Infectious Disease Clinics of North America,** v. 35, n. 2, p. 237-260, Jun. 2021. ISSN 0891-5520.

SHAFIEI, M. et al. History of the development of antifungal azoles: A review on structures, SAR, and mechanism of action. **Bioorganic Chemistry,** v. 104, p. 104240, Nov. 2020. ISSN 0045-2068.

SHEN, J. J. et al. The Emerging Terbinafine-Resistant *Trichophyton* Epidemic: What Is the Role of Antifungal Susceptibility Testing? **Dermatology,** v. 238, n. 1, p. 60-79, May. 2022. ISSN 1018-8665.

SILVEIRA, H. C. et al. Transcriptional profiling reveals genes in the human pathogen *Trichophyton rubrum* that are expressed in response to pH signaling. **Microbial Pathogenesis,** v. 48, n. 2, p. 91-6, Feb. 2010. ISSN 0882-4010.

SILVERMAN, S. J. et al. Chitin synthase 2 is essential for septum formation and cell division in *Saccharomyces cerevisiae*. **Proceedings of the National Academy of Sciences,** v. 85, n. 13, p. 4735-4739, Jul. 1988. ISSN 0027-8424.

SIMONSEN, J. K. et al. Deep dermatophytosis in an immunocompetent adult with no prior history of skin disease. In: (Ed.). **Medical Mycology Case Reports**. Netherlands: © 2023 The Authors., v.39, 2023. p.31-33. ISBN 2211-7539 (Print).

SONG, G. et al. Epidemiology of Onychomycosis in Chinese Mainland: A 30-year Retrospective Study. **Mycopathologia,** v. 187, n. 4, p. 323-331, Aug. 2022. ISSN 0301-486x.

SPALLONE, A.; SCHWARTZ, I. S. Emerging Fungal Infections. **Infectious Disease Clinics of North America,** v. 35, n. 2, p. 261-277, Jun. 2021. ISSN 0891-5520.

STANZIONE, I. et al. Innovative surface bio-functionalization by fungal hydrophobins and their engineered variants. **Frontiers Molecular Biosciences,** v. 9, p. 959166, Aug. 2022. ISSN 2296-889X.

SU, S. et al. The antifungal activity of caspofungin in combination with antifungals or non-antifungals against *Candida* species *in vitro* and in clinical therapy. **Expert Review of Anti-infective Therapy,** v. 20, n. 2, p. 161-178, Feb. 2022. ISSN 1478-7210.

SUCHER, A. J.; CHAHINE, E. B.; BALCER, H. E. Echinocandins: the newest class of antifungals. **Annals of Pharmacotherapy,** v. 43, n. 10, p. 1647-57, Oct. 2009. ISSN 1060-0280.

SUN, L.; LIAO, K. The Effect of Honokiol on Ergosterol Biosynthesis and Vacuole Function in *Candida albicans*. **Journal of Microbiology Biotechnology,** v. 30, n. 12, p. 1835-1842, Dec. 2020. ISSN 1017-7825.

SZUHANY, K. L.; SIMON, N. M. Anxiety Disorders: A Review. **Jama,** v. 328, n. 24, p. 2431-2445, Dec. 2022. ISSN 0098-7484.

SZYMAŃSKI, M. et al. Echinocandins - structure, mechanism of action and use in antifungal therapy. **Journal of Enzyme Inhibition and Medical Chemistry,** v. 37, n. 1, p. 876-894, Dec. 2022. ISSN 1475-6366.

TANAKA, T. et al. *Aspergillus* Hydrophobins: Physicochemical Properties, Biochemical Properties, and Functions in Solid Polymer Degradation. **Microorganisms,** v. 10, n. 8, Jul. 2022. ISSN 2076-2607.

TEKINTAŞ, Y. et al. Antifungal and Antibiofilm Activities of Selective Serotonin Reuptake Inhibitors Alone and in Combination with Fluconazole. **Turkish Journal of Pharmaceutical Sciences,** v. 17, n. 6, p. 667-672, Dec. 2020. ISSN 1304-530X.

THOMPSON, G. R., 3RD et al. Rezafungin versus caspofungin for treatment of candidaemia and invasive candidiasis (ReSTORE): a multicentre, double-blind, double-dummy, randomised phase 3 trial. **Lancet,** v. 401, n. 10370, p. 49-59, Jan. 2023. ISSN 0140-6736.

THORVALDSDÓTTIR, H.; ROBINSON, J. T.; MESIROV, J. P. Integrative Genomics Viewer (IGV): high-performance genomics data visualization and exploration. **Briefings in Bioinformatics,** v. 14, n. 2, p. 178-92, Mar. 2013. ISSN 1467-5463.

TREMAINE, L. M.; WELCH, W. M.; RONFELD, R. A. Metabolism and disposition of the 5-hydroxytryptamine uptake blocker sertraline in the rat and dog. **Drug metabolism and disposition,** v. 17, n. 5, p. 542-550, Sep-Oct. 1989. ISSN 0090-9556.

TREVIÑO-RANGEL RDE, J. et al. Activity of sertraline against *Cryptococcus neoformans*: *in vitro* and *in vivo* assays. **Medical Mycology,** v. 54, n. 3, p. 280-6, Mar. 2016. ISSN 1369-3786.

TREVIÑO-RANGEL, R. J. et al. *In vivo* evaluation of the antifungal activity of sertraline against *Aspergillus fumigatus*. **Journal of Antimicrobial Chemotherapy,** v. 74, n. 3, p. 663-666, Mar. 2019. ISSN 0305-7453.

TSENG, K. C. et al. Antidepressant Sertraline Is a Broad-Spectrum Inhibitor of Enteroviruses Targeting Viral Entry through Neutralization of Endolysosomal Acidification. **Viruses,** v. 14, n. 1, Jan. 2022. ISSN 1999-4915.

VALERO, C. et al. *Aspergillus fumigatus* Transcription Factors Involved in the Caspofungin Paradoxical Effect. **mBio,** v. 11, n. 3, Jun. 2020.

VELÁSQUEZ AGUDELO, V. et al. [Evaluation of the usefulness of nail biopsy in the diagnosis of onychomycosis]. **Revista Iberoamericana de Micología,** v. 36, n. 2, p. 72-78, Apr-Jun. 2019. ISSN 1130-1406.

VILLANUEVA-LOZANO, H. et al. Evaluation of the expanding spectrum of sertraline against uncommon fungal pathogens. **Journal of Infection and Chemotherapy,** v. 26, n. 3, p. 309-311, Mar. 2020. ISSN 1341-321x.

VILLANUEVA-LOZANO, H. et al. *In vitro* inhibitory activity of sertraline against clinical isolates of *Sporothrix schenckii*. **Revista Iberoamericana de Micología,** v. 36, n. 3, p. 139-141, Jul-Sep. 2019. ISSN 1130-1406.

VÊNCIO, R. Z. et al. BayGO: Bayesian analysis of ontology term enrichment in microarray data. **BMC Bioinformatics,** v. 7, p. 86, Feb. 2006. ISSN 1471-2105.

WANG, Y. et al. Antimicrobial Activity of Sertraline on Listeria monocytogenes. **International Journal Molecular Sciences,** v. 24, n. 5, Feb. 2023. ISSN 1422-0067.

XU, Y. et al. Spiro[benzoxazine-piperidin]-one derivatives as chitin synthase inhibitors and antifungal agents: Design, synthesis and biological evaluation. **European Journal of Medicinal Chemistry,** v. 243, p. 114723, Dec. 2022. ISSN 0223-5234.

YAMADA, T. et al. Gene Amplification of CYP51B: a New Mechanism of Resistance to Azole Compounds in *Trichophyton indotineae*. **Antimicrobial Agents and Chemotherapy,** v. 66, n. 6, Jun. 21 2022. ISSN 0066-4804.

YASSIN, Z. et al. Caspofungin resistance in clinical *Aspergillus flavus* isolates. **Journal of Medical Mycology,** v. 31, n. 4, p. 101166, Dec. 2021. ISSN 1156-5233.

YUN, S. K. et al. Deeper Dermal Dermatophytosis by *Trichophyton rubrum* Infection Mimicking Kaposi Sarcoma. **Mycopathologia,** v. 187, n. 5-6, p. 611-612, Dec. 2022. ISSN 0301-486x.

ZEESHAN, F.; SABIR, M.; UDDIN, F. The rising menace of antifungal resistance in dermatophytes among the patients of tinea capitis. **Journal of the Pakistan Medical Association,** v. 73, n. 1, p. 43-48, Jan. 2023. ISSN 0030-9982.

ZHAI, B. et al. The antidepressant sertraline provides a promising therapeutic option for neurotropic cryptococcal infections. **Antimicrobial agents and chemotherapy,** v. 56, n. 7, p. 3758-3766, Jul. 2012. ISSN 0066-4804.

ZHAN, P. et al. Phylogeny of dermatophytes with genomic character evaluation of clinically distinct *Trichophyton rubrum* and *T. violaceum*. **Studies and Mycology,** v. 89, p. 153-175, Mar. 2018. ISSN 0166-0616.

ZHANG, Q. et al. Drug repurposing strategies in the development of potential antifungal agents. **Applied Microbiology and Biotechnology,** v. 105, n. 13, p. 5259-5279, Jul. 2021. ISSN 0175-7598.

ZHAO, S. et al. Genomic and Molecular Identification of Genes Contributing to the Caspofungin Paradoxical Effect in *Aspergillus fumigatus*. **Microbiology Spectrum,** v. 10, n. 5, Oct. 2022. ISSN 2165-0497.

Anexos: Artigos Publicados

Journal of Fungi

MDPI

Article

Synergism between the Antidepressant Sertraline and Caspofungin as an Approach to Minimise the Virulence and Resistance in the Dermatophyte *Trichophyton rubrum*

Carlos H. Lopes Rocha, Flaviane M. Galvão Rocha, Tamires A. Bitencourt, Maíra P. Martins, Pablo R. Sanches, Antonio Rossi and Nilce M. Martinez-Rossi *

Department of Genetics, Ribeirão Preto Medical School, University of São Paulo, USP, Ribeirao Preto 14049-900, SP, Brazil; henriqueclr16@usp.br (C.H.L.R.); flavianerocha@usp.br (F.M.G.R.); tabitencourt@yahoo.com.br (T.A.B.); mairapompeu@hotmail.com (M.P.M.); psanches@usp.br (P.R.S.); anrossi@usp.br (A.R.)

* Correspondence: nmmrossi@usp.br

Abstract: *Trichophyton rubrum* is responsible for several superficial human mycoses. Novel strategies aimed at controlling this pathogen are being investigated. The objective of this study was to evaluate the antifungal activity of the antidepressant sertraline (SRT), either alone or in combination with caspofungin (CASP). We calculated the minimum inhibitory concentrations of SRT and CASP against *T. rubrum*. Interactions between SRT and CASP were evaluated using a broth microdilution chequerboard. We assessed the differential expression of *T. rubrum* cultivated in the presence of SRT or combinations of SRT and CASP. We used MTT and violet crystal assays to compare the effect of SRT alone on *T. rubrum* biofilms with that of the synergistic combination of SRT and CASP. A human nail infection assay was performed. SRT alone, or in combination with CASP, exhibited antifungal activity against *T. rubrum*. SRT targets genes involved in the biosyntheses of cell wall and ergosterol. Furthermore, the metabolic activity of the *T. rubrum* biofilm and its biomass were affected by SRT and the combination of SRT and CASP. SRT alone, or in combination, shows potential as an approach to minimise resistance and reduce virulence.

Keywords: *Trichophyton rubrum*; dermatophyte; synergistic combinations; antifungal resistance; sertraline; caspofungin and biofilm

check for updates

Citation: Rocha, C.H.L.; Rocha, F.M.G.; Bitencourt, T.A.; Martins, M.P.; Sanches, P.R.; Rossi, A.; Martinez-Rossi, N.M. Synergism between the Antidepressant Sertraline and Caspofungin as an Approach to Minimise the Virulence and Resistance in the Dermatophyte *Trichophyton rubrum*. *J. Fungi* **2022**, *8*, 815. https://doi.org/10.3390/jof8080815

Academic Editors: Aditya K. Gupta and Bianca Maria Piraccini

Received: 5 July 2022
Accepted: 29 July 2022
Published: 3 August 2022

Publisher's Note: MDPI stays neutral with regard to jurisdictional claims in published maps and institutional affiliations.

1. Introduction

Dermatophytosis is a common fungal infection caused by dermatophytes, a class of non-opportunistic pathogens that obtain nutrients from keratinised tissues such as hair, skin, and nails. *Trichophyton rubrum* is a cosmopolitan species often isolated from cutaneous infections and immunocompromised human hosts worldwide, resulting in severe conditions that may lead to public health issues [1]. It is estimates that dermatophytes affect approximately 25% of the world population, wherein 30–70% of adults act as carriers who do not present with clinical manifestations [2]. The damp climate and elevated temperatures of tropical and subtropical regions contribute to the high rate of dermatophytosis [1].

Treating *T. rubrum* infections is challenging because only a few therapeutic options, such as azoles and allylamines that interfere with the ergosterol biosynthesis pathway, are available. Furthermore, in addition to lengthy and costly treatments, several antifungal resistance cases have been reported [3]. Primary defence mechanisms of the host include skin peeling, decreased humidity, skin pH, elevated temperature, and fatty acids. In contrast, fungi develop adaptive responses to overcome these challenges [4]. Fungi trigger several mechanisms that overexpress drug efflux pumps, detoxify enzymes, and modify drug targets, all of which are aimed at tolerating or resisting the effects of antifungals [3,5].

Additionally, surface-based cell population complexes, termed biofilms, contribute to drug resistance, mainly by resisting penetration. These complex structures manifest in the form of an extracellular matrix, characterised by metabolic heterogeneity and upregulated efflux pump-related genes [6,7]; thus, the tracking and identification of compounds with antifungal activity are urgently required [8,9]. In this regard, drug repositioning appears to be an exciting alternative. When repurposing an existing drug for a newer use, drug characteristics, such as toxicity and pharmacokinetics, must already be established [10].

Combining sertraline (SRT), one of the most prescribed antidepressants explored for its antifungal properties, with commercial antifungals represents a promising therapeutic approach that would enhance the therapeutic efficacy [11,12]. SRT significantly reduced the pulmonary fungal burden associated with *Aspergillus fumigatus* infection in a murine aspergillosis model. The same study reported that SRT ensured the survival of 25% of infected larvae of a *Galleria mellonella* aspergillosis model, compared to the high mortality rates observed in infected and untreated larvae [13].

In mammals, SRT selectively inhibits serotonin reuptake by locking the 5-hydroxytryptamine (5-HT) transporter [14]. In yeast cells, SRT targets the phospholipid membranes of acidic organelles, which are part of an intracellular vesicle transport system [15]. SRT also exerts antifungal effects by disrupting translation, thereby inhibiting protein synthesis [11].

A synergistic combination of SRT and amphotericin B improves inhibitory activity against *A. fumigatus*. Notably, combining SRT with itraconazole was also synergistic [16]. Essays on *Cryptococcus neoformans* evidenced the antifungal activity of SRT, either in monotherapy or in synergic combination with fluconazole [16,17]. In addition, SRT exhibited synergistic effects against *Trichosporon asahii* planktonic cells with caspofungin (CASP) [18].

The activity of CASP against dermatophytes is not well defined. Pioneering works have demonstrated that CASP shows excellent activity against the dermatophytes *T. rubrum, Trichophyton interdigitale,* and *Microscoporum canis* [19,20]. Another study showed that CASP promotes several morphological changes, including shortening and induction of aberrant hyphae growth; however, it has reduced efficacy and incompletely inhibited in vitro growth [21].

There are few studies demonstrating the CASP effect with other antifungal agents. In most cases, the combination therapy of CASP with another agent is used for treating infections caused by the genus *Candida* [22,23]. In association with farnesol, CASP significantly inhibited the metabolic activity of *Candida parapsilosis* cells [24]. CASP, with fluconazole and posaconazole, is an effective strategy against *Candida glabrata* [22]. CASP belongs to a class of antifungal agents known as echinocandins, which inhibit the synthesis of the fungal cell wall component, beta-(1,3)-D-glucan.

Thus, owing to the necessity of expanding the range of therapeutics available against dermatophytosis, we hypothesised that SRT combined with CASP might help minimise drug resistance. Furthermore, we evaluated the expression of genes associated with the resistance of *T. rubrum* to SRT alone and its combination with CASP.

2. Materials and Methods

2.1. Strain and Growth Conditions

The *T. rubrum* strain, CBS118892 (Westerdijk Fungal Biodiversity Institute, Utrecht, Netherlands), obtained from a patient with onychomycosis, was cultivated on malt extract agar (Becton Dickinson, Franklin Lakes, NJ, USA) for 35 days at 28 °C, as previously described [25], for total RNA extraction. The fungal suspension was prepared in 0.9% NaCl, following which the conidia concentration was estimated using a Newbauer chamber. Approximately 1×10^6 conidia were added to 100 mL of liquid Sabouraud (SB) at pH 5.7 supplemented with 2% glucose and 1% peptone (Becton Dickinson, Franklin Lakes, NJ, USA), followed by incubation at 28 °C for 96 h under continuous shaking. The resulting mycelia were then transferred to 100 mL of SB in the presence of a sublethal dose (70 mg/L) of SRT (Cayman Chemical, Ann Arbor, MI, USA), in the presence of a sublethal

combination (sc) of 0.273 mg/L SRT + 10.93 mg/L CASP (Merck Sharp & Dohme, São Paulo, SP, Brazil), 0.273 mg/L SRT, 10.93 mg/L CASP, and in the absence of drugs (control), followed by incubation at 28 °C with shaking (120 rpm) for 3 h and 12 h.

2.2. Minimum Inhibitory Concentration (MIC) and Interaction between SRT and CASP

MICs were obtained according to the M38-A reference method recommended by the Clinical and Laboratory Standards Institute (CLSI) [26], with the following modification: 100 µL of the conidial suspension, amounting to 6×10^4 conidia/mL, was added to each well in the 96-well microtitre plate. The final conidial concentration was adjusted to approximately 3×10^4 conidia per well in RPMI 1640 (Sigma-Aldrich, St Louis, MO, USA) or SB medium. RPMI was buffered with 0.165 M morpholinepropanesulfonic acid (MOPS) (Sigma-Aldrich), and the pH was adjusted to 7.0. SRT and CASP were prepared as stock solutions in dimethyl sulfoxide (DMSO, Sigma-Aldrich): SRT (50,000 mg/L); and CASP (5000 mg/L). Serial dilutions of SRT and CASP were performed in RPMI medium, buffered with 0.165 M morpholinepropanesulfonic acid (MOPS), or SB medium. The final concentrations of SRT ranged between 0.78–200 mg/L, whereas those of CASP ranged between 0.98–250 mg/L. Interactions between SRT and CASP were evaluated using a broth microdilution chequerboard and quantified using the fractional inhibitory concentration index (FICI): FICI $\leq$ 0.5, FICI > 0.5 to $\leq$ 4.0, and FICI > 4.0 were categorised as synergism, indifference, and antagonism, respectively [27]. FICIs were calculated for all possible combinations of different concentrations. The results were expressed as the mean of FICIs. Assay plates were used to determine MICs, and the broth microdilution chequerboard was incubated at 28 °C for seven days. Growth controls were performed in wells containing only the fungal suspension and medium. Individual and combined MICs were defined by comparison with growth controls performed in wells containing only fungal suspension and media, with complete growth inhibition. All experiments were performed in triplicate.

2.3. Total RNA Extraction and cDNA Synthesis

Total RNA was extracted from *T. rubrum*, cultivated in the presence of SRT alone and SRT combined with CASP, using an Illustra RNAspin mini-isolation kit (GE Healthcare, Chicago, IL, USA). Mycelia were ground via mechanical pulverisation using a mortar and pestle in liquid nitrogen, and RNA samples were treated with RNase-free DNase I (Sigma-Aldrich). Complementary DNA (cDNA) was synthesised from each condition containing 1000 ng of total RNA in a 20 µL reaction volume using a High-Capacity cDNA Synthesis kit (Applied Biosystems, Waltham, MA, USA). Equal amounts of RNA from three independent biological replicates were used to synthesise cDNA.

2.4. RT-qPCR Analysis

Gene expression was quantified via qPCR using a StepOnePlus Real-Time PCR system (Applied Biosystems). PCR reactions were performed with specific primer pairs designed using Prime3Plus software (https://www.bioinformatics.nl/cgi-bin/primer3plus/primer3plus.cgi (accessed on 4 July 2022)) and specificity (Table S1). Each qPCR reaction was performed using a final volume of 12.5 µL: 0.5 µL primer, 6.25 µL SYBR Green PCR Master Mix (Applied Biosystem, Waltham, MA, USA), and 70 ng cDNA. The thermocycler conditions for RT-qPCR were 95 °C for 10 min, followed by 40 cycles of 95 °C for 15 s and 60 °C for 1 min. We selected genes encoding the enzymes glyceraldehyde 3 phosphate dehydrogenase (*gapdh*) and DNA-dependent RNA polymerase II (*rpb2*) as endogenous controls. Data were derived from three independent replicates, and the $2^{-\Delta\Delta ct}$ method was used to assess the relative quantification of responsive genes [28].

2.5. In Vitro Biofilm Formation

T. rubrum biofilms were formed according to a previously described method [29], with some modifications. *T. rubrum* CBS118892 was grown on malt extract agar for 15 days at 28 °C. The fungal suspension was prepared in 0.9% NaCl, and the conidial concentration

was adjusted to approximately 1×10^6 conidia/mL. The plates were initially incubated at 37 °C for 4 h without agitation for pre-adhesion.

2.6. Metabolic Activity of the Biofilm by MTT Assay

Following pre-adhesion, treatments consisting of 200 µL each of SRT (12.5 mg/L, and 3.12 mg/L), CASP (15.62 mg/L, and 1.95 mg/L), and SRT + CASP (3.12 mg/L + 1.95 mg/L respectively) prepared in RPMI 1640 medium, supplemented with 2% of glucose, were added into the wells. Biofilms were prepared at different time points (0, 24, 48, 72, and 96 h). Following each incubation, 2 µL of menadione (Sigma-Aldrich) and 20 µL of MTT (Sigma-Aldrich) at 5000 mg/L were added to each well. The plates were incubated at 37 °C for 4 h. Colorimetric changes were measured using an ELISA reader (Thermo Fisher Scientific, Waltham, MA, USA) at 550 nm. A control was prepared by adding 200 µL of untreated conidial suspension to each well.

2.7. Quantification of In Vitro Biofilm by Crystal Violet

Following pre-adhesion, the supernatant was removed from the wells and washed thrice with 0.9% sterile saline, after which 200 µL RPMI 1640 medium supplemented with 2% glucose was added to each well. Three independent biological replicates were incubated at 37 °C for 72 h for biofilm maturation. Following biofilm formation, culture medium was removed and treatments comprising 200 µL each of SRT 25 mg/L, SRT 6.25 mg/L, CASP 62.50 mg/L, CASP 1.95 mg/L, and SRT 6.25 mg/L + CASP 1.95 mg/L were added to wells. The treatments were prepared in RPMI 1640 medium supplemented with 2% glucose. Replicates were incubated at 37 °C for 3–7 days. Next, the drugs were removed, and each well was washed thrice with 0.01 M PBS (pH 7.2), following which 100 µL of crystal violet solution was added to each well to quantify biomass. Then, each well was washed twice with sterile water, treated with 100 µL of 95% ethanol and carefully homogenised. The resulting solution was transferred to a new 96-well plate and read using an ELISA reader at a wavelength of 550 nm. A control consisting of 200 µL of untreated conidial suspension was added to each well.

2.8. Assessment of Biofilms in Human Nails

The human nail infection assay was performed as previously described [29], with some modifications. Human nail fragments (1 mm^2) obtained from healthy donors were initially sterilised by autoclaving and transferred to water agar-containing 24-well plates. The fragments were infected with 2 mL suspension prepared in sterile saline 0.9% (NaCl), and conidia concentration was adjusted to approximately 3×10^4 conidia per well. After 4 h of pre-adhesion at 37 °C, the suspension was removed, and each well was washed thrice with 0.9% sterile saline. Next, 2 mL of 0.9% sterile saline was added to each well, following which the plates were incubated for 20 days at 28 °C. Then, 2 mL each of SRT 50 mg/L, SRT 12.5 mg/L, CASP 62.50 mg/L, CASP 3.90 mg/L, and SRT 12.5 mg/L + CASP 3.90 mg/L prepared in 0.9% sterile saline were added to wells daily for seven days. After seven days, the biofilms were analysed using scanning electron microscopy. The assay was conducted according to the Medical School Ethics Committee and approved per protocol number 4.304.317/2020.

2.9. Scanning Electron Microscopy

The samples were initially fixed using 3% glutaraldehyde in 0.1% phosphate buffer (*v*/*v*) (pH 7.2) at 4 °C for 24 h and rinsed with 0.1% phosphate buffer (pH 7.2). Osmium tetroxide (1%) was used during the post-fixation step. Subsequently, the samples were dehydrated in an increasing ethanol gradient involving successive baths of increasing ethanol concentrations. Gold was then spray-coated on these samples to visualise biofilms formed in human nails. A JEOL JSM-6610 LV scanning electron microscope at an acceleration voltage of 25 kV was used for visualisation.

2.10. Statistical Analysis

We calculated the gene expression using the comparative $2^{-\Delta\Delta CT}$ method. The paired Student's *t*-test was used to compare gene expression between treatment and control conditions at each time point. The results are reported as the mean ± standard deviation of three independent biological replicas. For comparing the biofilm's metabolic activity and quantification biomass, one-way ANOVA was used, followed by Tukey's post hoc test. For all tests, statistical significance was adopted at $p < 0.05$. Prism v. 5.1 (GraphPad Software, San Diego, CA, USA) was used to generate the graphs and statistical analyses.

3. Results

3.1. Antifungal Susceptibility and Interaction between SRT and CASP

SRT alone and in combination with CASP exhibited antifungal activity against *T. rubrum* free-flowing planktonic cells. The MIC of SRT required to inhibit *T. rubrum* in RPMI medium was 25 mg/L, whereas that of CASP was 31.25 mg/L. The MICs of SRT and CASP increased considerably when the assay was performed in the SB medium. In this medium, SRT showed a MIC of 100 mg/L, whereas CASP showed a MIC of 62.50 mg/L. The interactions between SRT/CASP in both culture media (RPMI or SB) could be considered synergistic (FICI ≤ 0.5). Assays performed in both media indicated that the FICIs corresponding to the SRT/CASP combination ranged between 0.1–0.5. The mean FICIs in the RPMI and SB medium were 0.28 and 0.25, respectively (Table 1). The combined MIC values associated with synergism between SRT and CASP are displayed (Table 2).

Table 1. MICs of sertraline (SRT) and caspofungin (CASP) against planktonic forms of *T. rubrum*. FICI and the mean of FICI of interactions between SRT and CASP.

Medium	MIC_{100}-mg/L		FICI Range	FICI (Mean)
	SRT	CASP	SRT/CASP	SRT/CASP
SB	100	62.50	0.1–0.50	0.25
RPMI	25	31.25	0.1–0.50	0.28

FICI ≤ 0.5, FICI > 0.5 to ≤4.0, and FICI > 4.0 were categorised as synergism, indifference, and antagonism, respectively.

Table 2. MICcb (combined MICs) values for analysis of synergism between sertraline (SRT) and caspofungin (CASP) in assays performed in RPMI medium and Sabouraud (SB) medium.

Medium	Drug	Concentrations Ranged of the SRT (mg/L)								
		200	100	50	25	12.5	6.25	3.12	1.56	0.78
SB	CASP	0	0	1.95	1.95	1.95	1.95	7.81	15.62	15.62
RPMI	(mg/mL)	0	0	0	0	0.98	0.98	1.95	1.95	3.90

3.2. RT-qPCR

RT-qPCR-based gene expression analysis revealed that an SRT concentration amounting to 70% of its MIC induced a gene encoding a transporter (*TERG_00162*) belonging to the major facilitator superfamily (MFS) at 3 and 12 h. In contrast, exposure to SRT for 3 and 12 h downregulated *TERG_12319*, a critical chitin synthase-associated gene linked to fungal virulence and cell wall remodelling. Furthermore, *TERG_04234*, encoding hydrophobin, a putative protein essential for fungal pathogenesis, and *TERG_06755*, encoding a c-8 sterol isomerase protein, required for the ergosterol pathway, were downregulated at 3 and 12 h, respectively (Figure 1).

Gene expression analysis using RT-qPCR was extended to examine *T. rubrum* growth in the presence of the SRT + antifungal CASP combination. SRT + CASP exposure downregulated gene transcription of the MFS multidrug transporter, *TERG_00162*, at 3 and 12 h, in contrast to the induction caused by the SRT alone. In contrast, SRT + CASP downregulated *TERG_04234* and *TERG_06755*, as well as the gene encoding the enzyme chitin synthase, *TERG_12319*, which was similar to that observed under conditions involving the use of SRT alone (Figure 2).

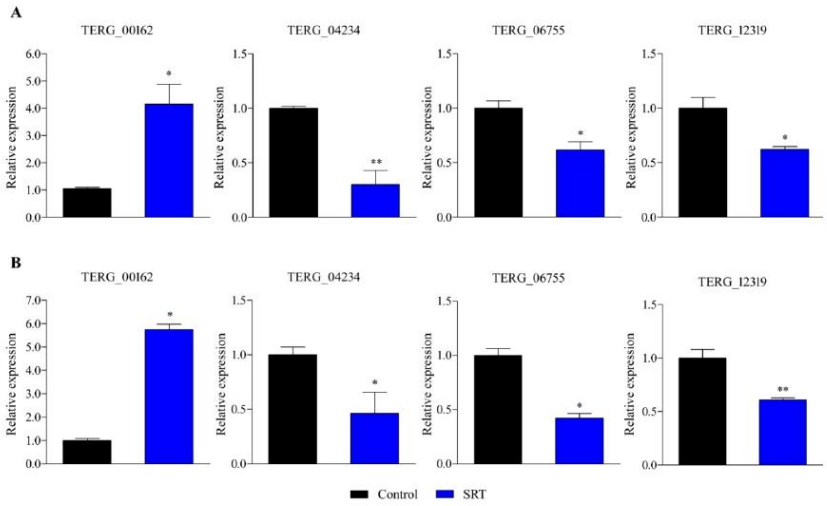

Figure 1. Differentially expressed genes in response to SRT, identified using RT-qPCR analysis. The relative expression of genes *TERG_00162* (MFS multidrug transporter), *TERG_04234* (Hydrophobin), *TERG_06755* (C-8 sterol isomerase), and *TERG_12319* (Chitin synthase 2) at 3 h (**A**) and 12 h (**B**) are represented. Asterisks indicate the statistical significance of the *t*-test compared to the control (SB drug absence). * $p < 0.05$; and ** $p < 0.01$.

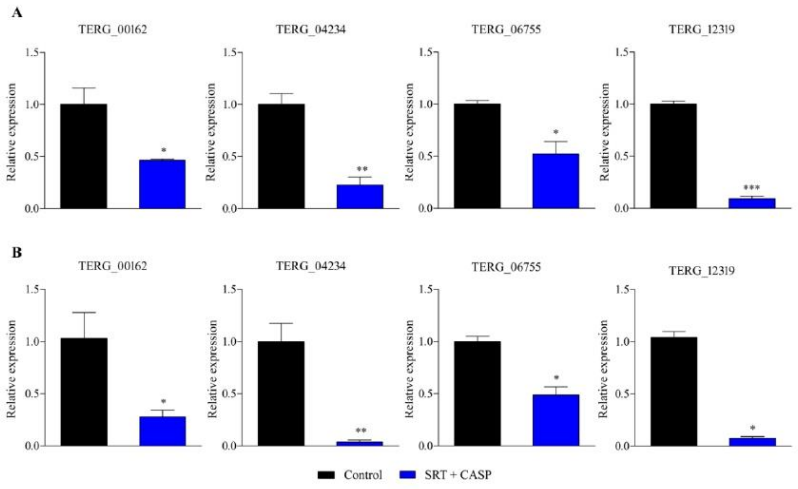

Figure 2. Genes encoding *TERG_00162* (MFS multidrug transporter), *TERG_04234* (Hydrophobin), *TERG_06755* (C-8 sterol isomerase), and *TERG_12319* (Chitin synthase 2) are differentially expressed in response to combinations of SRT with CASP. Asterisks indicate statistical significance determined by *t*-test as compared to the control (SB absence drug) at 3 h (**A**) and 12 h (**B**); * $p < 0.05$; ** $p < 0.01$; *** $p < 0.001$.

The effects of low concentrations of CASP and SRT on the expression levels of these genes in *T. rubrum* cultured in the presence of CASPsc or SRTsc were analysed. The results showed that SRTsc maintained the expression level of *TERG_00162*, which encodes

a multidrug transporter, at a level similar to that observed in the control at 3 h; in contrast, the expression of *TERG_00162* increased at 12 h. Moreover, a significant difference existed between the expression levels shown under these conditions and that of the control ($p < 0.05$). *TERG_06755* expression was downregulated at 3 h, but its expression at 12 h was similar to that of the control. *TERG_04234* and *TERG_12319* maintained their expression under both conditions (control and SRTsc) at 3 h and 12 h (Figure S1).

Exposure of *T. rubrum* to CASPsc resulted in *TERG_00162*, *TERG_04234*, *TERG_06755*, and *TERG_12319* presenting similar expression levels at 3 h or 12 h, compared to that of the untreated control. Therefore, no statistically significant differences existed between these treatment conditions (Figure S2).

3.3. Effects of SRT and Its Combination with CASP on the Activity of T. rubrum Biofilm

Metabolic activity in the biofilm was measured every 24 h. A significant increase in metabolic activity was observed up to 72 h, following which the activity stabilised. Therefore, 72 h was considered ideal for biofilm formation. The MTT assay results indicated that 12.5 mg/L SRT alone and of 15.62 mg/L CASP alone, as well as low concentrations of SRT + CASP (3.12 mg/L SRT+ 1.95 mg/L CASP), interfered significantly with the metabolic activities of the biofilm. Treatment with SRTsc or CASPsc did not reduce the metabolic activity of *T. rubrum* biofilms (Figure 3).

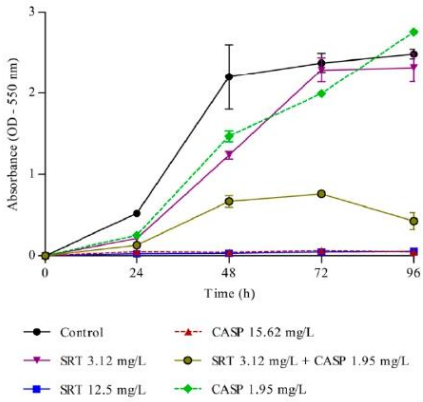

Figure 3. Metabolism of *T. rubrum* biofilm. Effects of sertraline (SRT), caspofungin (CASP), and SRT + CASP on the metabolic activity of *T. rubrum* biofilm.

The biomass of the biofilm was also affected by SRT, CASP, and SRT + CASP treatments. Three days after the biofilm was treated with 62.50 mg/L CASP, a significant reduction was observed in the biomass compared with that of the control ($p < 0.01$). Treatment with 25 mg/L SRT as well as 6.25 mg/L SRT + 1.95 mg/L CASP significantly reduced biomass. By contrast, 6.25 mg/L SRT or 1.95 mg/L CASP did not reduce biomass but instead increased production in a manner similar to that of the control (Figure 4).

After the biofilm matured for seven days, the 25 mg/L SRT, 62.50 mg/L CASP, or 6.25 mg/L SRT + 1.95 mg/L CASP treatments significantly reduced biomass when compared with the control ($p < 0.001$). However, treatment with 6.25 mg/L SRT or 1.95 mg/L CASP did not reduce the biomass of biofilm that had matured for three days. The biomass produced by these treatments was similar to that observed in the absence of drugs (Figure 5).

The results of the human nail infection assay corroborated the reduction in biomass and metabolic activity of the biofilm, observed via the MTT and crystal violet assays. Scanning electron microscopy revealed that *T. rubrum* forms mature biofilms in human nail fragments after 20 d. Its growth on the substrate was characterised by infinite filaments,

which were denser, interconnected, and spread in all directions to form an actual network of connected hyphae. The high antifungal tolerance in *T. rubrum* may be attributed to this network of connected hyphae. Thus, biofilm maturation in human nail fragments was considerably affected by SRT.

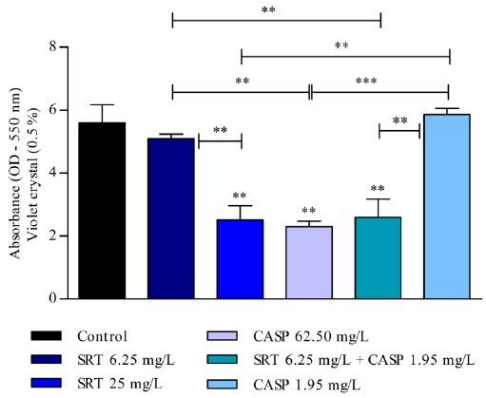

Figure 4. Evaluation of the effect of SRT, CASP, and the synergistic combination (SRT + CASP) on the biomass of *T. rubrum* biofilm stained with violet crystal. The treatments were performed 3 days after the biofilm matured. Statistical analyses showing significant differences ($p < 0.05$) between tested compounds and growth control were estimated using one-way ANOVA and Tukey's post hoc test; ** $p < 0.01$ and *** $p < 0.001$.

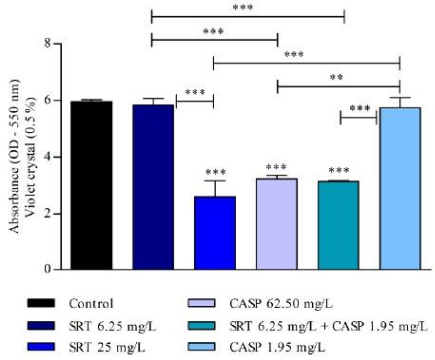

Figure 5. Effect of SRT, CASP, and SRT + CASP on the biomass of *T. rubrum* biofilm. Treatments were performed 7 days after the biofilm matured and stained with violet crystal. Significant differences between tested compounds and growth control were obtained using one-way ANOVA and Tukey's post hoc test. Asterisks indicate statistical significance: ** $p < 0.01$ and *** $p < 0.001$.

Filament density was significantly reduced by the treatments compared to that in the untreated control. A significant reduction in the thickness of filaments that formed the hyphal network was observed. Additionally, most hyphae could not complete their development to a level that enabled them to create a more uniform biofilm. In this context, the highest activity was observed after *T. rubrum* was treated with SRT and CASP at concentrations corresponding to 2 × MICs, which amounted to 50 mg/L, and 62.50 mg/L, respectively. Excellent biofilm reduction resulting from treatment with 12.5 mg/L SRT + 3.90 mg/L CASP

must be highlighted. However, we did not verify the reduction in filament density and the alterations mentioned earlier under isolated, uncombined conditions (Figure 6).

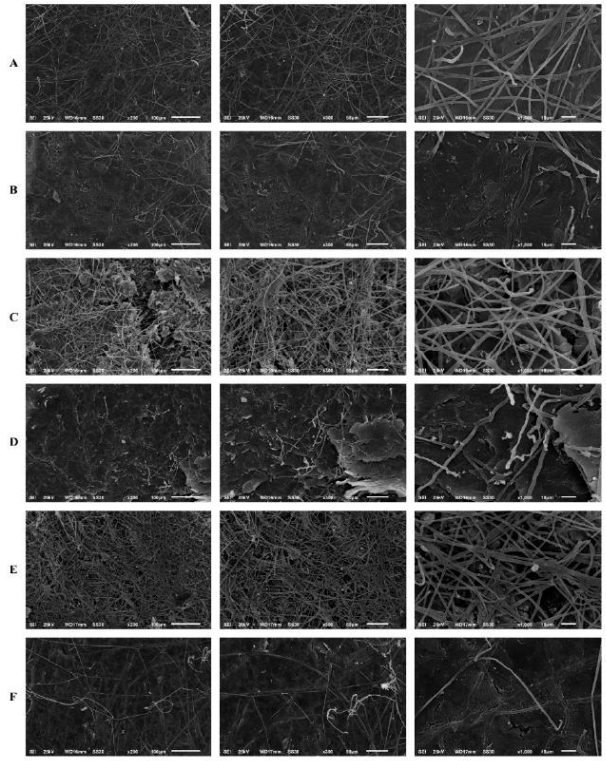

Figure 6. Scanning electron microscopy of the *T. rubrum* biofilm on a human nail. *T. rubrum* strain growth on nail fragments in the absence of drugs (**A**). Treatment with SRT 50 mg/L (**B**), SRT 12.5 mg/L (**C**), CASP 62.50 mg/L (**D**), CASP 3.90 mg/L (**E**) and SRT 12.5 mg/L + CASP 3.90 mg/L (**F**), 20 days of after biofilm matured.

4. Discussion

The human antidepressant, SRT, exhibited antifungal activity against planktonic forms of *T. rubrum* (100 mg/L SB and 25 mg/L RPMI media). When combined with CASP, SRT showed excellent synergistic effects by inhibiting *T. rubrum* in vitro. Interaction results showed that the combination of SRT and CASP decreased the concentration of antifungals required to inhibit the fungus by up to 30 times compared to antifungals used individually. These results suggest that repositioning SRT and combining it with CASP constitutes a promising therapy against *T. rubrum*. Several reports have demonstrated SRT activity against pathogenic fungi in vitro and in vivo, with particular reference to *Cryptococcus*, *Candida*, and *Aspergillus* [30–33]. To the best of our knowledge, we are the first to demonstrate its effect alone and in combination with CASP against the dermatophyte, *T. rubrum*, though a previous study has discussed the advantages of using a combination of SRT and CASP against *Trichosporon asahii* [18]. Moreover, the SRT concentration in the skin is much higher than that in blood; thus, the usefulness of SRT as a treatment against dermatophytosis appears to be promising [34].

We observed that an SRT concentration of 70% of its MIC induced a gene that encodes a transmembrane transporter (*TERG_00162*) belonging to the major facilitator superfamily (MFS). These transporters mediate increased drug efflux, the primary resistance mechanism in dermatophytes [35–37]. In this context, the combination of SRT and CASP reduced the transcript levels of the *TERG_00162* gene. Furthermore, exposure of *T. rubrum* to SRTsc or CASPsc (0.273 mg/L SRT or 10.93 mg/L CASP) showed that the expression level of the gene *TERG_00162* was associated with the amount of SRT in the cell and with the activity of the combination.

Fungi may evolve several adaptation mechanisms in response to environmental changes. The fungal cell wall, which enables fungi to interact dynamically with the ambient environment, constitutes a promising antifungal target. Furthermore, its structural integrity, which is actively modulated in response to stress conditions, plays a role in adhesion, signalling, and colonisation, making it essential for the survival of the pathogen [38,39]. Accordingly, other promising antifungal targets were revealed by the treatments, SRT alone and SRT + CASP, which downregulated critical genes that encode chitin synthase (*TERG_12319*) and hydrophobin (*TERG_04234*). However, the expression of these genes did not change when *T. rubrum* was cultured with SRTsc or CASPsc compared to that with the control. This suggested that the efficacy of activity against TERG_04234 and TERG_12319 is due exclusively to the combination of drugs and not to each drug used alone. Chitin, a linear protein that provides strength and protection to many eukaryotes, is vital for cell wall morphogenesis. Chitin is absent in mammalian cells; thus, its metabolism is an attractive target for highly specific antifungal agents [39]. Usually, upregulation of chitin synthesis-related genes is the primary response to cell wall stress [40,41]. The chitin synthase is essential for synthesising chitin in the primary septa of fungi [42]. Hydrophobin, a cysteine-rich protein secreted only by filamentous fungi, lowers the surface tension of water. Identifying drugs that downregulate the genes encoding hydrophobin may help develop novel strategies to treat infections caused by *T. rubrum*. This protein regulates water flux across the fungal cell wall and mediates the attachment of infective structures associated with fungal pathogenesis. Thus, its downregulation is associated with decreased fungal virulence [39,43].

We also identified the effects of SRT and SRT + CASP on the ergosterol pathway. SRT alone at a 70% of its MIC and low concentrations of SRT + CASP downregulated the *TERG_06755* gene, which encodes a c-8 sterol isomerase. This enzyme is involved in the ergosterol biosynthesis cascade [44].The relevance of drugs that target genes or proteins involved in ergosterol biosynthesis has been reported [45].

Our assays demonstrated the impact of SRT and its synergic combination on the metabolism and biomass of *T. rubrum* biofilms. We demonstrated that even low concentrations of SRT, when combined with CASP, are effective against *T. rubrum* biofilms; scanning electron microscopy results substantiated this inhibitory effect. Thus, our results indicate that SRT activity at high concentrations, as well as in combination with CASP, downregulate essential genes related to the formation and constitution of the cell wall, and a gene associated with the ergosterol pathway.

Despite the mechanisms that underlie the effects of CASP on the cell wall of yeasts being known [46], we excluded the possibility that alterations in the expression levels of genes involved in biofilms could be caused by this drug at low concentrations. Our studies indicated that CASP alone or in SC concentrations did not alter the expression of genes involved in cell wall constitution. It did not significantly affect *T. rubrum* biofilms in any of the aspects studied.

Although we used a single reference strain from the *T. rubrum* species, our findings indicate an alternative treatment for dermatophytosis caused by this fungus. SRT combined with CASP minimises fungal resistance and virulence in vitro. However, in vivo studies must also validate our findings and define their clinical utility.

Structural modifications of SRT and CASP molecules would also increase their spectrum of action as antifungal agents, thereby optimising their usefulness against other pathogenic fungi.

Supplementary Materials: The following supporting information can be downloaded at: https://www.mdpi.com/article/10.3390/jof8080815/s1, Table S1. Primer sets used for real-time quantitative reverse transcription polymerase chain reaction (RT-qPCR). Figure S1. Expression of *TERG_00162* (MFS multidrug transporter), *TERG_04234* (Hydrophobin), *TERG_06755* (C-8 sterol isomerase), and *TERG_12319* (Chitin synthase 2) following SRTsc exposure. Asterisks indicate statistical significance determined by the *t*-test, compared to the control (SB absence drug) at 3 h (A) and 12 h (B); * $p < 0.05$. Figure S2. Differentially expressed genes, *TERG_00162* (MFS multidrug transporter), *TERG_04234* (Hydrophobin), *TERG_06755* (C-8 sterol isomerase), and *TERG_12319* (Chitin synthase 2), following exposure to CASPsc compared to the control (SB absence drug) at 3 h (A) and 12 h (B).

Author Contributions: C.H.L.R. thoroughly reviewed the literature and wrote the manuscript. C.H.L.R. and F.M.G.R. performed the laboratory experiments. C.H.L.R., F.M.G.R. and P.R.S. were responsible for the illustrations. T.A.B. and M.P.M. helped with the laboratory experiments. N.M.M.-R. has supervised the investigation. N.M.M.-R. and A.R. obtained the resources, reviewed, and edited the manuscript. All authors have read and agreed to the published version of the manuscript.

Funding: This work was supported by grants from the Brazilian Agencies: São Paulo Research Foundation-FAPESP [proc. No. 2019/22596-9, and Fellowships No. 2015/23435-8 to T.A.B. and No. 2018/11319-1 to M.P.M.]; National Council for Scientific and Technological Development–CNPq [Grants Nos. 307871/2021-5 and 307876/2021-7], Coordenação de Aperfeiçoamento de Pessoal de Nível Superior (CAPES)-Finance Code 001; and Fundação de Apoio ao Ensino, Pesquisa e Assistência-FAEPA.

Institutional Review Board Statement: The Ethics Committee of the University Hospital of Ribeirão Preto Medical School, USP, Brazil (HCFMRP-USP) (Protocol No. 4.304.317/2020), approved this study.

Informed Consent Statement: Not applicable.

Data Availability Statement: The data presented in this study are available in this article and the accompanying Supplementary Data.

Acknowledgments: We thank V. M. Oliveira, M. Mazucato, and M. D. Martins for technical support.

Conflicts of Interest: The authors declare no conflict of interest.

References

1. Martinez-Rossi, N.M.; Peres, N.T.; Bitencourt, T.A.; Martins, M.P.; Rossi, A. State-of-the-art Dermatophyte infections: Epidemiology aspects, pathophysiology, and resistance mechanisms. *J. Fungi* **2021**, *7*, 629. [CrossRef] [PubMed]
2. De Hoog, S.; Monod, M.; Dawson, T.; Boekhout, T.; Mayser, P.; Gräser, Y. Skin Fungi from Colonization to Infection. *Microbiol. Spectr.* **2017**, *5*, 4. [CrossRef]
3. Martinez-Rossi, N.M.; Bitencourt, T.A.; Peres, N.T.; Lang, E.A.; Gomes, E.V.; Quaresemin, N.R.; Martins, M.P.; Lopes, L.; Rossi, A. Dermatophyte resistance to antifungal drugs: Mechanisms and prospectus. *Front. Microbiol.* **2018**, *9*, 1108. [CrossRef] [PubMed]
4. Mendes, N.S.; Bitencourt, T.A.; Sanches, P.R.; Silva-Rocha, R.; Martinez-Rossi, N.M.; Rossi, A. Transcriptome-wide survey of gene expression changes and alternative splicing in *Trichophyton rubrum* in response to undecanoic acid. *Sci. Rep.* **2018**, *8*, 2520. [CrossRef] [PubMed]
5. Yamada, T.; Yaguchi, T.; Tamura, T.; Pich, C.; Salamin, K.; Feuermann, M.; Monod, M. Itraconazole resistance of *Trichophyton rubrum* mediated by the ABC transporter TruMDR2. *Mycoses* **2021**, *64*, 936–946. [CrossRef] [PubMed]
6. Robbins, N.; Caplan, T.; Cowen, L.E. Molecular Evolution of Antifungal Drug Resistance. *Annu. Rev. Microbiol.* **2017**, *71*, 753–775. [CrossRef] [PubMed]
7. Brilhante, R.S.N.; Aguiar, L.; Sales, J.A.; Araújo, G.D.S.; Pereira, V.S.; Pereira-Neto, W.A.; Pinheiro, A.Q.; Paixão, G.C.; Cordeiro, R.A.; Sidrim, J.J.C.; et al. Ex vivo biofilm-forming ability of der-matophytes using dog and cat hair: An ethically viable approach for an infection model. *Biofouling* **2019**, *35*, 392–400. [CrossRef]
8. Zhai, B.; Zhou, H.; Yang, L.; Zhang, J.; Jung, K.; Giam, C.-Z.; Xiang, X.; Lin, X. Polymyxin B, in combination with fluconazole, exerts a potent fungicidal effect. *J. Antimicrob. Chemother.* **2010**, *65*, 931–938. [CrossRef]
9. Wang, Y.; Lu, C.; Zhao, X.; Wang, D.; Liu, Y.; Sun, S. Antifungal activity and potential mechanism of Asiatic acid alone and in combination with fluconazole against *Candida albicans*. *Biomed. Pharmacother.* **2021**, *139*, 111568. [CrossRef]
10. Ashburn, T.T.; Thor, K.B. Drug repositioning: Identifying and developing new uses for existing drugs. *Nat. Rev. Drug Discov.* **2004**, *3*, 673–683. [CrossRef]

11. Zhai, B.; Wu, C.; Wang, L.; Sachs, M.S.; Lin, X. The antidepressant sertraline provides a promising therapeutic option for neurotropic cryptococcal infections. *Antimicrob. Agents Chemother.* **2012**, *56*, 3758–3766. [CrossRef]
12. Katende, A.; Mbwanji, G.; Faini, D.; Nyuri, A.; Kalinjuma, A.V.; Mnzava, D.; Hullsiek, K.H.; Rhein, J.; Weisser, M.; Meya, D.B.; et al. Short-course amphotericin B in addition to sertraline and fluconazole for treatment of HIV-associated cryptococcal meningitis in rural Tanzania. *Mycoses* **2019**, *62*, 1127–1132. [CrossRef]
13. Treviño-Rangel, R.d.J.; Villanueva-Lozano, H.; Méndez-Galomo, K.S.; Solís-Villegas, E.M.; Becerril-García, M.A.; Montoya, A.M.; Robledo-Leal, E.R.; González, G.M. In vivo evaluation of the antifungal activity of sertraline against *Aspergillus fumigatus*. *J. Antimicrob. Chemother.* **2019**, *74*, 663–666. [CrossRef]
14. De Vane, C.L.; Liston, H.L.; Markowitz, J.S. Clinical pharmacokinetics of sertraline. *Clin. Pharmacokinet.* **2002**, *41*, 1247–1266. [CrossRef]
15. Rainey, M.M.; Korostyshevsky, D.; Lee, S.; Perlstein, E.O. The antidepressant sertraline targets intracellular vesiculogenic membranes in yeast. *Genetics* **2010**, *185*, 1221–1233. [CrossRef]
16. Heller, I.; Leitner, S.; Dierich, M.; Lass-Flörl, C. Serotonin (5-HT) enhances the activity of amphotericin B against *Aspergillus fumigatus* in vitro. *Int. J. Antimicrob. Agents* **2004**, *24*, 401–404. [CrossRef]
17. Breuer, M.R.; Dasgupta, A.; Vasselli, J.G.; Lin, X.; Shaw, B.D.; Sachs, M.S. The Antidepressant Sertraline Induces the For-mation of Supersized Lipid Droplets in the Human Pathogen *Cryptococcus neoformans*. *J. Fungi* **2022**, *8*, 642. [CrossRef]
18. Cong, L.; Liao, Y.; Yang, S.; Yang, R. In vitro antifungal activity of sertraline and synergistic effects in combination with antifungal drugs against planktonic forms and biofilms of clinical *Trichosporon asahii* isolates. *PLoS ONE* **2016**, *11*, e0167903. [CrossRef]
19. Badali, H.; Mohammadi, R.; Mashedi, O.; de Hoog, G.S.; Meis, J.F. In vitro susceptibility patterns of clinically important *Trichophyton* and *Epidermophyton* species against nine antifungal drugs. *Mycoses* **2015**, *58*, 303–307. [CrossRef]
20. Baghi, N.; Shokohi, T.; Badali, H.; Makimura, K.; Rezaei-Matehkolaei, A.; Abdollahi, M.; Didehdar, M.; Haghani, I.; Abasta-bar, M. In vitro activity of new azoles luliconazole and lanoconazole compared with ten other antifungal drugs against clinical dermatophyte isolates. *Med. Mycol.* **2016**, *54*, 757–763. [CrossRef]
21. Bao, Y.Q.; Wan, Z.; Li, R.Y. In vitro antifungal activity of micafungin and caspofungin against dermatophytes isolated from China. *Mycopathologia* **2013**, *175*, 141–145. [CrossRef]
22. Su, S.; Yan, H.; Min, L.; Wang, H.; Chen, X.; Shi, J.; Sun, S. The antifungal activity of caspofungin in combination with antifungals or non-antifungals against *Candida* species in vitro and in clinical therapy. *J. Fungi* **2021**, *20*, 161–178. [CrossRef]
23. Caballero, U.; Eraso, E.; Quindós, G.; Jauregizar, N. In vitro interaction and killing-kinetics of amphotericin B combined with anidulafungin or caspofungin against *Candida auris*. *Pharmaceutics* **2021**, *13*, 1333. [CrossRef]
24. Kovács, R.; Bozó, A.; Gesztelyi, R.; Domán, M.; Kardos, G.; Nagy, F.; Majoros, L. Effect of caspofungin and micafungin in combination with farnesol against *Candida parapsilosis* biofilms. *Int. J. Antimicrob. Agents* **2016**, *47*, 304–310. [CrossRef]
25. Peres, N.T.d.A.; Silva, L.G.d.; Santos, R.d.S.; Jacob, T.R.; Persinoti, G.F.; Rocha, L.B.; Falcao, J.P.; Rossi, A.; Martinez-Rossi, N.M. In vitro and ex vivo infection models help assess the molecular aspects of the interaction of *Trichophyton rubrum* with the host milieu. *Sabouraudia* **2016**, *54*, 420–427. [CrossRef] [PubMed]
26. *M38-A2*; Reference Method for Broth Dilution Antifungal Susceptibility Testing of Filamentous Fungi—Second Edition. Clinical and Laboratory Standards Institute: Wayne, PA, USA, 2008.
27. Gómez-López, A.; Cuenca-Estrella, M.; Mellado, E.; Rodríguez-Tudela, J.L. In vitro evaluation of combination of terbinafine with itraconazole or amphotericin B against Zygomycota. *Diagn. Microbiol. Infect. Dis.* **2003**, *45*, 199–202. [CrossRef]
28. Livak, K.J.; Schmittgen, T.D. Analysis of relative gene expression data using real-time quantitative PCR and the $2^{-\Delta\Delta CT}$ method. *Methods* **2001**, *25*, 402–408. [CrossRef] [PubMed]
29. Costa-Orlandi, C.; Sardi, J.; Santos, C.; Fusco-Almeida, A.; Mendes-Giannini, M.J.S. In vitro characterization of *Trichophyton rubrum* and *T. mentagrophytes* biofilms. *Biofouling* **2014**, *30*, 719–727. [CrossRef] [PubMed]
30. Lass-Flörl, C.; Dierich, M.; Fuchs, D.; Semenitz, E.; Jenewein, I.; Ledochowski, M. Antifungal properties of selective serotonin reuptake inhibitors against *Aspergillus* species in vitro. *J. Antimicrob. Chemother.* **2001**, *48*, 775–779. [CrossRef]
31. Liu, S.; Hou, Y.; Chen, X.; Gao, Y.; Li, H.; Sun, S. Combination of fluconazole with non-antifungal agents: A promising approach to cope with resistant *Candida albicans* infections and insight into new antifungal agent discovery. *Int. J. Antimicrob. Agents* **2014**, *43*, 395–402. [CrossRef]
32. Gowri, M.; Jayashree, B.; Jeyakanthan, J.; Girija, E.K. Sertraline as a promising antifungal agent: Inhibition of growth and biofilm of *Candida auris* with special focus on the mechanism of action in vitro. *J. Appl. Microbiol.* **2020**, *128*, 426–437. [CrossRef]
33. Villanueva-Lozano, H.; González, G.M.; Espinosa-Mora, J.E.; Bodden-Mendoza, B.A.; Andrade, A.; Martínez-Reséndez, M.F.; Treviño-Rangel, R.J. Evaluation of the expanding spectrum of sertraline against uncommon fungal pathogens. *J. Infect. Chemother.* **2020**, *26*, 309–311. [CrossRef]
34. Tremaine, L.M.; Welch, W.M.; Ronfeld, R.A. Metabolism and disposition of the 5-hydroxytryptamine uptake blocker sertraline in the rat and dog. *Drug Metab. Dispos.* **1989**, *17*, 542–550.
35. Scorzoni, L.; de Paula e Silva, A.C.; Marcos, C.M.; Assato, P.A.; de Melo, W.C.; de Oliveira, H.C.; Costa-Orlandi, C.B.; Mendes-Giannini, M.J.; Fusco-Almeida, A.M. Antifungal therapy: New advances in the understanding and treatment of mycosis. *Front. Microbiol.* **2017**, *8*, 36. [CrossRef]
36. Yamada, T.; Yaguchi, T.; Salamin, K.; Guenova, E.; Feuermann, M.; Monod, M. MFS1, a Pleiotropic Transporter in Derma-tophytes That Plays a Key Role in Their Intrinsic Resistance to Chloramphenicol and Fluconazole. *J. Fungi* **2021**, *7*, 542. [CrossRef]

37. Monod, M.; Feuermann, M.; Salamin, K.; Fratti, M.; Makino, M.; Alshahni, M.M.; Makimura, K.; Yamada, T. *Trichophyton rubrum* Azole Resistance Mediated by a New ABC Transporter, TruMDR3. *Antimicrob. Agents Chemother.* **2019**, *63*, e00863-19. [CrossRef]
38. Cowen, L.E.; Sanglard, D.; Howard, S.J.; Rogers, P.D.; Perlin, D.S. Mechanisms of antifungal drug resistance. *Cold Spring Harb. Perspect. Med.* **2015**, *5*, a019752. [CrossRef]
39. Martins, M.P.; Silva, L.G.; Rossi, A.; Sanches, P.R.; Souza, L.D.R.; Martinez-Rossi, N.M. Global Analysis of Cell Wall Genes Revealed Putative Virulence Factors in the Dermatophyte *Trichophyton rubrum*. *Front. Microbiol.* **2019**, *10*, 2168. [CrossRef]
40. Walker, L.A.; Munro, C.A.; De Bruijn, I.; Lenardon, M.D.; McKinnon, A.; Gow, N.A. Stimulation of chitin synthesis rescues *Candida albicans* from echinocandins. *PLoS Pathog.* **2008**, *4*, e1000040. [CrossRef]
41. Fortwendel, J.R.; Juvvadi, P.R.; Pinchai, N.; Perfect, B.Z.; Alspaugh, J.A.; Perfect, J.R.; Steinbach, W.J. Differential effects of inhibiting chitin and 1, 3-β-D-glucan synthesis in ras and calcineurin mutants of *Aspergillus Fumigatus*. *Antimicrob. Agents Chemother.* **2009**, *53*, 476–482. [CrossRef]
42. Silverman, S.J.; Sburlati, A.; Slater, M.L.; Cabib, E. Chitin synthase 2 is essential for septum formation and cell division in *Saccharomyces cerevisiae*. *Proc. Natl. Acad. Sci. USA* **1988**, *85*, 4735–4739. [CrossRef]
43. Lang, E.A.S.; Bitencourt, T.A.; Peres, N.T.A.; Lopes, L.; Silva, L.G.; Cazzaniga, R.A.; Rossi, A.; Martinez-Rossi, N.M. The stuA gene controls development, adaptation, stress tolerance, and virulence of the dermatophyte *Trichophyton rubrum*. *Microbiol. Res.* **2020**, *241*, 126592. [CrossRef]
44. Petrucelli, M.F.; Matsuda, J.B.; Peroni, K.; Sanches, P.R.; Silva, W.A.; Beleboni, R.O., Jr.; Martinez-Rossi, N.M.; Marins, M.; Fachin, A.L. The Transcriptional Profile of *Trichophyton rubrum* Co-Cultured with Human Keratinocytes Shows New In-sights about Gene Modulation by Terbinafine. *Pathogens* **2019**, *8*, 274. [CrossRef]
45. Zhang, W.; Yu, L.; Yang, J.; Wang, L.; Peng, J.; Jin, Q. Transcriptional profiles of response to terbinafine in *Trichophyton Rubrum*. *Appl. Microbiol. Biotechnol.* **2009**, *82*, 1123–1130. [CrossRef] [PubMed]
46. Odds, F.C.; Brown, A.J.; Gow, N.A. Antifungal agents: Mechanisms of action. *Trends Microbiol.* **2003**, *11*, 272–279. [CrossRef]

Journal of Fungi

MDPI

Article

The Antidepressant Sertraline Affects Cell Signaling and Metabolism in *Trichophyton rubrum*

Flaviane M. Galvão-Rocha [1], Carlos H. L. Rocha [1], Maíra P. Martins [1], Pablo R. Sanches [1], Tamires A. Bitencourt [1], Matthew S. Sachs [2], Nilce M. Martinez-Rossi [1] and Antonio Rossi [1,*]

[1] Department of Genetics, Ribeirao Preto Medical School, University of São Paulo, USP, Ribeirao Preto 14049-900, SP, Brazil
[2] Department of Biology, Texas A&M University, College Station, TX 77843-3258, USA
* Correspondence: anrossi@usp.br

Abstract: The dermatophyte *Trichophyton rubrum* is responsible for most human cutaneous infections. Its treatment is complex, mainly because there are only a few structural classes of fungal inhibitors. Therefore, new strategies addressing these problems are essential. The development of new drugs is time-consuming and expensive. The repositioning of drugs already used in medical practice has emerged as an alternative to discovering new drugs. The antidepressant sertraline (SRT) kills several important fungal pathogens. Accordingly, we investigated the inhibitory mechanism of SRT in *T. rubrum* to broaden the knowledge of its impact on eukaryotic microorganisms and to assess its potential for future use in dermatophytosis treatments. We performed next-generation sequencing (RNA-seq) to identify the genes responding to SRT at the transcript level. We identified that a major effect of SRT was to alter expression for genes involved in maintaining fungal cell wall and plasma membrane stability, including ergosterol biosynthetic genes. SRT also altered the expression of genes encoding enzymes related to fungal energy metabolism, cellular detoxification, and defense against oxidative stress. Our findings provide insights into a specific molecular network interaction that maintains metabolic stability and is perturbed by SRT, showing potential targets for its strategic use in dermatophytosis.

Keywords: RNA-seq; drug repositioning; dermatophyte; membrane damage; oxidative stress; ergosterol; sertraline; *Trichophyton rubrum*

Citation: Galvão-Rocha, F.M.; Rocha, C.H.L.; Martins, M.P.; Sanches, P.R.; Bitencourt, T.A.; Sachs, M.S.; Martinez-Rossi, N.M.; Rossi, A. The Antidepressant Sertraline Affects Cell Signaling and Metabolism in *Trichophyton rubrum*. *J. Fungi* **2023**, *9*, 275. https://doi.org/10.3390/jof9020275

Academic Editor: David S. Perlin

Received: 17 December 2022
Revised: 24 January 2023
Accepted: 8 February 2023
Published: 20 February 2023

1. Introduction

Dermatophytoses are skin infections caused by fungi. These dermatophytes are associated with keratinized tissues, such as skin, hair, and nails. Although dermatophytes do not usually cause deep lesions, the disease can progress to severe acute illness in hosts with poor immune protection [1]. *Trichophyton rubrum* is responsible for most onychomycosis cases in humans worldwide [2].

The number of antifungal agents available for the treatment of dermatophyte infections is limited. The most used drugs converge to a similar mechanism of action in fungal cells, targeting ergosterol biosynthesis. Consequently, intense selective pressure is exerted on clinical isolates, leading to the emergence of strains that are resistant to available drugs [3,4].

The development of new antifungal drugs is limited by the similarities between fungal and host cells, which restrict the number of cellular targets [4]. Furthermore, the time-consuming efforts and elevated costs required to achieve effective drugs engender the need to exploit alternatives for the management of fungal infections [4,5]. One approach is to evaluate the potential use of non-antifungal drugs as antifungals [6].

Numerous drugs used to treat non-infectious conditions such as inflammation, cardiovascular diseases, or depression are known to exhibit antimicrobial activities. The selective serotonin reuptake inhibitor (SSRI) sertraline (SRT), commonly used as an antidepressant, was revealed to have antifungal activity [7–10]. Furthermore, this drug interacts

synergistically in vitro with antifungals such as azoles, caspofungin, and amphotericin B, indicating its potential use as an adjuvant in treating fungal infections [11–15]. This synergistic association could decrease drug dosages and emerging drug resistance rates [6].

In the mammalian nervous system, SRT inhibits serotonin (5-hydroxytryptamine, 5-HT) reuptake, releasing serotonin into the synaptic cleft [16]. In addition, the drug enhances 5-HT synthesis by increasing the expression of tryptophan hydroxylase, the enzyme responsible for converting L-tryptophan to 5-HT [17]. SRT targets the serotonin transporter (5-HTT) responsible for 5-HT reuptake into presynaptic neurons in human cells. Interestingly, there is no conserved homolog of the 5-HT transporter in fungi, highlighting the occurrence of secondary targets for this drug [11]. However, the mechanisms underlying the antifungal activity of SRT remain unclear. It has been proposed that SRT intercalates into the phospholipid membranes of V-ATPase-acidified organelles [18]. Moreover, it is possible that the potent antifungal activity against *Cryptococcus neoformans* could also be driven by the inhibition of protein synthesis and/or other actions interfering with lipid metabolism [10,11].

Here, we evaluated the effects of sub-lethal doses of SRT against the dermatophyte *T. rubrum* through RNA-seq analysis. Our findings revealed changes in the comprehensive induction of the cellular antioxidant system, membrane transport-associated genes, and biosynthetic genes, resulting in changes in the cell membrane.

2. Materials and Methods

2.1. Strain and Culture Conditions for RNA-Seq Analysis

T. rubrum strain CBS118892 from the Westerdijk Fungal Biodiversity Institute (formerly CBS-KNAW Collections), The Netherlands, was maintained on malt extract agar (2% glucose, 2% malt extract, 0.1% peptone (*w/v*), pH 5.7). Conidial suspensions were obtained by flooding 21-day-old plates with sterile 0.9% NaCl, recovering the liquid, mixing by vortexing, and filtering through glass wool. We estimated the conidial concentration by counting in a Neubauer chamber. Approximately 1×10^6 conidia were inoculated into 100 mL Sabouraud dextrose broth (SDB; 2% (*w/v*) glucose, 1% (*w/v*) peptone) and incubated with agitation (120 rpm) at 28 °C for 96 h. Next, we aseptically transferred mycelia into new flasks containing 100 mL SDB media with 70 µg/mL of SRT hydrochloride (Cayman Chemical Co., Ann Arbor, MI, USA), corresponding to 70% of the minimal inhibitory concentration (MIC) [15], and in the absence of drugs (control). After 3 or 12 h of incubation at 28 °C with agitation, the resultant mycelia were collected, quick-frozen, and stored at −80 °C until RNA isolation.

2.2. RNA Isolation and cDNA Library Construction

Total RNA was isolated from ~100 mg mycelia using the Illustra RNAspin mini RNA isolation kit (GE Healthcare, Chicago, IL, USA). RNA concentrations were determined using a NanoDrop ND-1000 spectrophotometer (Thermo Fisher Scientific, Waltham, MA, USA). RNA quality was verified by agarose electrophoresis and an Agilent 2100 Bioanalyzer (Agilent Technologies, Santa Clara, CA, USA). Equal amounts of RNA from three independent biological replicates at each time point (3 and 12 h) were used for cDNA synthesis using the TruSeq RNA library kit (Illumina, San Diego, CA, USA) and sequenced using Illumina technology (HiSeq 2000 sequencer) according to the manufacturer's instructions. Paired-end reads were 150 bp in size.

2.3. Transcriptome Analysis

Raw read data obtained were filtered for quality control using the FastQC tool and trimmed using Trimmomatic [19] to remove adapters and Illumina-specific sequences. Trimmed paired-end reads from each sample were aligned to the reference genome using the STAR aligner [20]. We inspected the average coverage of transcripts and alignments using the Interactive Genomics Viewer (IGV) software [21]. We generated gene-level read

counts by STAR using the quantModeGeneCounts option. Differential expression was analyzed using the DESeq2 Bioconductor package [22].

After the above, the Benjamini–Hochberg correction was applied ($p < 0.05$) [23], and a cutoff threshold of ±1.5 log2 fold change was set to reveal statistically significant expression differences (genes surpassing these thresholds are referred to as differentially expressed genes (DEG)) [24]. We functionally categorized them using Gene Ontology (GO) terms assigned by the Blast2GO algorithm. Highly represented categories were determined by enrichment analysis using the BayGO algorithm [25].

2.4. Data Analysis and Gene Selection

We predicted transporter-associated domain-containing proteins in the *T. rubrum* CBS 118892 genome sequence using the HMMER v3.1 b2 pipeline [26]. We built the hidden Markov model (HMM) utilizing a Pfam [27] multiple alignment-based search of 55 sequences corresponding to the ABC domain-containing proteins and another Pfam multiple alignment-based search of 192 sequences corresponding to the MFS (major facilitator superfamily) domain-containing proteins, both from different organisms (https://pfam.xfam.org/family/PF00005 and https://pfam.xfam.org/family/PF07690, respectively—accessed on 10 June 2022). The resulting models with epitopes of the consensus sequences of transporter-associated domain-containing proteins were used to search for homologs in *T. rubrum* protein sequences. In addition, we identified proteins using the keywords "transporter", "transcription factor", and "kinase" in Ensembl Fungi (https://fungi.ensembl.org). We compared the gene codes for specific proteins with the DEGs identified in RNA-seq.

2.5. cDNA Synthesis and RT-qPCR Analysis

We treated total RNA with DNase I (Sigma-Aldrich, Milwaukee, WI, USA) to remove residual genomic DNA and generate complementary DNA (cDNA) using a High-Capacity cDNA Synthesis Kit (Applied Biosystems, Foster City, CA, USA). We performed RT-qPCR with a StepOnePlus Real-Time PCR system (Applied Biosystems). Reactions were run in 12.5 µL with Power SYBR Green PCR Master Mix (Applied Biosystems), 70 ng template cDNA, and forward and reverse primers (Table S1). We used glyceraldehyde-3-phosphate dehydrogenase (*gapdh*) and DNA-dependent RNA polymerase II (*rpb2*) as internal controls [28]. Thermocycler conditions included an initial PCR step at 95 °C for 10 min, followed by 40 cycles at 95 °C for 15 s and 60 °C for 1 min. Data were obtained from three independent replicates. The $2^{-\Delta\Delta ct}$ relative expression quantification method was used to calculate gene responsiveness [29]. For RNA-seq validation, we used 3 h and 12 h without SRT as the reference samples. Statistical analyses were performed using a *t*-test followed by Tukey's post-hoc test using GraphPad Prism v. 5.1 software (GraphPad, La Jolla, CA, USA). A significance level of 95% was considered; therefore, the measures were statistically different at $p < 0.05$.

2.6. Quantitation of Ergosterol Content

The *T. rubrum* strain CBS118892 was cultivated on Sabouraud dextrose agar (SDA) for 17 days at 28 °C. The mycelia were transferred to 50 mL of SDB for 24 h at 28 °C with agitation (200 rpm). After this period, the mycelium was recovered, inoculated in 20 mL of SDA containing a sub-inhibitory concentration of SRT (6.25 µg/mL), ketoconazole (KTC, 4 µg/mL; Sigma-Aldrich), or amphotericin B (AMB, 1.25 µg/mL; Sigma-Aldrich), and incubated for 48 h at 28 °C, 200 rpm. Mycelia were also inoculated in SDA without drugs (control). The resulting mycelia were filtered, the dry weight was measured, and the ergosterol content was determined following the protocol described by Arthington-Skaggs et al. [30], with modifications [31]. Briefly, 3 mL of 25% alcoholic potassium hydroxide solution was added to the dried mycelia and mixed by vortexing for 5 min. We incubated the mycelium at 85 °C for 1 h. The tubes were cooled to room temperature and sterile distilled water (1 mL) and 3 mL of *n*-heptane were added, followed by vigorous vortex mixing for 5 min. The heptane layer was transferred to a clean polystyrene tube, and a 20 µL aliquot

was diluted five-fold in 100% ethanol and scanned in a spectrophotometer between 230 and 300 nm. All assays were performed in triplicate. Both 24(28)-dehydroergosterol (a sterol pathway intermediate) and ergosterol absorb at 281.5 nm, but 24(28)-dehydroergosterol also absorbs at 230 nm, which was subtracted from the absorbance obtained at 281.5 nm [31]. We calculated the reduction in ergosterol content as the difference in the treatments compared to the growth control samples based on a standard curve of various concentrations of standard ergosterol (Sigma-Aldrich). The results are expressed as a percentage of ergosterol content compared with the growth control. One-way ANOVA was used to determine the amount of ergosterol in the control with the treatments, followed by Tukey's post-hoc test. Statistical significance was set at $p < 0.05$, and Prism v. 5.1 software was used to generate graphs and perform statistical analyses.

3. Results

3.1. Transcriptional Profiling of Trichophyton rubrum Challenged by SRT

We used next-generation sequencing to comprehensively analyze the *T. rubrum* global transcriptome in response to sub-lethal doses of the antidepressant SRT at two different time points. Approximately 535.5 million high-quality reads of 150-bp paired-end sequences were obtained (Table S2). In response to SRT exposure, 169 and 1197 genes were modulated at 3 and 12 h, respectively, when compared to the expression levels of the control. Three hundred seventy-two genes were modulated at both time points, totaling 1738 genes that were responsive to SRT (Figure 1A). SRT differentially upregulates more genes than it represses after 3 h of treatment. This profile was inverted at 12 h exposure with a less expressive difference between up- and downregulated genes compared to the 3 h time point (Figure 1B). We list the products of all genes modulated in response to SRT for each drug exposure time in Table S3 and present the most significantly up- and downregulated genes in Table 1.

A

B

Condition	Total genes	Up-regulated	Down-regulated
3 h	541	452	89
12 h	1569	768	801

Figure 1. SRT-induced differential gene expression. (**A**) Venn diagram presenting the time-dependent differential expression of 1738 genes after exposure to sub-lethal dose of SRT for 3 h and 12 h compared to the control samples without SRT. (**B**) Total up- and downregulated genes in each experimental condition.

Table 1. The most significantly up- or downregulated genes.

Upregulated		log_2 (Fold Change)	
ID	**Gene Product Name**	**3 h**	**12 h**
TERG_06548	hypothetical protein (oxidoreductase, *M. canis*)	10.86	11.80
TERG_00785	endoplasmic reticulum vesicle protein 25	8.60	
TERG_01782	hypothetical protein	8.34	9.02
TERG_00010	amidase family protein (*T. verrucosum*)		8.72
TERG_03829	FAD binding domain-containing protein (*T. equinum*)		6.92
TERG_04952	multidrug resistance protein (*T. equinum*)	6.87	7.69
TERG_08954	hypothetical protein	6.61	
TERG_06106	sulfate permease 2 (*T. tonsurans*)		6.45
TERG_08751	ABC multidrug transporter, putative (*A. benhamiae*)	5.82	6.33
TERG_01543	S-adenosylmethionine (SAM)-dependent methyltransferase (*M. gypseum*)	5.42	7.48
TERG_08041	aminotransferase, putative (*A. benhamiae*)	5.42	
TERG_04937	alpha/beta hydrolase (*T. equinum*)	5.41	6.40
TERG_07830	hypothetical protein	5.41	8.22
Downregulated		**log_2 (Fold Change)**	
ID	**Gene Product Name**	**3 h**	**12 h**
TERG_02653	hypothetical protein	−6.21	
TERG_02652	O-methyltransferase, putative (*T. verrucosum*)	−4.91	
TERG_04066	filamentation protein (Rhf1), putative (*T. verrucosum*)	−4.67	
TERG_02959	hypothetical protein	−4.16	
TERG_05816	hypothetical protein	−3.74	
TERG_02650	NmrA family protein (*T. equinum*)	−3.56	
TERG_12339	hypothetical protein	−3.31	
TERG_01619	toxin biosynthesis protein (Tri7), putative (*T. verrucosum*)	−3.20	
TERG_00490	erythromycin esterase (*T. tonsurans*)	−3.13	
TERG_03826	hypothetical protein	−2.77	
TERG_02959	hypothetical protein		−5.90
TERG_11536	hypothetical protein		−5.69
TERG_11771	hypothetical protein		−5.51
TERG_04742	hypothetical protein		−5.29
TERG_01148	hypothetical protein		−5.26
TERG_00490	erythromycin esterase (*T. tonsurans*)		−5.24
TERG_03919	phytoene dehydrogenase (*T. equinum*)		−5.20
TERG_01599	hypothetical protein		−4.95
TERG_12035	NB-ARC and TPR domain protein (*A. benhamiae*)		−4.87
TERG_11963	hypothetical protein		−4.79

The functional categorization of the modulated genes was performed using Blast2Go, which revealed the molecular mechanisms by which *T. rubrum* senses and responds to the challenge of SRT presence (Figure 2). Gene function analysis using GO enriched mainly molecular function terms after 3 h of treatment. Genes associated with catalytic and hydrolase activities and those related to transmembrane transport were upregulated. The oxidoreductase activity induces or represses many genes after 3 h of drug exposure (Figure 2A). The upregulated membrane-associated genes and downregulated genes associated with the oxidation–reduction process increased at 12 h compared to those after 3 h of treatment. The terms related to translation were all inhibited at the 12 h time point. The number of genes associated with hydrolase activity and transmembrane transport increased compared to those in the 3 h condition, remaining induced in response to 12 h of SRT exposure (Figure 2B).

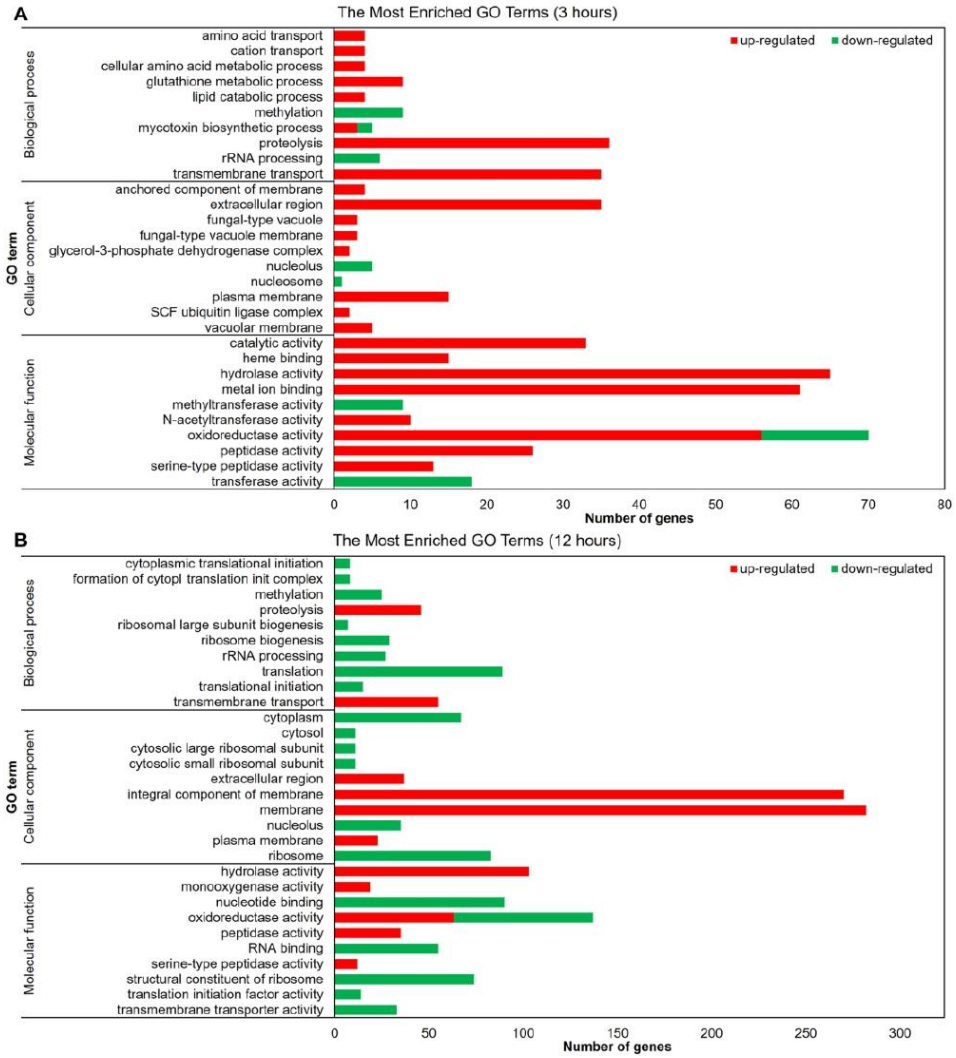

Figure 2. Gene ontology-based functional categorization of the most representative differentially expressed genes. The red and green bars indicate the number of up- and downregulated genes modulated by *T. rubrum* in response to SRT ($p < 0.05$). Results show genes after (**A**) 3 h and (**B**) 12 h drug exposure compared to the control without SRT.

To validate the RNA-seq results, we randomly selected 15 genes from the differentially expressed genes related to processes such as catalytic activity, transferase activity, and transmembrane transport (Figure 3). The RT-qPCR data and corresponding RNA-seq values obtained from biological replicates (Table 2) confirmed the reliability of the results (Pearson's correlation, $r > 0.92$, $p < 0.001$).

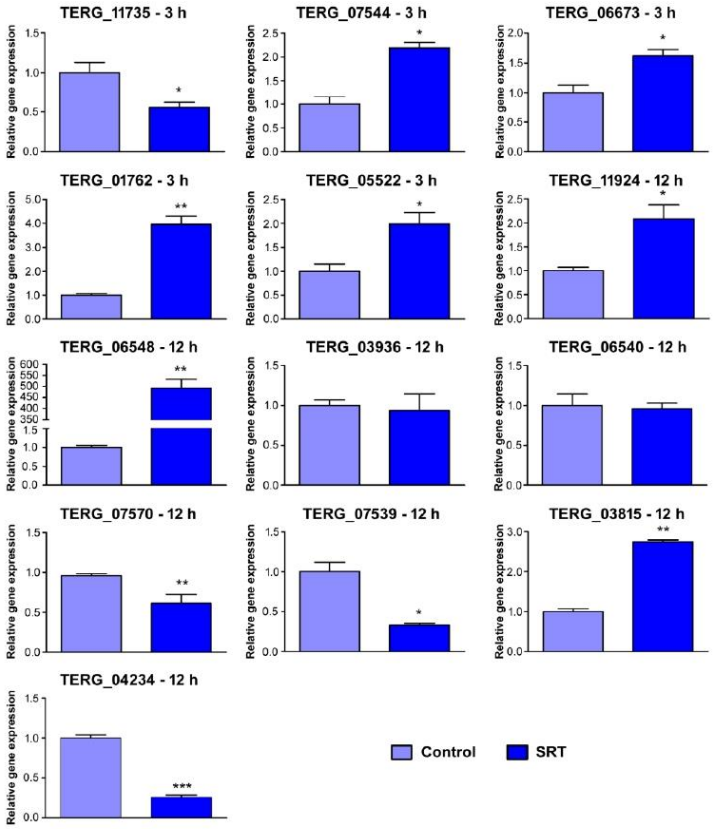

Figure 3. Validation by RT-qPCR of 15 genes differentially expressed in response to SRT exposure. Log2 fold change at each time point represents gene expression level changes at each time point. Expression levels are relative to the control without SRT. Asterisks indicate the statistical significance determined by the *t*-test followed by Tukey's post-hoc test (* $p < 0.05$; ** $p < 0.01$; *** $p < 0.001$). The identification of each gene is listed in Table 2.

Table 2. Comparison of the gene expression levels assayed by RNA sequencing and RT-qPCR.

ID	Condition	Gene Product Name	RNA-seq	RT-qPCR
TERG_11735	3 h	microtubule-associated protein (*T. tonsurans*)	−2.4	−1.41
TERG_07544	3 h	lipase (*T. tonsurans*)	2.02	1.13
TERG_06673	3 h	pachytene checkpoint component Pch2 (*T. tonsurans*)	2.0	0.70
TERG_01762	3 h	sulfite reductase (NADPH) hemoprotein beta-component	2.14	1.99
TERG_05522	3 h	lysophospholipase (*T. equinum*)	1.55	0.97
TERG_11924	12 h	ankyrin repeat protein (*T. tonsurans*)	3.85	1.06
TERG_06548	12 h	hypothetical protein (oxidoreductase, *M. canis*)	11.8	8.63
TERG_03936	12 h	CAMK protein kinase	−4.19	−0.09
TERG_06540	12 h	glutathione S-transferase (*T. tonsurans*)	−3.44	−0.07
TERG_07570	12 h	G-protein signaling regulator putative (*T. verrucosum*)	−3.47	−0.70
TERG_04234	12 h	hydrophobin putative (*T. verrucosum*)	−3.41	−1.98
TERG_07539	12 h	multidrug resistance protein (*T. tonsurans*)	−1.72	−1.61
TERG_03815	12 h	subtilisin-like protease 3	1.78	1.46

3.2. SRT Interferes with T. rubrum Signaling and Regulation

Few kinase- and transcription factor-coding genes were modulated in response to SRT. The *T. rubrum* kinome (protein kinase superfamily members) is predicted to comprise 170 coding genes [32]. In our results, 81 kinases were modulated (Figure S1), coding chiefly for serine/threonine–protein kinases and kinases belonging to the CMGC (cyclin-dependent kinases (CDKs)) group. Among the 15 serine/threonine–protein kinase genes modulated, only TERG_07509 was repressed after 12 h of treatment. Among the eight CMGC-type kinases modulated by SRT exposure, TERG_12259 (CMGC/CLK protein kinase), TERG_05893 (CMGC protein kinase), and TERG_07061 (CMGC/SRPK protein kinase) were repressed. The latter two belong to the SRPK family and are active in the regulation of splicing by phosphorylation [33]. SRPKs act synergistically with CLK protein kinases, a family of Cdc2-like kinases that can auto-phosphorylate tyrosine residues, but phosphorylate their substrates exclusively on serine/threonine residues. The associated activity of SRPKs and CLK proteins phosphorylates SR (serine/arginine-rich) proteins, which mediate the phosphorylation of SR proteins and direct pre-mRNA splicing [34].

The comparative evaluation between anthropophilic and zoophilic dermatophytes revealed that only kinases and transcription factor Interpro (IPR) domain families were enriched in anthropophilic dermatophytes, suggesting that the modulation of signaling pathways and transcriptional regulation are key factors in host specificity [32]. Here, the reduced number of transcription factors modulated in response to SRT challenge (Figure S2) suggests the restrained infective potential of *T. rubrum* under SRT exposure. Most modulated transcription factors code for zinc finger domain-containing proteins and are preferentially repressed, mainly after 12 h of SRT exposure (including TERG_02532, TERG_01042, and TERG_05497), for which transcript accumulation increased over time.

3.3. Cell Wall and Membrane Structure Are Affected by SRT

SRT modulates the expression of genes associated with the formation of glucans and chitins, which are important structural polysaccharides in the fungal cell wall. These genes include endoglucanases (TERG_08178, TERG_03353, TERG_06189, and TERG_04268), chitinases (TERG_05626 and TERG_05625), and chitin synthases (TERG_12318 and TERG_12319). While glucan-related genes were predominantly induced after 12 h of treatment, chitin-associated genes were repressed after 12 h of SRT challenge. The hydrophobin-coding gene (TERG_04234) was repressed after only 12 h of SRT exposure.

Furthermore, SRT was found to downregulate the expression of genes encoding components of the ergosterol biosynthetic pathway in *T. rubrum.* After 12 h, the genes that code for diphosphomevalonate decarboxylase (*erg*19; TERG_07616), C-8 sterol isomerase (*erg*1; TERG_06755), c-14 sterol reductase (*erg*24; TERG_04382), C-4 methylsterol oxidase (*erg*25; TERG_08545), ergosterol biosynthesis protein *erg*28 (TERG_04740), and sterol 24-C-methyltransferase/Delta (24(24[1]))-sterol reductase (*erg*4; TERG_06528/TERG_03102) were downregulated. The squalene epoxidase-coding gene (*erg*1; TERG_05717) was repressed after 3 and 12 h. The ergosterol dosage confirmed the inhibition of the biosynthetic pathway activity (Figure 4).

SRT, a cationic amphiphilic drug (CAD), causes drug-induced phospholipidosis (DIP) during excessive phospholipid storage within the lysosomes [18]. We observed the modulation of sphingomyelinase D (TERG_01406), lysosomal phospholipase A2 (TERG_03747), B (TERG_05522), and D (TERG_05303), and upregulation of secretory phospholipase A2 (TERG_00127).

Exposure to SRT led to the accumulation of transcripts of genes related to membrane transport. The number of modulated genes increased over time. Most downregulated genes at both time points are MFS transporters (3 of the 4 downregulated genes after 3 h, and 25 genes among the 38 downregulated genes after 12 h of SRT challenge). Among the upregulated genes, 23 remained upregulated after 3 and 12 h of drug challenge (Figure S3).

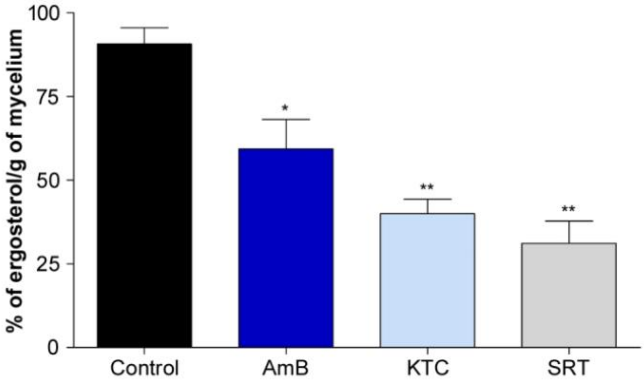

Figure 4. Effect of SRT on ergosterol content as a percentage of the wet weight of *T. rubrum*. Absence (negative control) and presence of amphotericin B (AMB, 1.25 µg/mL), ketoconazole (KTC, 4 µg/mL) (positive controls), and SRT (6.25 µg/mL). We tested the antifungals AMB and KTC at the minimal inhibitory concentration and the antidepressant SRT at a sub-inhibitory concentration. Asterisks represent statistical difference * $p < 0.05$ and ** $p < 0.01$ related to the control.

3.4. SRT Affects the Transcription of Oxidative Stress Genes in T. rubrum

Through upregulating the glutathione S-transferase (GST) genes (TERG 03390, TERG 04960, TERG 01405, TERG 07326, TERG 02041, TERG 00579, TERG 08208, and TERG 05135), *T. rubrum* could have an altered oxidative stress response when exposed to SRT. These genes participate in the sequestration of endogenous or xenobiotic compounds [35]. In the presence of SRT, two other GST genes (TERG_06540 and TERG_06578), as well as genes encoding catalase A (TERG_01252) and Fe-superoxide dismutase (TERG_04819), were downregulated. Additionally, SRT upregulated the gene encoding thioredoxin reductase (TERG_08849) and downregulated the thioredoxin gene (TERG_05849). Thioredoxins (TRX) are small ubiquitous redox proteins that play key roles in redox signaling and oxidative stress responses. The genes responsible for the conversion of melatonin into two metabolites, 6-hydroxymelatonin and N-acetyl-N-formyl-5-methoxykynuramine, were also upregulated by SRT (Figure 5). Finally, the most induced gene at both time points (TERG_06548) was an oxidoreductase ortholog identified in *Microsporum canis*.

3.5. Effect of SRT on T. rubrum Metabolism

SRT apparently interferes with the primary metabolism of *T. rubrum*. While genes involved in glycolysis are repressed, the genes involved in the glyoxylate cycle, ethanol and glycerol biosynthesis, and glycogen debranching are induced. The drug makes *T. rubrum* deviate from standard carbon metabolism to alternative pathways based on gene expression patterns (Figure 6). This repressive effect on glycolysis pathway genes counteracts the initial step performed by hexokinase (TERG_03229), which is induced. Metabolic reprogramming induced the expression of glyoxylate cycle-associated genes (TERG_11639, TERG_01281, TERG_08288, and TERG_08287) and glycerol biosynthesis genes (TERG_07273, TERG_12172, and TERG_12173). Additionally, SRT modulated ethanol- and glycerol-catabolism-related genes and induced a debranching enzyme (TERG_06681). This enzyme facilitates the breakdown of glycogen, which serves as a store of glucose.

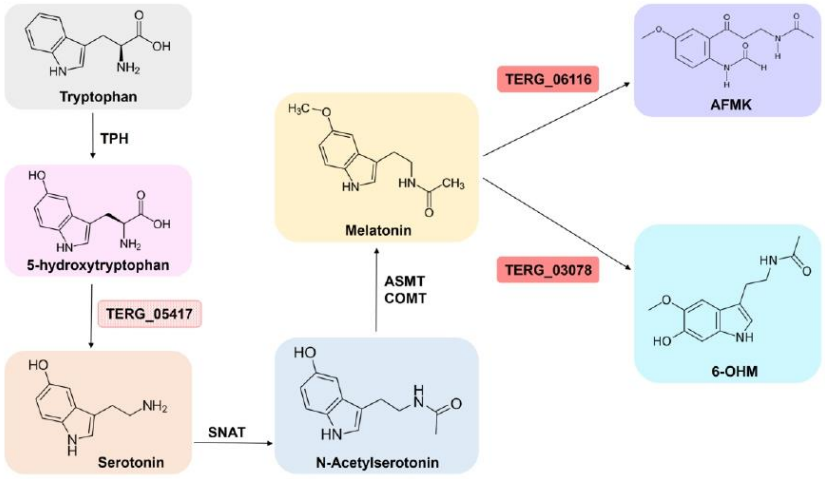

Figure 5. The biosynthetic pathway involved in synthesis of melatonin from tryptophan. Enzymatic steps from tryptophan to melatonin and the correlated metabolites. TPH: tryptophan hydroxylase; SNAT: serotonin N-acetyltransferase; ASMT: acetylserotonin O-methyltransferase; COMT: caffeic acid 3-O-methyltransferase; AFMK: N-acetyl-N-formyl-5-methoxykynuramine; 6-OHM: 6-hydroxymelatonin. The red genes are upregulated by *T. rubrum* in response to SRT. In pink, transcript accumulation is slightly below the log2 fold threshold (corresponding to 1.36 fold). Figure adapted from [36,37].

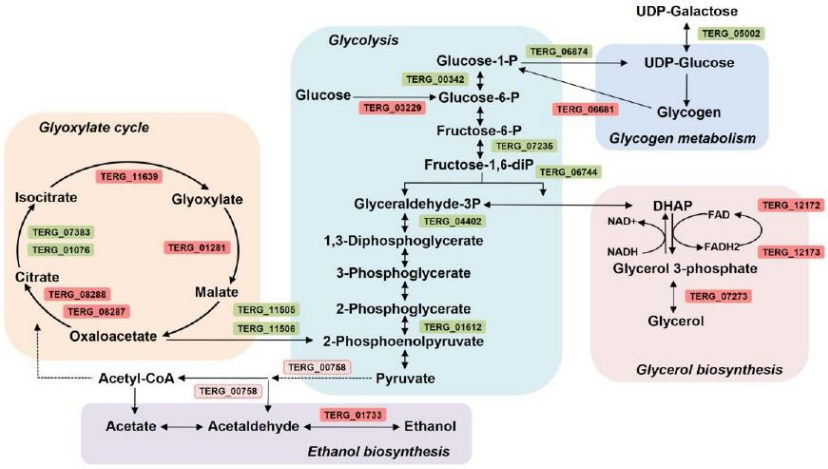

Figure 6. Schematic overview of the effect of SRT on the metabolism of *Trichophyton rubrum*. Genes induced (red) or repressed (green) considering log2 fold threshold ± 1.5. In pink, transcript accumulation is slightly below the log2 fold threshold (corresponding to 1.47 fold). UDP-galactose: uridine diphosphate galactose; UDP-glucose: uridine diphosphate glucose; DHAP: dihydroxyacetone phosphate.

4. Discussion

In addition to its use as an antidepressant, SRT has also been explored for other therapeutic applications. In vitro and in vivo studies have demonstrated its potential application in treating osteomyelitis infection [38] and cancer [39]. Furthermore, SRT presents antiparasitic [40], antibacterial [41], and antifungal activities against various pathogenic fungi, including *C. neoformans* [10,11], *Aspergillus fumigatus* [7], *Trichosporon asahii* [12], *Sporothrix schenckii* [9], and *T. rubrum* [15]. Through a drug repurposing approach, novel therapeutic options can rapidly enter clinical practice, as their safety and pharmacokinetics have been validated previously in patients. SRT is also effective alone or as an adjuvant therapeutic agent against fungal biofilm formation in vitro [15]. The synergistic effects of SRT combined with antifungals such as amphotericin B, caspofungin, or fluconazole have been documented in vitro [11–13,15]. Despite the potential therapeutic use of SRT in association with these drugs to control fungal infections, some are preferentially used intravenously.

4.1. SRT Affects Cell Signaling and Transcription in T. rubrum

Enrichment of the serine/threonine protein kinase domain (IPR002290), the catalytic domain of the protein kinase tyrosine, and the Zn(2)- C(6) fungal-like DNA-binding domain (IPR001138) has been reported in fungal anthropophilic organisms [32]. The transcriptional profile of *T. rubrum* after being challenged with SRT provided evidence that both kinases and transcriptional regulation-associated genes, when modulated, were preferentially induced, mainly at 12 h.

Phosphorylation by protein kinases is a critical mechanism that tunes cell activities, such as proliferation, metabolism, apoptosis, and gene expression. Cells possess thousands of kinases that phosphorylate specific sites in response to precise and controlled interactions [42]. The observed induced kinase modulation resulting from SRT exposure suggests the activation of specific signaling pathways. Our results indicate the activation of splicing events through the reversible phosphorylation of SR proteins. These phosphorylation events are dependent on both the SRPK and CLK families. The SRPK family of kinases phosphorylates SR proteins, promoting the nuclear import of SR proteins. Once in the nucleus, SR proteins may be further phosphorylated by the CLK family of kinases, which comprises a sequence of events essential for pre-mRNA splicing [33].

Conversely, the restricted number of protein kinase-coding genes modulated, considering the predicted whole kinome, implies the putative deactivation of other pathways. This deactivation strategy may represent a demand for energy conservation supported by, for example, the downregulation of ribosome biogenesis (Figure 2). Ribosome biogenesis is energetically expensive for cells. Consequently, unfavorable environmental conditions inhibit such processes [43].

Transcription factors are also associated with host specificity in dermatophytes [32]. We observed that a small number of transcriptional regulators were modulated, most of which had a zinc finger structural motif. Cells use transcription factors to dictate gene expression rates and regulate transcriptional networks [44]. Considering the relevance of transcription factor regulation and its key role in anthropophilic dermatophyte pathogenesis, we assume that drug challenge directly regulates transcription, possibly limiting energy expenditure under unfavorable conditions.

4.2. SRT Disturbs T. rubrum Cell Wall and Membrane

The fungal cell wall is a rigid layer with high plasticity that is essential for maintaining intracellular osmotic pressure [45]. β-1,3-glucan, chitin, and glycoproteins are primarily responsible for interactions between the cell and the environment. This wall is associated with a cell membrane that is predominantly composed of glycerophospholipids, sterols, and sphingolipids. Several molecules that form cell walls and membranes are exclusive to fungi and constitute suitable targets for antifungal development [45–47]. SRT exposure affects the expression of hydrolytic enzyme-coding genes in *T. rubrum*, which may contribute to changes in the cell wall structure.

Additionally, the repression of a beta-1,6 glucan synthetase that acts as a glycosidic linker suggests an imposed instability in cell wall assembly [48]. The overall repressive effects of SRT on the transcript levels for chitin synthases and chitinases may function as a compensatory mechanism to maintain cell wall integrity. This modulatory profile is similar to the effects of echinocandin antifungal agents on fungal cells. Echinocandins target the β-1,3-glucan synthase gene, deplete the glucan content of the cell wall, and increase chitin content.

Genes associated with ergosterol biosynthesis were downregulated after 12 h exposure to SRT, revealing that SRT affects plasma membrane properties. Moreover, SRT reduced ergosterol levels compared with amphotericin B and ketoconazole, which were used as positive controls (Figure 4). Amphotericin B complexes with ergosterol [49], whereas ketoconazole is a potent inhibitor of ergosterol biosynthesis [3]. Ergosterol modulates fluidity and permeability, interfering with water penetration [50]. The resultant alteration in the plasma membrane, together with the differential modulation of cell-wall-associated genes, suggests the occurrence of osmotic stress with alterations in the ergosterol composition of lipid bilayers, providing insights into the antifungal activity of SRT against *T. rubrum*.

Phospholipase A_2 and sphingomyelinase D activities are downregulated after 12 h treatment with SRT. Lysosomal phospholipase A_2 inhibition robustly correlates with drugs causing phospholipidosis [51], whereas the enzyme acid sphingomyelinase has been investigated as a potential target for antidepressant action [52]. Conversely, phospholipase B is upregulated at the initial SRT exposure, and phospholipase D is upregulated over time. Phospholipase B has hydrolase activity that cleaves fatty acids from phospholipids and lysophospholipids [53]. Phospholipase D comprises enzymes responsible for generating phosphatidic acid (PA), a putative secondary messenger implicated in the regulation of vesicular trafficking [54]. We observed that SRT also modulated genes involved in vesicular trafficking, including the induction of V-SNARE-coding genes (TERG_06294, TERG_07174) and the endoplasmic reticulum vesicle protein (TERG_00785) 25,388-fold induced after 3 h (log2 = 8.6). The secretory system of *T. rubrum* is essential for pathogenesis. Several keratinolytic enzymes are involved in the breakdown of keratin molecules, which may be assisted by ammonia and urea secretion [55]. The extra-vesicular content of *T. rubrum* is still not well understood. However, the vesicles of the dermatophyte *Trichophyton interdigitale* modulate the host immune response [56].

Besides affecting the cell wall structure and composition, global transcriptional analysis in response to SRT demonstrated the induction of drug resistance genes, mainly of the MFS genes, as a cellular stress response. The MFS is one of the largest groups of secondary active transporters and plays multiple roles in transporting a broad range of substrates, including sugars, amino acids, and drugs. The overall upregulated profile suggests a detoxification activity that increases with time since this family of proteins includes those encoding drug resistance transporters. However, at the 12 h time point, the downregulation of specific genes could represent an attempt to retain molecules such as phosphate (TERG_05891; MFS phosphate transporter) or monosaccharides (TERG_12194, TERG_04308; MFS sugar transporter), aiming to overcome the toxic drug effects.

4.3. SRT Overbalances Oxidative Stress Response

After 3 h of exposure to SRT, *T. rubrum* induced the expression of glutathione S-transferase genes to overcome its toxic effects. GSTs are small cytosolic proteins that contain a redox-active sulfhydryl group and are involved in cellular detoxification. Xenobiotics and endogenous products of oxidative stress are conjugated to glutathione (GSH) and secreted through vacuoles [57]. Endogenous toxic metabolites are removed through GSH-dependent detoxification processes. Thus, it confers protection against formaldehyde produced by methanol metabolism or against methylglyoxal, a byproduct of glycolysis [58,59]. Drug interactions with GSTs also facilitate their detoxification through GSH conjugation [60].

However, after 12 h of drug exposure, the downregulation of two glutathione transferase genes may reduce the efficiency of xenobiotic extrusion. Simultaneously, SRT down-

regulates Fe superoxide dismutase and catalase A genes, which neutralize reactive oxygen species (ROS).

The genes encoding thioredoxin and thioredoxin reductase were oppositely modulated after 12 h of SRT exposure. The thioredoxin/thioredoxin reductase system (Trx/TrxR) confers redox homeostasis to fungal cells [61]. Because SRT downregulates TrxR, the control of the cellular redox balance remains compromised. In *A. fumigatus* and *C. neoformans*, the TrxR-encoding gene is essential for growth under in vitro conditions and shows weak homology to its human ortholog, making it a potential antifungal target [60,62].

Saccharomyces cerevisiae subjected to oxidative stress induced by H_2O_2 shows increased *TRX* transcription; melatonin, an antioxidant agent, partially mitigates oxidative stress by enhancing *TRX* mRNA accumulation in cells exposed to H_2O_2 [63]. Here, the upregulation of the genes encoding the enzymes responsible for the conversion of melatonin into its metabolites indicates a decrease in melatonin availability (Figure 5), followed by the upregulation of the *Trx* gene and the downregulation of *TrxR*. These data support the speculated dependency between *Trx* and melatonin availability, suggesting the counterbalanced expression of the thioredoxin/thioredoxin reductase system under experimental conditions.

In humans, SSRI drugs increase serotonin levels in synaptic spaces. Based on our data, SRT increased in *T. rubrum* transcripts of the gene encoding an aromatic-L-amino acid decarboxylase (EC 4.1.1.28) slightly below the log2 fold threshold (1.36 fold) (Figure 5). This enzyme catalyzes the conversion of 5-hydroxytryptophan to serotonin [36,37]. In *Aspergillus* spp., serotonin can directly kill fungi in vitro [64].

4.4. SRT Imposes Dynamic Metabolic Modulation

The overall profile showed flexibility in metabolic modulation in response to the toxic effect of SRT, activating alternative carbon metabolism. In general, microorganisms deplete preferred nutrients such as glucose by activating a regulatory cascade that represses the consumption of alternative carbon sources such as maltose, galactose, or ethanol [65]. The induction of a glycogen debranching enzyme and sugar transporters indicates the cellular effort to release glucose through glycogen degradation in response to energy deficiency. In our results based on analyses of transcript levels, although glucose is available (at least through glycogen metabolism) and the enzyme hexokinase is induced, activating the initial step of glycolysis that is responsible for the phosphorylation of glucose by ATP to glucose-6-P, the glycolytic fluxes are not directed downward toward the synthesis of two 2-phosphoenolpyruvate molecules. Carbon catabolite repression (CCR) is a mechanism that handles the utilization of an energy-efficient and readily available carbon source preferentially over a relatively less easily degradable carbon source. This mechanism helps microorganisms to obtain the maximum amount of glucose to provide carbon for biosynthetic processes [66]. We hypothesize that *T. rubrum* triggers a different strategy in response to SRT challenge, overcoming CCR and redirecting gene expression patterns, activating genes responsible for the catabolism of less favored carbon sources. A glucose reservoir may, somehow, counteract the harmful effects caused by SRT exposure.

SRT treatment resulted in the repression of genes encoding glycolytic enzymes and an increase in the transcript levels of genes involved in alternative carbon utilization pathways, including the glyoxylate cycle. The induction of isocitrate lyase (TERG_11639) and malate synthase, glyoxysomal (TERG_01281) at the 3 h time point, and ATP-citrate synthases (TERG_08288/7) after 12 h drug exposure show the anabolic activity of the glyoxylate cycle counterbalancing glycolysis downregulation. The induction of the same isocitrate lyase (TERG_11639) at 48 and 96 h of *T. rubrum* incubation in keratin as the sole carbon source [55], coupled with the repression of genes related to glycolysis, suggests the promotion of a virulence response under both conditions. Glyoxylate cycle activation is directly associated with fungal pathogenicity [67,68]. Specifically, isocitrate lyase is a key enzyme in the glyoxylate cycle [69]. Our results suggest that the metabolic flexibility

observed in *T. rubrum* in vitro presumably contributes to its fitness and pathogenicity in vivo.

Based on transcriptional profiling, we hypothesize that SRT induced ethanol metabolism via alcohol dehydrogenase activity, and glycerol metabolism via glycerol kinase modulation. Transcript accumulation of pyruvate decarboxylase (TERG_00758) slightly below the log2 fold threshold (corresponding to 1.47 fold) suggests the enzymatic catalysis of pyruvic acid to acetaldehyde and the subsequent ethanol production. Pyruvate decarboxylase catalyzes the decarboxylation of pyruvate to acetaldehyde with the release of carbon dioxide and is a key enzyme in ethanol fermentation [70]; thus, it directs the metabolic activity of *T. rubrum* to different alternative carbon pathways in response to SRT exposure.

5. Concluding Remarks, Challenges, and Perspectives

The limited number of antifungals available in the market and the increase in antifungal resistance highlight the urgent need for new antifungals with new targets. This approach requires detailed knowledge of the basic biology of the organism and intracellular processes essential for its growth and survival in the human host. Here, we assessed the transcriptional profile of the dermatophyte *T. rubrum*, focusing on the mechanisms activated to counteract the antifungal activity of SRT. The repositioning of SRT as an antifungal drug seems to be reliable from a molecular perspective. This drug targets important molecular events and metabolic pathways. With our results, it was possible to perceive the depth of the complexity of the regulatory systems that operate to restore damage but that can be useful to direct innovative strategies focusing on the weaknesses of dermatophytes, taking advantage of well-tolerated drugs for human use. SRT challenge analysis provided clues to understand the response and adaptive mechanisms of *T. rubrum* to drug exposure. Although its clinical use as an antifungal agent is promising, further studies are needed to validate our findings.

Supplementary Materials: The following supporting information can be downloaded at: https://www.mdpi.com/article/10.3390/jof9020275/s1, Supplementary Figure S1. Kinase-related genes modulated in response to SRT. Supplementary Figure S2. Transcription-factor-related genes modulated in response to SRT. Supplementary Figure S3. *Trichophyton rubrum* membrane transporter genes modulated in response to SRT. Supplementary Table S1. List of primers used in RT-qPCR assays. Supplementary Table S2. General features of RNA-seq reads mapped to the *Trichophyton rubrum* reference genome. Supplementary Table S3. *Trichophyton rubrum* genes modulated in response to SRT exposure at each time point.

Author Contributions: N.M.M.-R. and A.R. designed the project. F.M.G.-R. and C.H.L.R. performed the laboratory experiments. T.A.B. and M.P.M. helped with some laboratory experiments and assisted in RNA-seq construction. P.R.S. performed the bioinformatics analyses. F.M.G.-R., C.H.L.R., P.R.S. and M.P.M. composed the figures. F.M.G.-R., M.P.M. and A.R. wrote the manuscript. N.M.M.-R. and A.R. provided funds, supervised the study, and edited the manuscript. M.S.S. discussed the results and edited the manuscript. All authors have read and agreed to the published version of the manuscript.

Funding: This work was supported by research grants from the following Brazilian funding agencies: São Paulo Research Foundation (FAPESP; Grant No. 2019/22596-9, and Fellowships No. 2018/11319-1 to M.M. and No. 2015/23435-8 to T.B.), National Council for Scientific and Technological Development (CNPq; Grant Nos. 307871/2021-5 and 307876/2021-7), Coordenação de Aperfeiçoamento de Pessoal de Nível Superior (CAPES; Finance Code 001), and Fundação de Apoio ao Ensino, Pesquisa e Assistência (FAEPA).

Institutional Review Board Statement: The Ethics Committee of the University Hospital of Ribeirão Preto Medical School, USP, Brazil (HCFMRP-USP) (Protocol No. 4.278.367/2020), approved this study.

Informed Consent Statement: Not applicable.

Data Availability Statement: We deposited RNA-sequencing (RNA-seq) data in the Gene Expression Omnibus (GEO) database under accession number GSE218521.

Acknowledgments: We thank V. M. de Oliveira, M. Mazucato, and M. D. Martins for the technical assistance.

Conflicts of Interest: The authors declare no conflict of interest.

References

1. Rouzaud, C.; Hay, R.; Chosidow, O.; Dupin, N.; Puel, A.; Lortholary, O.; Lanternier, F. Severe Dermatophytosis and Acquired or Innate Immunodeficiency: A Review. *J. Fungi* **2015**, *2*, 4. [CrossRef] [PubMed]
2. Piraccini, B.M.; Alessandrini, A. Onychomycosis: A Review. *J. Fungi* **2015**, *1*, 30–43. [CrossRef] [PubMed]
3. Martinez-Rossi, N.M.; Peres, N.T.; Bitencourt, T.A.; Martins, M.P.; Rossi, A. State-of-the-art Dermatophyte infections: Epidemiology aspects, pathophysiology, and resistance mechanisms. *J. Fungi* **2021**, *7*, 629. [CrossRef] [PubMed]
4. Martinez-Rossi, N.M.; Bitencourt, T.A.; Peres, N.T.A.; Lang, E.A.S.; Gomes, E.V.; Quaresemin, N.R.; Martins, M.P.; Lopes, L.; Rossi, A. Dermatophyte Resistance to Antifungal Drugs: Mechanisms and Prospectus. *Front. Microbiol.* **2018**, *9*, 1108. [CrossRef]
5. Rossi, A.; Martins, M.r.P.; Bitencourt, T.A.; Peres, N.T.A.; Rocha, C.H.L.; Rocha, F.M.G.; Neves-da-Rocha, J.o.; Lopes, M.E.R.; Sanches, P.R.; Bortolossi, J.C. Reassessing the use of undecanoic acid as a therapeutic strategy for treating fungal infections. *Mycopathologia* **2021**, *186*, 327–340. [CrossRef]
6. Zhang, Q.; Liu, F.; Zeng, M.; Mao, Y.; Song, Z. Drug repurposing strategies in the development of potential antifungal agents. *Appl. Microbiol. Biotechnol.* **2021**, *105*, 5259–5279. [CrossRef]
7. Lass-Flörl, C.; Dierich, M.; Fuchs, D.; Semenitz, E.; Jenewein, I.; Ledochowski, M. Antifungal properties of selective serotonin reuptake inhibitors against *Aspergillus* species in vitro. *J. Antimicrob. Chemother.* **2001**, *48*, 775–779. [CrossRef]
8. Ayaz, M.; Subhan, F.; Ahmed, J.; Khan, A.U.; Ullah, F.; Ullah, I.; Ali, G.; Syed, N.I.; Hussain, S. Sertraline enhances the activity of antimicrobial agents against pathogens of clinical relevance. *J. Biol. Res.* **2015**, *22*, 4. [CrossRef]
9. Villanueva-Lozano, H.; Treviño-Rangel, R.J.; Téllez-Marroquín, R.; Bonifaz, A.; Rojas, O.C.; Hernández-Rodríguez, P.A.; González, G.M. In vitro inhibitory activity of sertraline against clinical isolates of *Sporothrix schenckii*. *Rev. Iberoam. Micol.* **2019**, *36*, 139–141. [CrossRef]
10. Breuer, M.R.; Dasgupta, A.; Vasselli, J.G.; Lin, X.; Shaw, B.D.; Sachs, M.S. The Antidepressant Sertraline Induces the Formation of Supersized Lipid Droplets in the Human Pathogen *Cryptococcus neoformans*. *J. Fungi* **2022**, *8*, 642. [CrossRef]
11. Zhai, B.; Wu, C.; Wang, L.; Sachs, M.S.; Lin, X. The antidepressant sertraline provides a promising therapeutic option for neurotropic cryptococcal infections. *Antimicrob. Agents Chemother.* **2012**, *56*, 3758–3766. [CrossRef]
12. Cong, L.; Liao, Y.; Yang, S.; Yang, R. *In vitro* antifungal activity of sertraline and synergistic effects in combination with antifungal drugs against planktonic forms and biofilms of clinical *Trichosporon asahii* isolates. *PLoS ONE* **2016**, *11*, e0167903. [CrossRef]
13. Rossato, L.; Loreto, É.S.; Zanette, R.A.; Chassot, F.; Santurio, J.M.; Alves, S.H. *In vitro* synergistic effects of chlorpromazine and sertraline in combination with amphotericin B against *Cryptococcus neoformans* var. grubii. *Folia Microbiol.* **2016**, *61*, 399–403. [CrossRef]
14. Villanueva-Lozano, H.; González, G.M.; Espinosa-Mora, J.E.; Bodden-Mendoza, B.A.; Andrade, A.; Martínez-Reséndez, M.F.; Treviño-Rangel, R.J. Evaluation of the expanding spectrum of sertraline against uncommon fungal pathogens. *J. Infect. Chemother.* **2020**, *26*, 309–311. [CrossRef]
15. Rocha, C.H.L.; Rocha, F.M.G.; Bitencourt, T.A.; Martins, M.P.; Sanches, P.R.; Rossi, A.; Martinez-Rossi, N.M. Synergism between the Antidepressant Sertraline and Caspofungin as an Approach to Minimise the Virulence and Resistance in the Dermatophyte *Trichophyton rubrum*. *J. Fungi* **2022**, *8*, 815. [CrossRef]
16. Sangkuhl, K.; Klein, T.E.; Altman, R.B. Selective serotonin reuptake inhibitors pathway. *Pharm. Genom.* **2009**, *19*, 907–909. [CrossRef]
17. Kim, S.W.; Park, S.Y.; Hwang, O. Up-regulation of tryptophan hydroxylase expression and serotonin synthesis by sertraline. *Mol. Pharmacol.* **2002**, *61*, 778–785. [CrossRef]
18. Rainey, M.M.; Korostyshevsky, D.; Lee, S.; Perlstein, E.O. The antidepressant sertraline targets intracellular vesiculogenic membranes in yeast. *Genetics* **2010**, *185*, 1221–1233. [CrossRef]
19. Bolger, A.M.; Lohse, M.; Usadel, B. Trimmomatic: A flexible trimmer for Illumina sequence data. *Bioinformatics* **2014**, *30*, 2114–2120. [CrossRef]
20. Dobin, A.; Davis, C.A.; Schlesinger, F.; Drenkow, J.; Zaleski, C.; Jha, S.; Batut, P.; Chaisson, M.; Gingeras, T.R. STAR: Ultrafast universal RNA-seq aligner. *Bioinformatics* **2013**, *29*, 15–21. [CrossRef]
21. Thorvaldsdóttir, H.; Robinson, J.T.; Mesirov, J.P. Integrative Genomics Viewer (IGV): High-performance genomics data visualization and exploration. *Brief. Bioinform.* **2013**, *14*, 178–192. [CrossRef] [PubMed]
22. Love, M.I.; Huber, W.; Anders, S. Moderated estimation of fold change and dispersion for RNA-seq data with DESeq2. *Genome Biol.* **2014**, *15*, 550. [CrossRef] [PubMed]
23. Benjamini, Y.; Hochberg, Y. Controlling the False Discovery Rate: A Practical and Powerful Approach to Multiple Testing. *J. R. Stat. Soc. Ser. B Methodol.* **1995**, *57*, 289–300. [CrossRef]
24. Persinoti, G.F.; de Aguiar Peres, N.T.; Jacob, T.R.; Rossi, A.; Vêncio, R.Z.; Martinez-Rossi, N.M. RNA-sequencing analysis of *Trichophyton rubrum* transcriptome in response to sublethal doses of acriflavine. *BMC Genom.* **2014**, *15* (Suppl 7), S1. [CrossRef] [PubMed]

25. Vencio, R.Z.; Koide, T.; Gomes, S.L.; Pereira, C.A. BayGO: Bayesian analysis of ontology term enrichment in microarray data. *BMC Bioinform.* **2006**, *7*, 86. [CrossRef]
26. Finn, R.D.; Clements, J.; Eddy, S.R. HMMER web server: Interactive sequence similarity searching. *Nucleic Acids Res.* **2011**, *39*, W29–W37. [CrossRef]
27. Finn, R.D.; Bateman, A.; Clements, J.; Coggill, P.; Eberhardt, R.Y.; Eddy, S.R.; Heger, A.; Hetherington, K.; Holm, L.; Mistry, J.; et al. Pfam: The protein families database. *Nucleic Acids Res.* **2014**, *42*, D222–D230. [CrossRef]
28. Jacob, T.R.; Peres, N.T.A.; Persinoti, G.F.; Silva, L.G.; Mazucato, M.; Rossi, A.; Martinez-Rossi, N.M. *rpb2* is a reliable reference gene for quantitative gene expression analysis in the dermatophyte *Trichophyton rubrum*. *Med. Mycol.* **2012**, *50*, 368–377. [CrossRef]
29. Livak, K.J.; Schmittgen, T.D. Analysis of relative gene expression data using real-time quantitative PCR and the $2^{-\Delta\Delta CT}$ method. *Methods* **2001**, *25*, 402–408. [CrossRef]
30. Arthington-Skaggs, B.A.; Jradi, H.; Desai, T.; Morrison, C.J. Quantitation of ergosterol content: Novel method for determination of fluconazole susceptibility of *Candida albicans*. *J. Clin. Microbiol.* **1999**, *37*, 3332–3337. [CrossRef]
31. Mendes, N.S.; Bitencourt, T.A.; Sanches, P.R.; Silva-Rocha, R.; Martinez-Rossi, N.M.; Rossi, A. Transcriptome-wide survey of gene expression changes and alternative splicing in *Trichophyton rubrum* in response to undecanoic acid. *Sci. Rep.* **2018**, *8*, 14. [CrossRef]
32. Martinez, D.A.; Oliver, B.G.; Graser, Y.; Goldberg, J.M.; Li, W.; Martinez-Rossi, N.M.; Monod, M.; Shelest, E.; Barton, R.C.; Birch, E.; et al. Comparative Genome Analysis of *Trichophyton rubrum* and Related Dermatophytes Reveals Candidate Genes Involved in Infection. *MBio* **2012**, *3*, e00259-12. [CrossRef]
33. Zhou, Z.; Fu, X.D. Regulation of splicing by SR proteins and SR protein-specific kinases. *Chromosoma* **2013**, *122*, 191–207. [CrossRef]
34. Bullock, A.N.; Das, S.; Debreczeni, J.E.; Rellos, P.; Fedorov, O.; Niesen, F.H.; Guo, K.; Papagrigoriou, E.; Amos, A.L.; Cho, S.; et al. Kinase domain insertions define distinct roles of CLK kinases in SR protein phosphorylation. *Structure* **2009**, *17*, 352–362. [CrossRef]
35. Hayes, J.D.; Strange, R.C. Glutathione S-transferase polymorphisms and their biological consequences. *Pharmacology* **2000**, *61*, 154–166. [CrossRef]
36. Muñiz-Calvo, S.; Bisquert, R.; Fernández-Cruz, E.; García-Parrilla, M.C.; Guillamón, J.M. Deciphering the melatonin metabolism in *Saccharomyces cerevisiae* by the bioconversion of related metabolites. *J. Pineal Res.* **2019**, *66*, e12554. [CrossRef]
37. Gallardo-Fernández, M.; Valls-Fonayet, J.; Valero, E.; Hornedo-Ortega, R.; Richard, T.; Troncoso, A.M.; Garcia-Parrilla, M.C. Isotopic labelling-based analysis elucidates biosynthesis pathways in *Saccharomyces cerevisiae* for Melatonin, Serotonin and Hydroxytyrosol formation. *Food Chem.* **2022**, *374*, 131742. [CrossRef]
38. Muthu, D.; Gowri, M.; Suresh Kumar, G.; Kattimani, V.S.; Girija, E.K. Repurposing of antidepression drug sertraline for antimicrobial activity against *Staphylococcus aureus*: A potential approach for the treatment of osteomyelitis. *New J. Chem.* **2019**, *43*, 5315–5324. [CrossRef]
39. Baú-Carneiro, J.L.; Akemi Guirao Sumida, I.; Gallon, M.; Zaleski, T.; Boia-Ferreira, M.; Bridi Cavassin, F. Sertraline repositioning: An overview of its potential use as a chemotherapeutic agent after four decades of tumor reversal studies. *Transl. Oncol.* **2022**, *16*, 101303. [CrossRef]
40. Ferreira, D.D.; Mesquita, J.T.; da Costa Silva, T.A.; Romanelli, M.M.; da Gama Jaen Batista, D.; da Silva, C.F.; da Gama, A.N.S.; Neves, B.J.; Melo-Filho, C.C.; Correia Soeiro, M.N.; et al. Efficacy of sertraline against *Trypanosoma cruzi*: An in vitro and in silico study. *J. Venom. Anim. Toxins Incl. Trop. Dis.* **2018**, *24*, 30. [CrossRef]
41. Krzyżek, P.; Franiczek, R.; Krzyżanowska, B.; Laczmański, L.; Migdal, P.; Gościniak, G. In Vitro Activity of Sertraline, an Antidepressant, Against Antibiotic-Susceptible and Antibiotic-Resistant *Helicobacter pylori* Strains. *Pathogens* **2019**, *8*, 228. [CrossRef] [PubMed]
42. Watson, N.A.; Cartwright, T.N.; Lawless, C.; Cámara-Donoso, M.; Sen, O.; Sako, K.; Hirota, T.; Kimura, H.; Higgins, J.M.G. Kinase inhibition profiles as a tool to identify kinases for specific phosphorylation sites. *Nat. Commun.* **2020**, *11*, 1684. [CrossRef] [PubMed]
43. Piazzi, M.; Bavelloni, A.; Gallo, A.; Faenza, I.; Blalock, W.L. Signal Transduction in Ribosome Biogenesis: A Recipe to Avoid Disaster. *Int. J. Mol. Sci.* **2019**, *20*, 2718. [CrossRef] [PubMed]
44. Shelest, E. Transcription factors in fungi. *FEMS Microbiol. Lett.* **2008**, *286*, 145–151. [CrossRef]
45. Beauvais, A.; Latgé, J.-P. Special Issue: Fungal Cell Wall. *J. Fungi* **2018**, *4*, 91. [CrossRef]
46. Martins, M.P.; Silva, L.G.; Rossi, A.; Sanches, P.R.; Souza, L.D.R.; Martinez-Rossi, N.M. Global Analysis of Cell Wall Genes Revealed Putative Virulence Factors in the Dermatophyte *Trichophyton rubrum*. *Front. Microbiol.* **2019**, *10*, 2168. [CrossRef]
47. Ibe, C.; Munro, C.A. Fungal cell wall: An underexploited target for antifungal therapies. *PLoS Pathog.* **2021**, *17*, e1009470. [CrossRef]
48. Roncero, C.; Vázquez de Aldana, C.R. Glucanases and Chitinases. *Curr. Top. Microbiol. Immunol.* **2020**, *425*, 131–166.
49. Yamamoto, T.; Umegawa, Y.; Tsuchikawa, H.; Hanashima, S.; Matsumori, N.; Funahashi, K.; Seo, S.; Shinoda, W.; Murata, M. The Amphotericin B-Ergosterol Complex Spans a Lipid Bilayer as a Single-Length Assembly. *Biochemistry* **2019**, *58*, 5188–5196. [CrossRef]
50. Abe, F.; Usui, K.; Hiraki, T. Fluconazole modulates membrane rigidity, heterogeneity, and water penetration into the plasma membrane in *Saccharomyces cerevisiae*. *Biochemistry* **2009**, *48*, 8494–8504. [CrossRef]

51. Hinkovska-Galcheva, V.; Treadwell, T.; Shillingford, J.M.; Lee, A.; Abe, A.; Tesmer, J.J.G.; Shayman, J.A. Inhibition of lysosomal phospholipase A2 predicts drug-induced phospholipidosis. *J. Lipid Res.* **2021**, *62*, 100089. [CrossRef]
52. Rhein, C.; Reichel, M.; Kramer, M.; Rotter, A.; Lenz, B.; Mühle, C.; Gulbins, E.; Kornhuber, J. Alternative *splicing* of SMPD1 coding for acid sphingomyelinase in major depression. *J. Affect. Disord.* **2017**, *209*, 10–15. [CrossRef]
53. Ramrakhiani, L.; Chand, S. Recent progress on phospholipases: Different sources, assay methods, industrial potential and pathogenicity. *Appl. Biochem. Biotechnol.* **2011**, *164*, 991–1022. [CrossRef]
54. O'Luanaigh, N.; Pardo, R.; Fensome, A.; Allen-Baume, V.; Jones, D.; Holt, M.R.; Cockcroft, S. Continual production of phosphatidic acid by phospholipase D is essential for antigen-stimulated membrane ruffling in cultured mast cells. *Mol. Biol. Cell* **2002**, *13*, 3730–3746. [CrossRef]
55. Martins, M.P.; Rossi, A.; Sanches, P.R.; Bortolossi, J.C.; Martinez-Rossi, N.M. Comprehensive analysis of the dermatophyte *Trichophyton rubrum* transcriptional profile reveals dynamic metabolic modulation. *Biochem. J.* **2020**, *477*, 873–885. [CrossRef]
56. Bitencourt, T.A.; Rezende, C.P.; Quaresemin, N.R.; Moreno, P.; Hatanaka, O.; Rossi, A.; Martinez-Rossi, N.M.; Almeida, F. Extracellular Vesicles From the Dermatophyte *Trichophyton interdigitale* Modulate Macrophage and Keratinocyte Functions. *Front. Immunol.* **2018**, *9*, 2343. [CrossRef]
57. Sato, I.; Shimizu, M.; Hoshino, T.; Takaya, N. The glutathione system of *Aspergillus nidulans* involves a fungus-specific glutathione S-transferase. *J. Biol. Chem.* **2009**, *284*, 8042–8053. [CrossRef]
58. Pócsi, I.; Prade, R.A.; Penninckx, M.J. Glutathione, altruistic metabolite in fungi. *Adv. Microb. Physiol.* **2004**, *49*, 1–76.
59. He, Y.; Zhou, C.; Huang, M.; Tang, C.; Liu, X.; Yue, Y.; Diao, Q.; Zheng, Z.; Liu, D. Glyoxalase system: A systematic review of its biological activity, related-diseases, screening methods and small molecule regulators. *Biomed. Pharmacother.* **2020**, *131*, 110663. [CrossRef]
60. Missall, T.A.; Lodge, J.K. Function of the thioredoxin proteins in *Cryptococcus neoformans* during stress or virulence and regulation by putative transcriptional modulators. *Mol. Microbiol.* **2005**, *57*, 847–858. [CrossRef]
61. Pannala, V.R.; Dash, R.K. Mechanistic characterization of the thioredoxin system in the removal of hydrogen peroxide. *Free Radic. Biol. Med.* **2015**, *78*, 42–55. [CrossRef] [PubMed]
62. Binder, J.; Shadkchan, Y.; Osherov, N.; Krappmann, S. The Essential Thioredoxin Reductase of the Human Pathogenic Mold *Aspergillus fumigatus* Is a Promising Antifungal Target. *Front. Microbiol.* **2020**, *11*, 1383. [CrossRef] [PubMed]
63. Vázquez, J.; González, B.; Sempere, V.; Mas, A.; Torija, M.J.; Beltran, G. Melatonin Reduces Oxidative Stress Damage Induced by Hydrogen Peroxide in *Saccharomyces cerevisiae*. *Front. Microbiol.* **2017**, *8*, 1066. [CrossRef] [PubMed]
64. Perkhofer, S.; Niederegger, H.; Blum, G.; Burgstaller, W.; Ledochowski, M.; Dierich, M.P.; Lass-Flörl, C. Interaction of 5-hydroxytryptamine (serotonin) against *Aspergillus* spp. in vitro. *Int. J. Antimicrob. Agents* **2007**, *29*, 424–429. [CrossRef]
65. New, A.M.; Cerulus, B.; Govers, S.K.; Perez-Samper, G.; Zhu, B.; Boogmans, S.; Xavier, J.B.; Verstrepen, K.J. Different levels of catabolite repression optimize growth in stable and variable environments. *PLoS Biol.* **2014**, *12*, e1001764. [CrossRef]
66. Adnan, M.; Zheng, W.; Islam, W.; Arif, M.; Abubakar, Y.S.; Wang, Z.; Lu, G. Carbon Catabolite Repression in Filamentous Fungi. *Int. J. Mol. Sci.* **2017**, *19*, 48. [CrossRef]
67. Lorenz, M.C.; Fink, G.R. The glyoxylate cycle is required for fungal virulence. *Nature* **2001**, *412*, 83–86. [CrossRef]
68. Cruz, A.H.S.; Santos, R.S.; Martins, M.P.; Peres, N.T.A.; Trevisan, G.L.; Mendes, N.S.; Martinez-Rossi, N.M.; Rossi, A. Relevance of Nutrient-Sensing in the Pathogenesis of *Trichophyton rubrum* and *Trichophyton interdigitale*. *Front. Fungal Biol.* **2022**, *3*. [CrossRef]
69. Chew, S.Y.; Ho, K.L.; Cheah, Y.K.; Ng, T.S.; Sandai, D.; Brown, A.J.P.; Than, L.T.L. Glyoxylate cycle gene ICL1 is essential for the metabolic flexibility and virulence of Candida glabrata. *Sci. Rep.* **2019**, *9*, 2843. [CrossRef]
70. Ishchuk, O.P.; Voronovsky, A.Y.; Stasyk, O.V.; Gayda, G.Z.; Gonchar, M.V.; Abbas, C.A.; Sibirny, A.A. Overexpression of pyruvate decarboxylase in the yeast Hansenula polymorpha results in increased ethanol yield in high-temperature fermentation of xylose. *FEMS Yeast Res.* **2008**, *8*, 1164–1174. [CrossRef]

Mycopathologia
https://doi.org/10.1007/s11046-021-00550-4

REVIEW

Reassessing the Use of Undecanoic Acid as a Therapeutic Strategy for Treating Fungal Infections

Antonio Rossi · Maíra P. Martins · Tamires A. Bitencourt · Nalu T. A. Peres · Carlos H. L. Rocha · Flaviane M. G. Rocha · João Neves-da-Rocha · Marcos E. R. Lopes · Pablo R. Sanches · Júlio C. Bortolossi · Nilce M. Martinez-Rossi

Received: 11 December 2020 / Accepted: 21 March 2021

Abstract Treating fungal infections is challenging and frequently requires long-term courses of antifungal drugs. Considering the limited number of existing antifungal drugs, it is crucial to evaluate the possibility of repositioning drugs with antifungal properties and to revisit older antifungals for applications in combined therapy, which could widen the range of therapeutic possibilities. Undecanoic acid is a saturated medium-chain fatty acid with known antifungal effects; however, its antifungal properties have not been extensively explored. Recent advances indicate that the toxic effect of undecanoic acid involves modulation of fungal metabolism through its effects on the expression of fungal genes that are critical for virulence. Additionally, undecanoic acid is suitable for chemical modification and might be useful in synergic therapies. This review highlights the use of undecanoic acid in antifungal treatments, reinforcing its known activity against dermatophytes. Specifically, in *Trichophyton rubrum*, against which the activity of undecanoic acid has been most widely studied, undecanoic acid elicits profound effects on pivotal processes in the cell wall, membrane assembly, lipid metabolism, pathogenesis, and even mRNA processing. Considering the known antifungal activities and associated mechanisms of undecanoic acid, its potential use in combination therapy, and the ability to modify the parent compound structure, undecanoic acid shows promise as a novel therapeutic against fungal infections.

Keywords Fatty acid · Undecanoic acid · Dermatophyte · Antifungal resistance · Synergistic · Pre-mRNA processing

Handling Editor: Vishnu Chaturvedi.

A. Rossi · M. P. Martins · T. A. Bitencourt · C. H. L. Rocha · F. M. G. Rocha · J. Neves-da-Rocha · M. E. R. Lopes · P. R. Sanches · J. C. Bortolossi · N. M. Martinez-Rossi (✉)
Department of Genetics, Ribeirão Preto Medical School, University of São Paulo, USP, Ribeirão Preto, SP 14049-900, Brazil
e-mail: nmmrossi@usp.br

N. T. A. Peres
Department of Microbiology, Institute of Biological Sciences, Federal University of Minas Gerais, Belo Horizonte, MG, Brazil

Introduction

Antifungal therapy is based on drugs that block cellular processes, such as cell wall assembly, cell membrane biosynthesis and maintenance, microtubule formation, and nucleic acid biosynthesis. The limited arsenal of antifungal drugs, the increasing prevalence of fungal infections, and the isolation of strains resistant to current medicines have motivated researchers to search for new therapeutic strategies

Published online: 09 April 2021

to control these infections [1]. The search for new antifungal drugs has involved studies of compounds derived from plants and other microorganisms that display antifungal properties [2, 3]. Various approaches have been evaluated to improve the efficacies of antifungal treatments. For example, combination therapy involves the use of clinically approved medicines that act synergistically with low toxicity and enhanced effectiveness. Novel technologies have been developed, especially those using nanoparticles, which have enabled improved drug delivery and availability, and decreased toxicity [4].

The therapeutic use of fatty acids (FA) has been known for a long time, especially against fungal skin infections. Their presence in the human skin represents a chemical barrier against opportunistic and pathogenic bacteria and fungi and is essential in maintaining skin integrity. FAs are also produced by the hydrolysis of phospholipids in keratinocytes, sebaceous glands, or the stratum corneum. In addition to their antimicrobial activities, they also play essential roles in maintaining acidification in the stratum corneum, making the skin a hostile environment for most pathogenic microorganisms [5, 6].

The antimycotic properties of organic acids have been evaluated since the nineteenth century [7]. In the 1940s, ointments containing propionate and undecylenate were proposed for treating dermatophytosis [8]. In addition, using a preparation of zinc undecylenate ($C_{22}H_{38}O_4Zn$) and undecylenic acid ($C_{11}H_{20}O_2$) (Fig. 1) in a vanishing emulsion base led to a complete clinical cure in the great majority of tinea pedis and tinea cruris cases [9]. Furthermore, the superiority of the propionate-caprylate mixture was verified in vitro and in vivo against dermatophytes, demonstrating that this combination seemed to be more effective than any other fatty acids previously used to treat these diseases [10]. At that time, studies were aimed at evaluating the fungistatic or fungicidal effect of FAs, particularly those found in human sweat (such as propionic, caproic, and caprylic acid); perspiration was attributed a protective activity against fungal infections [10].

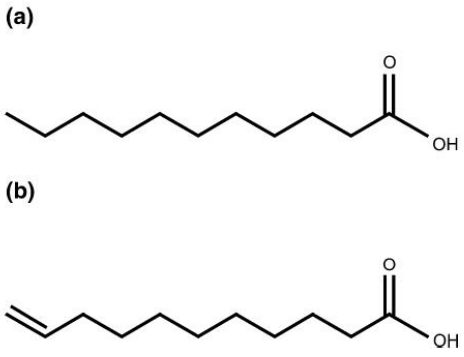

Fig. 1 Chemical structure of **a** undecanoic acid and **b** undecylenic acid

The antifungal activity of FAs was believed to be directly proportional to the number of carbon atoms in the molecule [11] or associated with the pH of the medium used in the assay. FAs with six or fewer carbon atoms exhibited higher antifungal activity in acidic medium, whereas FAs with more than seven carbons ($C_{7:0}$–$C_{12:0}$) exhibited higher activities at pH 7.0 or 8.0 [12]. The hypothesis of a relationship between antifungal activity and the number of carbon atoms in FA molecules was refuted when valeric acid, a FA with 5 carbon atoms, displayed the strongest fungicide activity of all the acids analyzed, including formic acid (1 carbon atom) to capric acid (10 carbon atoms), as well as the unsaturated undecylenic acid [13]. Further tests against dermatophytes demonstrated short-chain saturated FAs (C_7 to C_{11}) to be more toxic than long-chain molecules (> C_{12}), and undecanoic acid (UDA, a medium-chain saturated C_{11}) (Fig. 1) was the most toxic within the $C_{7:0}$-$C_{18:0}$ carbon atom series [14]. Interestingly, this FA is also found naturally in human sweat.

Studies on the activities of FAs in fungi have shown that they inhibit several biological processes, including respiration [15], cellular FA accumulation, and pigment formation in the dermatophyte *Trichophyton rubrum* [16]. FAs also reduced phosphate uptake and glucose fermentation in *Saccharomyces cerevisiae* [17]. UDA inhibited the growth of *T. rubrum*, conidia germination [18], phospholipid biosynthesis [19], and extracellular keratinase and lipase activities, but enhanced the activity of phospholipase A [20]. But, at low doses, UDA increased the lipid content [21]. Moreover, UDA-resistant strains have lowered virulence and important pathogenic traits are compromised by this FA [20, 22]. Recently, our group showed that UDA exposure affected the integrity, stability, and assembly of the cell wall and membrane of *T. rubrum*, and caused a decrease in the ergosterol level. These studies showed that UDA influenced the

expression of several genes involved in lipid metabolism, oxidative stress, cell wall and plasma membrane assembly, and pathogenesis [23, 24]. Furthermore, UDA affected the splicing of genes essential for cellular metabolism, intracellular signaling, and adaptation to stress [24–26].

Avrahami and Shai showed that UDA conjugation with antimicrobial lipopeptides can broaden their spectrum of actions, making them useful against several microorganisms [27]. These authors discussed the potential for increasing the activities of antimicrobial peptides by exploiting the property of synthetic lipopeptides in which they act directly on plasma membranes, thereby altering membrane permeability and facilitating drug uptake. UDA also causes damage to the cell wall and plasma membrane of fungi, suggesting it contributes to the synergistic effect of these two antimicrobial substances.

Combination treatment with UDA and quinic acid (QA), a compound derived from plants, synergistically inhibited the growth of *Candida albicans*, *Candida glabrata,* and *Candida tropicalis* by affecting several traits involved in virulence, such as biofilm formation and the production of proteases and phospholipases [28]. UDA was also effective inhibiting hyphal growth, a key step in *C. albicans* biofilm development, mimicking the quorum-sensing molecule farnesol that usually inhibits the yeast-to-hyphal transition [29]. In this review, we discuss recent findings highlighting the feasibility of using UDA as a cost-effective compound for antifungal treatment. We also discuss the suitability of UDA for chemical modification, conjugation with other molecules, and combination therapy.

Chemical Aspects, Molecule Modification, and Synergism

UDA, an 11-carbon, saturated medium-chain FA, is naturally present in the human skin and eliminated through sweat, and is industrially prepared from castor oil. UDA is a white crystalline solid, is insoluble in water, and is possibly involved in stimulating triacylglycerol synthesis [14, 30].

Although the therapeutic effectiveness of UDA against dermatophytes has been established for many years [14, 31], the enormous potential of this molecule remains poorly explored. Various studies demonstrated the therapeutic effectiveness of UDA when administered alone, enhanced activity when chemically modified, and synergistic activity when administered in combination with other compounds, such as antimicrobial peptides. The hydroxamate derivative of UDA, 10-undecanhydroxamic acid, functions as a novel antimicrobial agent with increased efficacy and a greater spectrum of activity by controlling the growth of clinically relevant microorganisms, including bacteria (such as *Escherichia coli* and *Enterococcus faecalis*) and fungi (*C. albicans* and *Aspergillus niger*). Its enhanced effectiveness is due to the introduction of an iron-chelating chemical group in the molecule, which interferes with iron homeostasis [31]. Disturbances in iron homeostasis have been associated with the effect of UDA against *T. rubrum*. Over time, UDA exposure accentuated the inhibitory effects on the expression of genes related to iron-binding activity [24]. The initial maintenance of the iron-acquisition system, with some upmodulated genes, occurs in response to UDA stress. After a 12-h UDA exposure, the repression of genes related to iron metabolism and many other categories is suggestive of widespread damage.

In another study, the activity of UDA was reduced by introducing acetylenic or ethylenic unsaturation into the UDA molecule in different positions from $C11\Delta^2$ to $C11\Delta^{10}$. These results established the saturated molecule as the most effective form of UDA. The effects of unsaturated UDA derivatives were evaluated against *Streptococcus pyogenes*. Comparatively, acetylenic compounds were slightly more active than the ethylenic isomers. The position of the ethylenic unsaturation site exerted minor effects against bacteria, whereas significant differences were observed with acetylenic derivatives, depending on the location of the unsaturated position [32].

Most antimicrobial peptides with high antibacterial activity are not active toward fungi. However, chemical modification of antimicrobial peptides can change this scenery. An antibacterial peptide, a magainin analog, exhibited antifungal activity when conjugated with lipophilic acids [33]. Also, conjugating UDA with this antibacterial lipopeptide resulted in high potency against some fungi [27]. These results led to the proposal of a new group of lipopeptide candidates with antifungal activity. Additionally, conjugating UDA to a weakly active diastereomeric lytic peptide containing Lys and Leu ([D]-K_5L_7) produced a highly potent lipopeptide. This compound was active against

gram-negative bacteria (*E. coli* and *Pseudomonas aeruginosa*), gram-positive bacteria (*Bacillus subtilis* and *Staphylococcus aureus*), yeasts (*C. albicans* and *Cryptococcus neoformans*), and the opportunistic fungus *Aspergillus fumigatus* [27].

Finally, the combined use of QA and UDA significantly repressed the major virulence genes of *C. albicans*. The synergistic interaction between these two compounds significantly inhibited important perpetuation-related aspects, such as biofilm formation and the filamentation capability [28]. The results obtained after combination therapy with UDA and other compounds with antifungal properties emphasized that such treatment represents a viable and promising alternative strategy.

In general, the use of UDA is mostly associated with antimycotic and antibacterial activity. However, the molecule also exhibits toxicity toward ticks and chiggers and displays repellent properties against fleas, house flies, *Anopheles quadrimaculatus*, and *Aedes aegypti* [34, 35]. It also inhibits oviposition in the phloem-feeding insect *Bemisia tabaci*, which is important for managing plant pests [36].

The well-known properties of UDA and its promising capacity for chemical modification and/or synergistic use highlight its potential importance in controlling fungal infections. The diverse strategies used to enhance its antimicrobial efficacy and its use in widespread applications, particularly its antifungal properties, establish UDA as a promising substance in the pharmaceutical field.

Impact of UDA on Fungal Metabolism

The antifungal activity of UDA has been demonstrated with various fungal species such as *Aspergillus nidulans* [37, 38], *Candida* spp. [28], *Trichophyton* spp. [14, 19], *Albifimbria verrucaria* (formerly *Myrothecium verrucaria*) [39], *S. cerevisiae* [40], and *Trichoderma viride* [39].

The possible mechanisms of action of medium-chain FAs, as previously described for *C. albicans*, include regulating cellular-membrane fluidity, mitochondrial activity changes, impaired formation of hyphae, and biofilm formation [41, 42]. Data from a recent study demonstrated that combination treatment with UDA and QA caused decreased secretion of aspartyl proteinases and lipase biosynthesis [28]. The same study showed a significant reduction in polysaccharide and lipid levels in the extracellular polymeric substance (EPS) of *Candida* spp. biofilm. Moreover, the inhibitory effect of QA-UDA combinations resulted in a prominent decrease in *C. albicans* filamentous growth [28]. UDA exhibited antibiofilm and anti-hyphal forming properties against *Candida* species [29], and antibiofilm activity against *Serratia marcescens* [43], suggesting UDA could be used to control the development of pathogenic biofilms.

A previous investigation of *S. cerevisiae* that assessed aspects of FA uptake and metabolism demonstrated the influence of the ergosterol pathway, specifically the *erg4* gene, in terms of the capacity of fungi to cope with exogenous FAs, such as UDA [40]. Several lines of evidence suggest that UDA is involved in FA and energy metabolism, as previously described for *Umbelopsis isabellina* (formerly *Mortierella isabellina*) [44]. UDA impacts the cellular lipid pattern of this fungus by inhibiting mitochondrial enzymes, blocking the elongation and acetylation of FAs, and making it difficult to incorporate these FAs into lipids in the cell. Moreover, data from a previous study demonstrated the effect of FAs on the growth of *Aspergillus flavus*, correlating with imbalanced peroxisome function, which ultimately resulted in aflatoxin production [45]. Also, *A. nidulans* exposed to sublethal doses of UDA led to decreased conidia germination [46], showed a significant decrease in extracellular lipase activity, and a reduction of approximately 70% in both intracellular and extracellular esterase activities [37].

Among studies exploring the antifungal properties of UDA, many were conducted against dermatophytes, mostly *T. rubrum*. Das and colleagues exploited the toxic effects of UDA against *T. rubrum* and confirmed the growth-inhibitory activity against this fungus [18–21]. UDA changed the lipid composition by lowering the synthesis of glycerides, sterol esters, and phospholipids, thus promoting changes in the fungal membrane and inhibiting its growth [21].

Treating *Trichophyton interdigitale* H6 (previously identified as *T. rubrum*, and reclassified based on genome sequencing) [47, 48] with UDA resulted in the induction of regulatory genes, such as *AURR1* (DW005378), a transcription factor that regulates aurofusarin biosynthesis, and the cellular regulator DopA (EZF34453.1), which is required for correct cell

morphology [49]. In addition, the susceptibility of *T. interdigitale* to UDA was nutrient-dependent [22].

It has been reported that UDA inhibits the growth of *T. rubrum* in concentrations ranging from 25 to 30 μg/mL [20, 24, 50]. In addition, other assays showed how UDA affects the production of exocellular enzymes by *T. rubrum*, inhibiting lipases and keratinases, which are necessary for the infection process [20]. Molecular studies on the effects of UDA on dermatophytes were performed to elucidate the strategies fungi use to overcome the effects triggered by the entry of UDA into fungal cells. UDA was assumed to alter *T. rubrum* lipid composition by possibly affecting an unknown control mechanism of lipid synthesis or breakdown [21]. The utilization of UDA in phospholipid biosynthesis was corroborated through the upregulation of a sterol carrier protein, followed by the induction of several genes related to FA synthesis and elongation, notably after 3 h of UDA exposure [24]. UDA also led to positive modulation of the beta-oxidation pathway. Fungal cells direct the degradation of FAs through different pathways, such as the beta-oxidation pathway, to overcome toxicity [51]; however, increased beta-oxidation activity significantly induced the overproduction of reactive oxygen species, which led to oxidative stress [24]. Also, ergosterol production was markedly reduced, which was reflected in impaired membrane fluidity. In addition, cellular detoxification pathways were activated to reverse the damage due to oxidative stress. The authors showed that most of these metabolic changes occurred after 3 h of exposure to UDA, which was due to the high toxicity of this FA. As mentioned above, dermatophytes use these strategies to overcome the deleterious effects of UDA that cause remodeling of the cell membrane and cell wall. A vital part of this strategy is the ability to use a sophisticated regulatory mechanism to alter gene expression [24] (Fig. 2).

Cells form integrated systems and, therefore, cellular physiology depends on a delicate balance between the synthesis and degradation of molecules involved in cell maintenance and metabolism. Once this balance is dysregulated, multiple cellular effects are triggered, which cannot be analyzed separately. A broader analysis of these effects is necessary to understand the overall effects of a drug, which may have secondary effects that should be considered. A transcriptomics study of *T. rubrum* exposed to sublethal doses of UDA shed insight on the refined cellular processes triggered by the drug [24]. The processes underlying these effects revealed that cellular-membrane damage had effects on the dermatophyte cell wall. Moreover, coordinated gene regulation might account for restructuring of the cell wall by modifications in its biochemical composition. The glycosyl hydrolase gene was upregulated after a 3-h challenge with UDA, which was a possible response to offset the damage caused by the drug during the early exposure period. However, the gene encoding the protein hydrophobin (TERG_04234), a cysteine-rich protein produced exclusively by filamentous fungi that is related to cell wall remodeling, was downregulated shortly after exposure to UDA. This observation merits attention because of the importance of hydrophobin to cell wall integrity, which was affected by damage to the plasma membrane, demonstrating the breadth of the responses by the fungus to overcome the toxic action of UDA [23].

An attractive approach for antifungal therapy is to target the gene-expression machinery, which is essential, given the network of cellular interactions that occur inside cells. Cells often fine-tune the levels of transcription to generate an appropriate response to a given stimulus. Positive and negative influences on gene expression must be balanced for correct mRNA synthesis [52]. Focusing on specific genes is becoming crucial for the development of drugs, such as transcription factors, which are of primary importance for all organisms [53]. Therefore, a drug capable of affecting transcription factors and disrupting a network of cellular interactions, thereby preventing fungi from responding correctly to developmental and environmental conditions, is an ideal solution. Importantly, the modulation of *T. rubrum* transcription factors is affected by UDA exposure, demonstrating that its toxic effects likewise affect the expression of genes closely related to regulating metabolic pathways in dermatophytes [24].

Taken together, the results of several reports have reinforced UDA as a compound with a broad spectrum of activity that triggers multiple effects in fungal cells, while being non-toxic to mammalian cells in vitro and to *Caenorhabditis elegans* [28, 54].

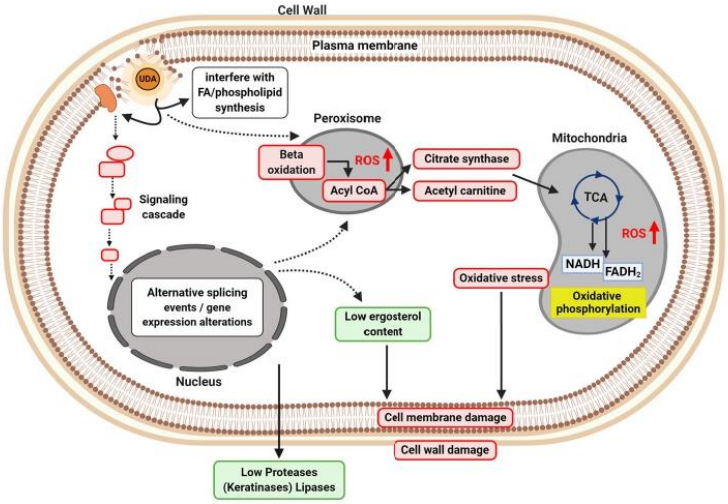

Fig. 2 Proposed mechanism of action of undecanoic acid (UDA) against fungal viability. UDA triggers oxidative stress, leading to changes in fatty acid (FA), phospholipid, and ergosterol synthesis. Increased levels of reactive oxygen species (ROS) cause damage to the cell membrane and cell wall. UDA also decreases the expression and activity of proteases and induces alternative splicing in genes involved in several cellular processes. Inhibited or downregulated processes are represented in green, while increased or upregulated processes are represented in red. Dashed lines represent pathways or processes that have not yet been fully elucidated. (Color figure online)

Fungal Resistance to UDA

A fundamental approach for evaluating the inhibitory potential of antifungals is to investigate the natural resistance mechanisms of fungi [38]. Pathogenic fungi deploy several molecular tools to handle the stress caused by toxic substances produced by host cells or that are present in the environment. For instance, *T. rubrum* responds to UDA mainly by modulating the expression of genes related to FA metabolism, oxidative stress, and proteases [24].

Thus, a mechanism that *T. rubrum* uses against UDA is its incorporation into phospholipid synthesis and degradation of the phospholipids by the β-oxidation enzymes as the acyl oxidase (TERG_02909) and ketoacyl thiolase (TERG_12530) [24]. These enzymes were notably induced after a 3-h exposure to UDA (Table 1). Another vigorous defense involves the induction of antioxidant enzymes to reduce the levels of reactive oxygen species [24].

Analysis of the results obtained through RNA-sequencing (RNA-seq) of *T. rubrum* exposed to acriflavine and UDA revealed upregulation of the ABC and MFS multidrug-resistance (MDR) transporters [23, 55]. MDR transporters are transmembrane components that function as efflux pumps. Overexpression of these proteins results in a resistant phenotype by preventing the over-accumulation of toxic compounds inside cells [56, 57]. Interestingly, the modulation of different transporter genes was observed in the presence of each of these drugs [23, 58], corroborating the idea that an adaptive response occurs in a drug-dependent manner [59]. Previous data revealed that the upregulation of MDR transporters occurred as a rapid response in the first hour after UDA exposure [58]. The presence of several different MDRs in the dermatophyte genome enables it to counteract many classes of drugs, which demonstrates the complexity of such regulation. Furthermore, compensatory expression of *mdr4*, due to the deletion of the *mdr2* gene, was observed in *T. interdigitale* grown in media containing the antifungal medicine griseofulvin [60].

In microorganisms, the biofilm structure is known to provide high resistance against external agents. Indeed, this structure constitutes a significant medical

Table 1 Genes associated with oxidative stress and fatty acid metabolism, grouped in terms of Gene Ontology enrichment

Gene ID	Gene product name	3 h	12 h
GO:0006979—response to oxidative stress			
TERG_01252	Catalase A		2.37
TERG_01463	Cytochrome c peroxidase (*T. tonsurans*)	3.17	2.15
TERG_02735	Fatty acid oxygenase PpoC, putative (*A. benhamiae*)	− 2.06	
TERG_06354	SVP1-like protein (*T. tonsurans*)	1.79	
TERG_08226	hypothetical protein	− 1.79	
GO:0034599—cellular response to oxidative stress			
TERG_01349	Glutathione peroxidase (*T. tonsurans*)	2.41	1.60
TERG_05769	NAD(P)H-dependent D-xylose reductase (*T. equinum*)	1.98	2.02
GO:0006631—fatty acid metabolic process			
TERG_05621	Short-chain dehydrogenase/reductase family oxidoreductase, putative (*A. benhamiae*)	4.02	
TERG_02909	Acyl-CoA oxidase, putative (*T. verrucosum*)	3.81	
TERG_07659	Peroxisomal 3-ketoacyl-coA thiolase (Kat1), putative (*A. benhamiae*)	3.01	
TERG_08170	Fatty acid elongase gig30 (*T. equinum*)	2.27	1.89
TERG_08952	Long-chain-fatty-acid-CoA ligase (*T. equinum*)	1.65	
TERG_06240	Peroxisomal biogenesis factor 2 (*T. tonsurans*)	1.60	
GO:0016747—transferase activity			
TERG_12530	3-Ketoacyl-CoA thiolase peroxisomal A (*T. tonsurans*)	4.19	1.50
TERG_07691	Sterol carrier protein (*T. tonsurans*)	2.73	
TERG_03390	Glutation S-transferase (*T. equinum*)	3.00	
TERG_04960	Glutathione S-transferase Ure2-like, putative (*A. benhamiae*)	6.15	
TERG_00284	Peroxin 14 (*T. tonsurans*)	2.52	
TERG_06361	ATP-dependent protease La	2.13	
TERG_01759	Peroxisome assembly protein 10 (*T. equinum*)	1.94	

Transcriptional modulation is indicated according to the exposure time to undecanoic acid [24]. Gene-expression values are expressed as log2-fold change between the indicated time point and the reference sample (without drug exposure)

problem, since most hospital-acquired infections are associated with biofilms on medical devices such as catheters, dentures, contact lenses, heart valves, and prostheses [61, 62]. Biofilm formation is frequently encountered in fungi; *Candida* spp. have been reported to be proficient in forming biofilms on both biotic and inert surfaces [63]. As mentioned above, combined UDA and QA therapy had a considerable effect on the biofilm structures of *Candida* spp. [28].

Another mechanism of resistance to UDA was described for *A. nidulans*, in which ultraviolet light-induced mutations in the *udaA* gene resulted in the resistant strains *udaA1* and *udaA2* [37]. Interestingly, it was observed that mutations in the *lipA* gene also conferred UDA resistance in *A. nidulans*. In this case, a point mutation in a particular locus caused a Glu-to-Lys substitution during translation, which potentially lowered the rate of enzymatic catalysis or the catalytic affinity of the enzyme for the substrate, or promoted enzymatic inactivation [38]. In addition, a recent study showed that UDA susceptibility was related to chromosome 7 trisomy in *C. albicans* and that resistance was due to chromosomal loss [64]. This study also showed that all susceptible isolates carrying a deletion of the transcription factor DAL81, and that acquired UDA resistance, had lost a copy of chromosome 7. Thus, these data draw a particular, but rather unclear, relationship between aneuploidy and antifungal resistance; a possibility that was corroborated by data from similar studies [65, 66].

A study carried out with a UDA-resistant strain (UDA^r) of *T. interdigitale* demonstrated that tolerance to UDA could also be displayed by a naturally non-resistant strain (H6) under specific nutritional

conditions [22]. Culturing the UDA^r and H6 strains in a protein-rich medium (minimal medium [MM] supplemented with 1% commercial low-fat dry milk) resulted in significant differences in survival rates at UDA concentrations above 50 mg/L. In contrast, culturing the same strains in a lipid-rich medium (MM supplemented with 1% Tween 20 as the sole carbon source) completely prevented the survival effect on the susceptible strain, even at high drug concentrations. The same nullifying effect on the inhibitory potential of UDA was observed when the strains were cultured in a keratin-rich medium (MM supplemented with keratin powder, 2.5 g/L) [22].

The possibility that nutrient conditions are crucial for establishing the susceptibility to a given drug is very relevant for isolating and characterizing resistant strains. Factoring in this possibility is also helpful when screening new antifungal agents [22]. Importantly, resistance acquired by wild-type strains due to environmental conditions (such as the carbon source) can serve as a determinant for the emergence of genetically resistant lineages. This process is a consequence of the population stabilization provided by the resistant phenotype so that mutations, recombination, and selection can occur. Events of environmentally induced resistance occurring before genetic resistance are well described and pose a real challenge for antifungal therapy [67, 68].

Resistance strategies like those described here are adaptive responses that have mostly been shaped by long-term natural selection involving co-evolutionary dynamics with hosts [69]. Despite the activation of common pathways related to stress responses, antifungals can cause high mortality rates, precisely because they correspond to substances that fungi have not experienced prolonged contact with during their evolution. Therefore, the misuse of antifungal drugs exacerbates opportunistic fungal infections by enabling the emergence of resistant strains [70]. Further investigation on this matter will be crucial for better guiding clinical efforts against recidivist pathogenic fungi that are mostly opportunistic.

Effect of UDA Exposure on Pre-mRNA Processing in Dermatophytes

Alternative splicing (AS) is an essential and highly complex process of post-transcriptional regulation that enables increased numbers of transcript isoforms for a single gene [71, 72]. AS powerfully enhances proteome diversity and functionality and thus fulfills paramount functions in adaptive responses [24, 73, 74].

The spliceosome machinery drives RNA processing after detecting exon boundaries (5′ and 3′ splice sites) [75]. The activity of the spliceosome is highly dynamic and coordinated. Splicing factors play essential roles in the activation and maintenance of this machinery [75, 76]. Recent work has shown differences in the modulation of splice factor genes in response to different environmental stimuli in the dermatophyte *T. rubrum* [77], which might ultimately influence the occurrence of AS. Indeed, changes in the relative rates of spliceosome assembly might be a means of AS regulation [78].

Patterns of AS that occur include the use of alternate 5′ or 3′ splice sites, exon skipping, intron retention (IR), and mutually exclusive events [72]. Although AS is not fully understood, fungal pathogens show a higher tendency to undergo AS than non-pathogenic fungi. If we consider only human pathogenic fungi, the relative proportion is even higher [79]. Moreover, evidence suggests the involvement of AS in complex regulatory network wiring in fungal cells that culminates in adaptive responses toward a plethora of stimuli. For example, antifungal signalling, nutrient supply, and host interactions have been reported to influence AS in *Neurospora crassa*, *T. rubrum*, *A. nidulans*, *A. fumigatus*, and *Candida* spp. [24, 73, 80, 81].

The RNA-seq tool consists of a robust and reliable source of data for the analysis of AS because it provides genome-wide information on exon coverage and splice junctions [82, 83]. It is noteworthy that in fungi, IR comprises the most predominant AS pattern [72, 81], and previous reports also demonstrated that only 14% of differentially expressed genes (DEGs) overlap with AS [81], which reinforces that AS occurs as a regulatory mechanism for specific adaptive responses.

Recent RNA-seq data showed the occurrence of AS events (in terms of exon usage and IR) in *T. rubrum* genes after UDA exposure [24]. Approximately 516 genes exhibited differences in exon usage after UDA exposure, distributed among 302 and 214 genes for the 3 h and 12 h time point, respectively (Fig. 3). About 967 genes underwent IR after UDA exposure,

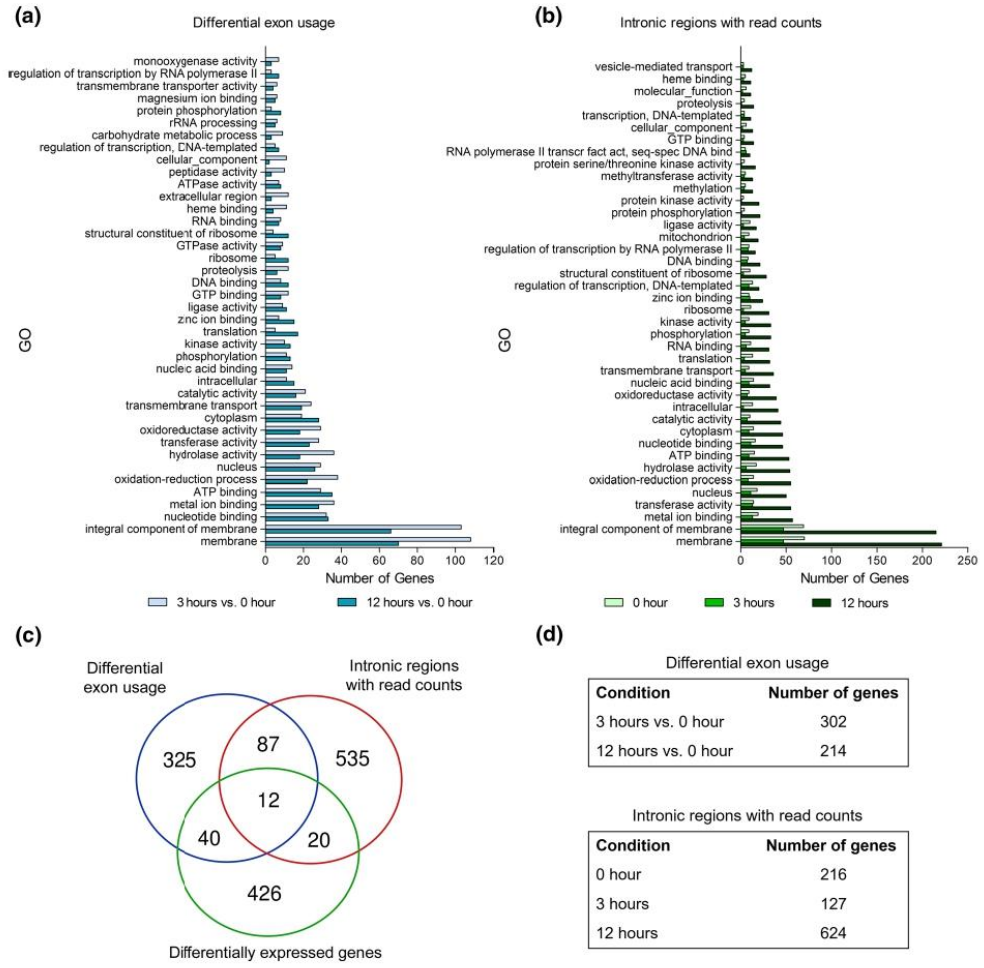

Fig. 3 In silico identification of genes presenting **a** differential exon usage or **b** intron retention, in response to undecanoic acid (UDA) exposure. Analysis was conducted by identifying significantly enriched Gene Ontology terms using previously published RNA-sequencing data [24]. **c** Venn diagram showing the number of transcripts modulated in *Trichophyton rubrum* cells following UDA exposure, and the number of genes that underwent alternative splicing events, differential exon usage, or intron retention. **d** Number of genes presenting differential exon usage and the number of intronic regions with read counts at each time point

distributed among 216 genes at 0 h, 127 genes at 3 h, and 624 genes at 12 h. While exon use events prevailed after a 3 h UDA exposure, IR was observed mainly after 12 h of contact with the drug (Fig. 3d). In both cases, the predominant group of genes subject to AS was related to membrane composition (Fig. 3a, b), associating UDA damage to the membrane with splicing events under the tested conditions. In addition, a small percentage of DEGs (approximately 15%) was associated with a type of AS, IR, or exon skipping (Fig. 3c), reiterating that the aforementioned

regulatory mechanism of AS contributes to adaptive strategies.

It was also reported that pre-mRNA coding for phosphoglucomutase underwent exon skipping and the pre-mRNA coding for inosine monophosphate dehydrogenase underwent IR. In both cases, the encoded enzymes are involved in critical energy metabolism. However, the proteins resulting from either form of AS presented a loss of essential domains and probably had impaired function [24]. These results demonstrated the existence of tight regulation promoted by AS between fungal energy metabolism and cellular signaling in response to UDA exposure. In addition, *T. rubrum* exposed to UDA presented IR events in two genes that encode heat shock proteins (HSPs): Hsp7-like protein (TERG_03206) and Hsp75-like protein (TERG_01883) [26]. In silico analysis revealed that conventional processing of the respective pre-mRNAs of both genes led to functional proteins. In contrast, the AS events caused by IR promoted open reading frame disruptions, resulting in premature mRNA stop codons and the generation of truncated proteins with probable functional impairment. Modulation of the Hsp7-like protein isoforms was compared after *T. rubrum* exposure to UDA and terbinafine. UDA exposure promoted dysregulated gene processing and decreased levels of transcripts coding for functional proteins. In contrast, terbinafine exposure caused increased transcript levels coding for functional proteins after a 3 h UDA exposure, and no difference in modulation of the retained isoform was observed between control and drug-treated cells. These results raised the possibility that a regulatory pathway is involved in HSPs processing, which is probably related to optimization in response to different chemical exposures (cellular conditions). Indeed, refined mechanisms for protein production, co-translation, protein folding, and disposal have been described, each of which plays paramount roles in maintaining cellular homeostasis and proper metabolism [84–86].

The occurrence of IR events in two genes that encode heat shock proteins in *T. rubrum* exposed to UDA was revealed in the pre-mRNA coding for STE/PAKA kinase, as an autoregulatory mechanism for this kinase [25]. Increased IR levels were observed after a 3-h UDA exposure. In silico analyses showed a change in the open reading frame for the kinase due to IR, which was responsible for the production of at least two independent polypeptides. One polypeptide contained the entire kinase catalytic domain, but lacked the regulatory domain. This finding suggests that an alternative pre-mRNA splicing played a role in activating the STE20/PAKA kinase in *T. rubrum*, independent of caspase cleavage or molecular signaling that is normally required for its canonical activation. These results also suggest that the MAPK pathway was activated to varying extents and regulated by different sets of molecules by external stimuli. Based on these lines of evidence, we hypothesize that different sources of isoforms could be generated by AS, leading to potentially functional proteins or proteins with impaired function, which is mainly influenced by the roles each gene plays within cells. In addition, these events rely on a complex signaling cascade that culminates in the optimization of protein production according to the needs of a fungus.

Concluding Remarks and Perspectives

In this review, we highlight known and novel perspectives related to the antifungal properties of UDA. The limited antifungal options currently available have led to increased attention on the potential use of UDA as a therapeutic strategy against fungal infections. This potential use is strengthened by the broad-spectrum activity of UDA, which includes potent antimycotic activity against several human pathogenic fungi, such as *Aspergillus* spp., *Candida* spp., and *Trichophyton* spp. The main effects of UDA exposure on some fungi are compiled in Table 2. Furthermore, UDA is suitable for chemical modifications enabling it to serve as a model scaffold for designing novel and more efficient antimicrobial molecules, it displays synergistic activity with other compounds, and it is non-toxic to mammalian cells and worms. In summary, the data discussed here highlight this overlooked compound as a potentially safe and effective antifungal agent.

Author contributions All authors wrote sections of the manuscript. NM-R, MM, and AR edited the manuscript. All authors read and approved the submitted version.

Funding We thank the Brazilian funding agencies for the continuous support to our projects: São Paulo Research Foundation - FAPESP (proc. Nos. 2019/22596-9, 2018/11319-

Table 2 Main effects observed in some microorganisms following exposure to undecanoic acid

Microorganism	Observed effect	Working doses	References
Trichophyton rubrum	Lipid composition increased when UDA^s was grown in low concentration of UDA	30 μg ml^{-1}	[21]
	Inhibited conidial germination of UDA^s and UDA^r	UDA^s at 30 μg ml^{-1} and UDA^r 120 μg ml^{-1}	[18]
	Inhibited production of exocellular lipase and keratinase	27.5 μg ml^{-1}	[20]
	Inhibited phospholipid metabolism	50 μg ml^{-1}	[19]
	Affected fungal metabolism and pre-mRNA processing regulatory events	17.5 μg mL^{-1}	[24]
Trichophyton interdigitale	Inhibited growth in response to UDA and carbon source for both wild type and UDA^r strains	Concentration is dependent on the carbon source	[22]
	Affected gene-expression profile	50 μg mL^{-1}	[49]
Serratia marcescens	Impaired biofilm formation	ranging from 20 to 160 μg/ml	[43]
Candida albicans		2 μg ml^{-1}	[29]
		QA (50–800 μg mL^{-1}) in combination with UDA (5–80 μg mL^{-1})	[28]
Aspergillus nidulans	Decreased extracellular lipase activity	200 μg mL^{-1}	[37]
	Impaired conidia germination	0 to 300 μg mL^{-1}	[46]
Saccharomyces cerevisiae	Inhibited growth	0.5 mM, 1 mM or 2 mM	[40]
Umbelopsis isabellina	Inhibited biosynthesis of long-chain fatty acids	Concentration is dependent on the carbon source	[44]

QA = quinic acid; UDA = undecanoic acid; UDA^s = UDA sensitive strain; UDA^r = UDA resistant strain

1, 2018/15458-6, 2015/23435-8, 2009/08411-4); National Council for Scientific and Technological Development -CNPq (proc. Nos. 305797/2017-4, and 304989/2017-7); Coordenação de Aperfeiçoamento de Pessoal de Nível Superior - CAPES (Finance Code 001), and Fundação de Apoio ao Ensino, Pesquisa e Assistência - FAEPA.

Declarations

Conflict of interest The authors declare that they have no conflicts of interest.

Research involving human participants and/or animals This manuscript does not contain any studies with human participants or animals performed by any of the authors.

References

1. Martinez-Rossi NM, Bitencourt TA, Peres NTA, Lang EAS, Gomes EV, Quaresemin NR, et al. Dermatophyte resistance to antifungal drugs: mechanisms and prospectus. Front Microbiol. 2018;9:1108.
2. Cordoba S, Vivot W, Szusz W, Albo G. Antifungal activity of essential oils against *Candida* species isolated from clinical samples. Mycopathologia. 2019;184(5):615–23.
3. Lopes AI, Tavaria FK, Pintado ME. Conventional and natural compounds for the treatment of dermatophytosis. Med Mycol. 2020;58(6):707–20.
4. Souza ACO, Amaral AC. Antifungal therapy for systemic mycosis and the nanobiotechnology era: improving efficacy, biodistribution and toxicity. Front Microbiol. 2017;8:336.
5. Drake DR, Brogden KA, Dawson DV, Wertz PW. Thematic review series: skin lipids—antimicrobial lipids at the skin surface. J Lipid Res. 2008;49(1):4–11.
6. Feingold KR. The outer frontier: the importance of lipid metabolism in the skin. J Lipid Res. 2009;50:S417–22.
7. Clark JF. On the toxic effect of deleterious agents on the germination and development of certain filamentous fungi. Bot Gaz. 1899;28(5):289–327.
8. Keeney EL, Ajello L, Broyles EN, Lankford E. Propionate and undecylenate ointments in the treatment of tinea pedis and an *in vitro* comparison of their fungistatic and antibacterial effects with other ointments. Bull Johns Hopkins Hosp. 1944;74:417–39.
9. Shapiro AL, Rothman S. Undecylenic acid in the treatment of dermatomycosis. Arch Dermatol. 1945;119(4):345–50.
10. Peck SM, Russ WR. Propionate-caprylate mixtures in the treatment of dermatomycoses, with a review of fatty acid therapy in general. Arch Derm Syphilol. 1947;56(5):601–13.

11. Kiesel A. Recherches sur L'action de divers acides et sels acides sur le développement de L'*Aspergillus niger*. Ann Inst Pasteur. 1913;27:391–420.
12. Hoffman C, Schweitzer TR, Dalby G. Fungistatic properties of the fatty acids and possible biochemical significance. J Food Sci. 1939;4(6):539–45.
13. Peck SM, Rosenfeld H. The effects of hydrogen ion concentration, fatty acids and vitamin C on the growth of fungi. J Invest Dermatol. 1938;1(4):237–65.
14. Garg AP, Muller J. Fungitoxicity of fatty acids against dermatophytes. Mycoses. 1993;36(1–2):51–63.
15. Vicher EE, Lyon I, White EL. Studies on the respiration of *Trichophyton rubrum*. Mycopathol Mycol Appl. 1959;11:185–95.
16. Vicher EE, Kostiw LL, Lyon I, Bolewicz BM. The effect of sodium propionate and sodium caprylate on the fatty acid content of *Trichophyton rubrum*. Mycopathol Mycol Appl. 1968;35(3):208–14.
17. Samson FE, Katz AM, Harris DL. Effects of acetate and other short-chain fatty acids on yeast metabolism. Arch Biochem Biophys. 1955;54(2):406–23.
18. Das SK, Adhya S, Banerjee AB. Effect of undecanoic acid on germination of microconidia of wild and undecanoic acid resistant mutant of *Trichophyton rubrum*. Mycopathologia. 1977;61(2):121–3.
19. Das SK, Banerjee AB. Effect of undecanoic acid on phospholipid-metabolism in *Trichophyton rubrum*. Sabouraudia-J Med Vet Mycol. 1982;20(4):267–72.
20. Das SK, Banerjee AB. Effect of undecanoic acid on the production of exocellular lipolytic and keratinolytic enzymes by undecanoic acid-sensitive and -resistant strains of *Trichophyton rubrum*. Sabouraudia. 1982;20(3):179–84.
21. Das SK, Banerjee AB. Effect of undecanoic acid on lipid composition of *Trichophyton rubrum*. Mycopathologia. 1983;83(1):35–9.
22. Peres NTA, Cursino-Santos JR, Rossi A, Martinez-Rossi NM. *In vitro* susceptibility to antimycotic drug undecanoic acid, a medium-chain fatty acid, is nutrient-dependent in the dermatophyte *Trichophyton rubrum*. World J Microbiol Biotechnol. 2011;27(7):1719–23.
23. Martins MP, Silva LG, Rossi A, Sanches PR, Souza LDR. Martinez-Rossi NM. Global analysis of cell wall genes revealed putative virulence factors in the dermatophyte *Trichophyton rubrum*. Front Microbiol. 2019;10:2168.
24. Mendes NS, Bitencourt TA, Sanches PR, Silva-Rocha R, Martinez-Rossi NM, Rossi A. Transcriptome-wide survey of gene expression changes and alternative splicing in *Trichophyton rubrum* in response to undecanoic acid. Sci Rep. 2018;8(1):2520.
25. Gomes EV, Bortolossi JC, Sanches PR, Mendes NS, Martinez-Rossi NM, Rossi A. STE20/PAKA protein kinase gene releases an autoinhibitory domain through pre-mRNA alternative splicing in the dermatophyte *Trichophyton rubrum*. Int J Mol Sci. 2018;19(11):3654.
26. Neves-da-Rocha J, Bitencourt TA, de Oliveira VM, Sanches PR, Rossi A, Martinez-Rossi NM. Alternative splicing in heat shock protein transcripts as a mechanism of cell adaptation in *Trichophyton rubrum*. Cells. 2019;8(10):1206.
27. Avrahami D, Shai Y. Bestowing antifungal and antibacterial activities by lipophilic acid conjugation to D, L-amino acid-containing antimicrobial peptides: a plausible mode of action. Biochemistry. 2003;42(50):14946–56.
28. Muthamil S, Balasubramaniam B, Balamurugan K, Pandian SK. Synergistic effect of quinic acid derived from *Syzygium cumini* and undecanoic acid against *Candida* spp. biofilm and virulence. Front Microbiol. 2018;9:2835.
29. Lee JH, Kim YG, Khadke SK, Lee J. Antibiofilm and antifungal activities of medium-chain fatty acids against *Candida albicans* via mimicking of the quorum-sensing molecule farnesol. Microb Biotechnol. 2020.
30. Hastings J, Owen G, Dekker A, Ennis M, Kale N, Muthukrishnan V, et al. ChEBI in 2016: improved services and an expanding collection of metabolites. Nucleic Acids Res. 2016;44(D1):D1214–9.
31. Ammendola S, Lembo A, Battistoni A, Tagliatesta P, Ghisalberti C, Desideri A. 10-undecanhydroxamic acid, a hydroxamate derivative of the undecanoic acid, has strong antimicrobial activity through a mechanism that limits iron availability. FEMS Microbiol Lett. 2009;294(1):61–7.
32. Kabara JJ, Vrable R. Antimicrobial lipids: natural and synthetic fatty acids and monoglycerides. Lipids. 1977;12(9):753–9.
33. Avrahami D, Shai Y. Conjugation of a magainin analogue with lipophilic acids controls hydrophobicity, solution assembly, and cell selectivity. Biochemistry. 2002;41(7):2254–63.
34. Jones AM, Klun JA, Cantrell CL, Ragone D, Chauhan KR, Brown PN, et al. Isolation and identification of mosquito (*Aedes aegypti*) biting deterrent fatty acids from male inflorescences of breadfruit (*Artocarpus altilis* (Parkinson) Fosberg). J Agric Food Chem. 2012;60(15):3867–73.
35. Ali A, Cantrell CL, Bernier UR, Duke SO, Schneider JC, Agramonte NM, et al. *Aedes aegypti* (Diptera: Culicidae) biting deterrence: structure–activity relationship of saturated and unsaturated fatty acids. J Med Entomol. 2012;49(6):1370–8.
36. Cruz-Estrada A, Ruiz-Sanchez E, Cristobal-Alejo J, Gonzalez-Coloma A, Andres MF, Gamboa-Angulo M. Medium-chain fatty acids from *Eugenia winzerlingii* leaves causing insect settling deterrent, nematicidal, and phytotoxic effects. Molecules. 2019;24(9):1724.
37. Brito-Madurro AG, Cuadros-Orellana S, Madurro JM, Martinez-Rossi N, Rossi A. Effect of undecanoic acid on the production of esterases and lipases by *Aspergillus nidulans*. Ann Microbiol. 2005;55(4):291–4.
38. Brito-Madurro AG, Prade RA, Madurro JM, Santos MA, Peres NT, Cursino-Santos JR, et al. A single amino acid substitution in one of the lipases of *Aspergillus nidulans* confers resistance to the antimycotic drug undecanoic acid. Biochem Genet. 2008;46(9–10):557–65.
39. Gershon H, Shanks L. Antifungal activity of fatty acids and derivatives: structure–activity relationships. In: Kabarra JJ, editor. The pharmacological effect of lipids. American Oil Chemists Society; 1978.
40. McDonough V, Stukey J, Cavanagh T. Mutations in *erg4* affect the sensitivity of *Saccharomyces cerevisiae* to medium-chain fatty acids. Biochim Biophys Acta Mol Cell Biol Lipids. 2002;1581(3):109–18.
41. Shi D, Zhao Y, Yan H, Fu H, Shen Y, Lu G, et al. Antifungal effects of undecylenic acid on the biofilm formation of

Candida albicans. Int J Clin Pharmacol Ther. 2016;54(5):343–53.
42. Mionic Ebersold M, Petrovic M, Fong WK, Bonvin D, Hofmann H, Milosevic I. Hexosomes with undecylenic acid efficient against *Candida albicans*. Nanomaterials (Basel). 2018;8(2):91.
43. Salini R, Sindhulakshmi M, Poongothai T, Pandian SK. Inhibition of quorum sensing mediated biofilm development and virulence in uropathogens by *Hyptis suaveolens*. Antonie Van Leeuwenhoek. 2015;107(4):1095–106.
44. Hortmann L, Rehm HJ. Inhibitory effect of undecanoic acid on the biosynthesis of long-chain fatty acids in *Mortierella isabellina*. Appl Microbiol Biotechnol. 1984;20(2):139–45.
45. Reverberi M, Punelli M, Smith CA, Zjalic S, Scarpari M, Scala V, et al. How peroxisomes affect aflatoxin biosynthesis in *Aspergillus flavus*. PLoS ONE. 2012;7(10):e48097.
46. Brito-Madurro AG, Cuadros-Orellana S, Martinez-Rossi NM, Rossi A. Undecanoic acid resistance in filamentous fungi: Identification and linkage mapping of the *Aspergillus nidulans udaA* gene. J Gen Appl Microbiol. 2005;51(1):47–9.
47. Persinoti GF, Martinez DA, Li W, Dogen A, Billmyre RB, Averette A, et al. Whole-genome analysis illustrates global clonal population structure of the ubiquitous dermatophyte pathogen *Trichophyton rubrum*. Genetics. 2018;208(4):1657–69.
48. Chaturvedi V, de Hoog GS. Onygenalean fungi as major human and animal pathogens. Mycopathologia. 2020;185(1):1–8.
49. Paião FG, Segato F, Cursino-Santos JR, Peres NT, Martinez-Rossi NM. Analysis of *Trichophyton rubrum* gene expression in response to cytotoxic drugs. FEMS Microbiol Lett. 2007;271(2):180–6.
50. Das SK, Banerjee AB. Effect of undecanoic acid on cell-permeability and respiration of *Trichophyton rubrum*. Acta Microbiol Pol. 1981;30(3):295–8.
51. Hiltunen JK, Mursula AM, Rottensteiner H, Wierenga RK, Kastaniotis AJ, Gurvitz A. The biochemistry of peroxisomal beta-oxidation in the yeast *Saccharomyces cerevisiae*. FEMS Microbiol Rev. 2003;27(1):35–64.
52. Shelest E. Transcription factors in fungi. FEMS Microbiol Lett. 2008;286(2):145–51.
53. Bahn YS. Exploiting fungal virulence-regulating transcription factors as novel antifungal drug targets. PLoS Pathog. 2015;11(7):e1004936.
54. Li XC, Jacob MR, Khan SI, Ashfaq MK, Babu KS, Agarwal AK, et al. Potent *in vitro* antifungal activities of naturally occurring acetylenic acids. Antimicrob Agents Chemother. 2008;52(7):2442–8.
55. Persinoti GF, Peres NTA, Jacob TR, Rossi A, Vencio RZ, Martinez-Rossi NM. RNA-sequencing analysis of *Trichophyton rubrum* transcriptome in response to sublethal doses of acriflavine. BMC Genomics. 2014;15(Suppl 7):S1.
56. Prasad R, Rawal MK. Efflux pump proteins in antifungal resistance. Front Pharmacol. 2014;5:202.
57. Aneke CI, Rhimi W, Otranto D, Cafarchia C. Synergistic effects of efflux pump modulators on the azole antifungal susceptibility of *Microsporum canis*. Mycopathologia. 2020;185(2):279–88.
58. Martins MP, Rossi A, Sanches PR, Martinez-Rossi NM. Differential expression of multidrug-resistance genes in *Trichophyton rubrum*. J Integr OMICS. 2019;9(2):1–81.
59. Fachin AL, Ferreira-Nozawa MS, Maccheroni W Jr, Martinez-Rossi NM. Role of the ABC transporter TruMDR2 in terbinafine, 4-nitroquinoline N-oxide and ethidium bromide susceptibility in *Trichophyton rubrum*. J Med Microbiol. 2006;55(Pt 8):1093–9.
60. Martins MP, Franceschini AC, Jacob TR, Rossi A, Martinez-Rossi NM. Compensatory expression of multidrug-resistance genes encoding ABC transporters in dermatophytes. J Med Microbiol. 2016;65(7):605–10.
61. Chandra J, Mukherjee PK, Ghannoum MA. *Candida* biofilms associated with CVC and medical devices. Mycoses. 2012;55:46–57.
62. Nett JE, Zarnowski R, Cabezas-Olcoz J, Brooks EG, Bernhardt J, Marchillo K, et al. Host contributions to construction of three device-associated *Candida albicans* biofilms. Infect Immun. 2015;83(12):4630–8.
63. Mayer FL, Wilson D, Hube B. *Candida albicans* pathogenicity mechanisms. Virulence. 2013;4(2):119–28.
64. Ma QX, Ola M, Iracane E, Butler G. Susceptibility to medium-chain fatty acids is associated with trisomy of chromosome 7 in *Candida albicans*. mSphere. 2019;4(3):e00402–19.
65. Selmecki A, Forche A, Berman J. Aneuploidy and isochromosome formation in drug-resistant *Candida albicans*. Science. 2006;313(5785):367–70.
66. Pavelka N, Rancati G, Zhu J, Bradford WD, Saraf A, Florens L, et al. Aneuploidy confers quantitative proteome changes and phenotypic variation in budding yeast. Nature. 2010;468(7321):321–5.
67. Cowen LE, Carpenter AE, Matangkasombut O, Fink GR, Lindquist S. Genetic architecture of Hsp90-dependent drug resistance. Eukaryot Cell. 2006;5(12):2184–8.
68. Cowen LE, Lindquist S. Hsp90 potentiates the rapid evolution of new traits: drug resistance in diverse fungi. Science. 2005;309(5744):2185–9.
69. Decaestecker E, Gaba S, Raeymaekers JAM, Stoks R, Van Kerckhoven L, Ebert D, et al. Host-parasite "Red Queen" dynamics archived in pond sediment. Nature. 2007;450(7171):870-U16.
70. Martinez-Rossi NM, Peres NT, Rossi A. Antifungal resistance mechanisms in dermatophytes. Mycopathologia. 2008;166(5–6):369–83.
71. Kelemen O, Convertini P, Zhang Z, Wen Y, Shen M, Falaleeva M, et al. Function of alternative splicing. Gene. 2013;514(1):1–30.
72. Kempken F. Alternative splicing in ascomycetes. Appl Microbiol Biotechnol. 2013;97(10):4235–41.
73. Mendes NS, Silva PM, Silva-Rocha R, Martinez-Rossi NM, Rossi A. Pre-mRNA splicing is modulated by antifungal drugs in the filamentous fungus *Neurospora crassa*. FEBS Open Bio. 2016;6(4):358–68.
74. Laloum T, Martin G, Duque P. Alternative splicing control of abiotic stress responses. Trends Plant Sci. 2018;23(2):140–50.
75. Chen W, Moore MJ. Spliceosomes. Curr Biol. 2015;25(5):R181-3.
76. Koncz C, Dejong F, Villacorta N, Szakonyi D, Koncz Z. The spliceosome-activating complex: molecular

mechanisms underlying the function of a pleiotropic regulator. Front Plant Sci. 2012;3:9.
77. Bitencourt TA, Oliveira FB, Sanches PR, Rossi A, Martinez-Rossi NM. The prp4 kinase gene and related spliceosome factor genes in *Trichophyton rubrum* respond to nutrients and antifungals. J Med Microbiol. 2019;68(4):591–9.
78. Black DL. Mechanisms of alternative pre-messenger RNA splicing. Annu Rev Biochem. 2003;72:291–336.
79. Grutzmann K, Szafranski K, Pohl M, Voigt K, Petzold A, Schuster S. Fungal alternative splicing is associated with multicellular complexity and virulence: a genome-wide multi-species study. DNA Res. 2014;21(1):27–39.
80. Leal J, Squina FM, Freitas JS, Silva EM, Ono CJ, Martinez-Rossi NM, et al. A splice variant of the *Neurospora crassa hex-1* transcript, which encodes the major protein of the Woronin body, is modulated by extracellular phosphate and pH changes. FEBS Lett. 2009;583(1):180–4.
81. Sieber P, Voigt K, Kammer P, Brunke S, Schuster S, Linde J. Comparative study on alternative splicing in human fungal pathogens suggests its involvement during host invasion. Front Microbiol. 2018;9:2313.
82. Roberts A, Pimentel H, Trapnell C, Pachter L. Identification of novel transcripts in annotated genomes using RNA-Seq. Bioinformatics. 2011;27(17):2325–9.
83. Goldstein LD, Cao Y, Pau G, Lawrence M, Wu TD, Seshagiri S, et al. prediction and quantification of splice events from RNA-Seq data. PLoS ONE. 2016;11(5):e0156132.
84. Hug N, Longman D, Caceres JF. Mechanism and regulation of the nonsense-mediated decay pathway. Nucleic Acids Res. 2016;44(4):1483–95.
85. Yu CH, Dang Y, Zhou Z, Wu C, Zhao F, Sachs MS, et al. Codon usage influences the local rate of translation elongation to regulate co-translational protein folding. Mol Cell. 2016;59(5):744–54.
86. Zhou Z, Dang Y, Zhou M, Yuan H, Liu Y. Codon usage biases co-evolve with transcription termination machinery to suppress premature cleavage and polyadenylation. Elife. 2018;7:29.